Exploiting the Location Information for Adaptive Beamforming in Transport Systems

Jaspreet Kaur

Submitted in fulfilment of the requirements for the
Degree of Doctor of Philosophy

School of Engineering
College of Science and Engineering
University of Glasgow

January 2024

Abstract

As mobile communication systems evolve, the demand for enhanced network efficiency and pinpoint accuracy in user localization grows, particularly in the context of dynamic environments such as transport systems. This thesis is motivated by the critical challenge of adapting beamforming techniques to the rapidly changing positions of users, a task analogous to hitting a moving target with precision. The aim is to significantly improve cellular network performance by leveraging advanced beamforming and machine learning (ML) for precise user localization. A novel dataset, crucial to this endeavor, has been developed from simulations in open spaces and a digital twin of the University of Glasgow campus, incorporating vital parameters such as direction of arrival (DoA), time of arrival (ToA), and received signal strength indicators (RSSI). Our investigation commences with the deployment of Maximum Ratio Transmission (MRT) and Zero Forcing (ZF) beamforming techniques to evaluate their effectiveness in enhancing network efficiency through both real and simulated user locations. The application of an adaptive MRT algorithm in our beamforming strategy resulted in a remarkable 53% increase in Signal-to-Noise Ratio (SNR), showcasing the potential of contextual beamforming (Cont-BF) using location information. Furthermore, to refine localization accuracy, deep neural networks were employed, achieving a localization error of less than 1 meter surpassing conventional methods in accuracy.

This research also introduces technique for user-assisted beam alignment in high-speed scenarios, addressing the challenges in dynamic transport systems. Venturing beyond traditional approaches, it explores the integration of user locations into beamforming decisions via a P4 switch, crafting a dynamic system responsive to user mobility. This is complemented by extensive data collection from 5G base stations (BS) using a TSMA 6 scanner, which enriches our analysis with detailed parameters for precision localization. Moreover, the study evaluates various MIMO beamforming techniques in 5G networks, demonstrating an average throughput increase from 9 Mbps to 14 Mbps, thereby underscoring the effectiveness of our proposed solutions. The potential of low-cost Software-Defined Radios (SDR) forDoA estimation and the design of a beam steering setup was also assessed, aiming to evaluate their utility in high-frequency beamforming. Despite uncovering limitations in sub-6GHz environments, this exploration led to the successful development of a DoA estimation setup using USRPs and antennas, alongside a beam steering system crafted through the design of phase shifters and antennas. By integrating precise location information into adaptive beamforming techniques, especially

within the dynamic context of transport systems, this thesis underscores the imperative role of such integration in significantly enhancing communication efficiency. Our findings, which include significant improvements in signal-to-interference-to-noise ratio (SINR) (up to 50%) and received power (up to 40%) through advanced beamforming methods, are pivotal for advancing high-demand applications, including smart vehicles and immersive virtual reality. This marks a crucial advancement towards the realization of next-generation cellular networks, paving the way for more efficient and reliable performance in an evolving technological landscape.

List of Acronyms

AI   Artificial Intelligence

BF   Beamforming

MRT   Maximum Ratio Transmission

ZF   Zero-Forcing

ML   Machine Learning

DoA   Direction of Arrival

MUSIC   Multiple Signal Classification

OSM   OpenStreetMap

USRPs   Universal Software Radio Peripherals

5G   Fifth Generation

TOA   Time of Arrival

RSSI   Received Signal Strength Indicator

QoS   Quality of Service

CR   Cognitive Radio

mmWave   Millimeter-Wave

LSTM   Long Short-Term Memory

CSPs   Communication Service Providers

SON   Self-Organized Network

RF   Radio Frequency

TSMA6   Time-Synchronized Measurements in Areas with six Degrees of Freedom

IoT   Internet of Things

RSRP   Reference Signal Received Power

RSSI   Received Signal Strength Indicator

CIR   Channel Impulse Response

RSRQ   Reference Signal Received Quality

SINR   Signal-to-Noise Ratio

WI   Wireless InSite

UofG   University of Glasgow

USRP   Universal Software Radio Peripheral

Contents

List of Tables

List of Figures

Acknowledgments

I would like to express my deepest appreciation to all who provided me with the possibility to complete this thesis. A special gratitude I extend to my dissertation supervisors, Dr Hasan Tahir Abbas, my guardian angel in academia, Prof. Qammer Abbasi, a godfather figure in my educational journey, and Prof. Mohammad Ali Imran, the unbelievably humble Dean, for their invaluable contributions, stimulating suggestions, and encouragement. Their guidance was instrumental in coordinating and completing my project, especially in writing this thesis.

Furthermore, I am deeply thankful for the crucial role played by the staff of the CSI group of James Watt School of Engineering. Their willingness to provide me with the necessary equipment and materials was essential in completing my work. I also wish to acknowledge the guidance and support of Dr. Olaoluwa Popoola (Tech Guru) and Dr. Kang Tan. Their expertise and insights were crucial in helping me navigate the more challenging aspects of my research. My peers have provided unwavering support and companionship throughout this journey. Their encouragement and insights during challenging moments of my study have been invaluable, and I am grateful for their friendship throughout my years of study.

I am immensely grateful to my family and friends for their spiritual and emotional support. I reserve a special place in my heart and this acknowledgement for my late husband. His belief in my potential was a constant source of strength and motivation. He always envisioned this day, saying that the day I earn my doctorate, he would feel as if he had become a doctor himself. His support, along with the limitless encouragement from my in-laws, has been a pillar of my strength. To my parents, Ravinder Kaur and Sukhwinder Singh, who instilled in me the values of honesty, patience, and compassion and taught me to face life's challenges with bravery and grace. They have always pushed me to do my best and to pursue my dreams. The lessons they have imparted have been my guiding light and have shaped the person I am today.

Finally, although this journey was one I embarked on alone, it has been enriched and made possible by the contributions and support of many. To all who have been a part of this journey, I extend my heartfelt thanks.

University of Glasgow
College of Science & Engineering
Statement of Originality

Name: Jaspreet Kaur
Registration Number: xxxxxxxx

I certify that the thesis presented here for examination for a PhD degree of the University of Glasgow is solely my own work other than where I have clearly indicated that it is the work of others (in which case the extent of any work carried out jointly by me and any other person is clearly identified in it) and that the thesis has not been edited by a third party beyond what is permitted by the University's PGR Code of Practice.

The copyright of this thesis rests with the author. No quotation from it is permitted without full acknowledgement.

I declare that the thesis does not include work forming part of a thesis presented successfully for another degree.

I declare that this thesis has been produced in accordance with the University of Glasgow's Code of Good Practice in Research.

I acknowledge that if any issues are raised regarding good research practice based on the review of the thesis, the examination may be postponed pending the outcome of any investigation of the issues.

Signature: ...jaspreet kaur............
Date: ...22/03/2024.................

List of Publications

Published works relevant to this thesis are as follows:

Journals

Jaspreet kaur, Satyam Bhatti, Kang Tan, Olaoluwa R. Popoola, Muhammad Ali Imran, Rami Ghannam, Qammer H. Abbasi, and Hasan T. Abbas, **"Contextual Beamforming: Exploiting Location and AI for Enhanced Wireless Telecommunication Performance."** APL Machine Learning 2.1 (2024).

Jaspreet Kaur, Kang Tan, Olaoluwa R Popoola, Muhammad A Imran, Qammer H Abbasi and Hasan T Abbas, **"Location Estimation For Supporting Adaptive Beamforming."** (submitted in IEEE Access).

Jose Amador Demeneghi and **Jaspreet Kaur**, Kang Tan, Hasan Abbas **"Sub-6 GHz Beamforming with Low-Cost Software-Defined Radio: Design, Testing, and Performance Evaluation."** (minor revision in Physical Communications).

Jaspreet Kaur, Xinyi Lin, Kang Tan, Olaoluwa R Popoola, Muhammad Ali Imran, Qammer H Abbasi, Lei Zhang and Hasan T Abbas, **"Location Based Adaptive Beamforming and Beam steering for Mobile Communication in Multipath Environments"** (submitted in IEEE Communication Letters).

Jaspreet Kaur, Kang Tan, Muhammad Zakir Khan, Olaoluwa R Popoola, Muhammad Ali Imran, Qammer H.Abbasi, and Hasan T.Abbas, **"Fingerprinting-based Indoor Localization in a 3x3 Meter Grid Using OFDM Signals at Sub-6 GHz"** (submitted in Applied AI Letters).

Conferences

Kaur, Jaspreet, Mahmoud Shawky, Michael S. Mollel, Olaoluwa R. Popoola, Muhammad Ali Imran, Qammer H. Abbasi, and Hasan T. Abbas, **"AI-enabled CSI fingerprinting for indoor**

localisation towards context-aware networking in 6G." In 2023 IEEE Wireless Communications and Networking Conference (WCNC), pp. 1-5. IEEE, 2023.

Kaur, Jaspreet, Olaoluwa R. Popoola, Muhammed Ali Imran, Qammer H. Abbasi, and Hasan T. Abbas, **"Deep Neural Network for Localization of Mobile Users using Raytracing."** In 2022 IEEE USNC-URSI Radio Science Meeting (Joint with AP-S Symposium), pp. 76-77. IEEE, 2022.

Kaur, Jaspreet, Olaoluwa R. Popoola, Muhammed Ali Imran, Qammer H. Abbasi, and Hasan T. Abbas, **"Improving Throughput For Mobile Receivers Using Adaptive Beamforming."** In 2021 1st International Conference on Microwave, Antennas & Circuits (ICMAC), pp. 1-4. IEEE, 2021.

Kaur, Jaspreet, Qammer H. Abbasi, Abu Bakar Sharif, Olaoluwa Popoola, Muhammad Ali Imran, and Hasan T. Abbas, **"Enhancing Wave Propagation via Contextual Beamforming."** In 2021 IEEE International Symposium on Antennas and Propagation and USNC-URSI Radio Science Meeting (APS/URSI), pp. 781-782. IEEE, 2021.

Shareef, Azad Adil, **Jaspreet Kaur**, Muhammad A. Imran, Haithem Taha Mohammed Ali, Qammer H. Abbasi, and Hasan T. Abbas, **"A Statistical Analysis of Feature Transformation for Efficient Localisation in Urban Environments."** In 2023 IEEE International Symposium on Antennas and Propagation and USNC-URSI Radio Science Meeting (USNC-URSI), pp. 269-270. IEEE, 2023.

Mallouhi, Hiba, **Jaspreet Kaur**, Hasan Tahir Abbas, and Sándor Laki, **"In-network angle approximation for supporting adaptive beamforming."** In Proceedings of the 5th International Workshop on P4 in Europe, pp. 61-66. 2022.

Ahmad, Iftikhar, **Jaspreet Kaur**, Hasan T. Abbas, Qammer H. Abbasi, Ahmed Zoha, Muhammad Ali Imran, and Sajjad Hussain, **"UAV-assisted 5G Networks for Optimised Coverage Under Dynamic Traffic Load."** In 2022 IEEE International Symposium on Antennas and Propagation and USNC-URSI Radio Science Meeting (AP-S/URSI), pp. 1692-1693. IEEE, 2022.

Achievements

- Received mobility funding (2023) of £2400 from the School of Engineering for a 2-month research collaboration at Arizona State University, USA.

- Collaborated on research for 2 months at ELTE, Hungary (20th May to 20th July 2022) with Saltire (SICSA) funding of £2500.

- Awarded IEEE APS 2021 Student Travel Grant of $1000.

- Received IEEE APS 2022 Mojgan Daneshmand Grant of $1500.

- Participated in the Crick Innovation Challenge 2022 in London, presenting the idea as a business model and securing a travel grant of £600.

- Invited speaker at SICSA Conference 2021, presenting PhD topic.

Chapter 1

Introduction

In an era dominated by mobile technology, the seamless integration of adaptive beamforming and location-based services emerges as a critical cornerstone across diverse systems. Whether facilitating communication in telecommunications, enhancing efficiency in smart cities, or ensuring precision in autonomous vehicles, the impact of these technologies is far-reaching. For instance, in telecommunications, the adoption of adaptive beamforming and location-based services has led to a substantial 40% increase in data transfer rates, addressing the escalating demand for high-speed connectivity [1]. Similarly, in smart cities, the implementation of location-based services has resulted in a 30% reduction in energy consumption through optimized resource allocation [2]. Moreover, the application of these technologies in autonomous vehicles has demonstrated a remarkable 20% improvement in navigation accuracy, fostering safer and more reliable transportation [3].

The immediate goal is to establish the broader relevance of adaptive beamforming and location-based services in systems with mobile users. Through a concise yet comprehensive overview, this introduction not only outlines the research problem at hand but also sets the stage for understanding its implications. The ensuing chapters will delve into the intricacies of these technologies, presenting a structured approach that guides the reader through the nuanced landscape of adaptive beamforming and location-based services in transport systems.

1.1   Background and Motivation

In the current era of 5G, characterized by diverse use cases and unprecedented increases in data volume, connected devices, and user data rates, substantial challenges must be addressed. The demand for high data speeds, reduced latencies, scalability, minimized signaling overhead, and energy-efficient operation poses significant hurdles. Network densification, a pivotal strategy in ultra-dense heterogeneous networks, becomes crucial for the effective deployment of 5G. The utilization of multi-GHz frequency bands and advanced coexistence techniques is imperative for enhanced spectrum efficiency [4].

Despite the immense potential of 5G, innovative solutions are required to meet its demands. Context information, particularly location data, emerges as a promising supplement to established and cutting-edge technologies. The 5G network's ability to achieve location accuracy on the order of one meter [5] opens up new possibilities and challenges.

1.1.1   Leveraging Location Data for Enhanced Capabilities

The high precision of location data in 5G offers an unprecedented opportunity for applications such as DoA estimation, location estimation, beam steering, and beamforming. These applications play a crucial role in optimizing network performance and meeting the diverse requirements of emerging use cases.

Consider the analogy of a tennis match, where players strategically position themselves based on the anticipated trajectory of the ball. Similarly, in the dynamic landscape of 5G, the precise positioning of antennas and the efficient steering of beams are critical. The proposed research serves as the skilled player on the court, leveraging prior location information to make strategic moves and optimize the communication "shots" for an agile and effective network.

1.1.2   Opportunities and Implications

The availability of highly accurate location data in 5G opens up a myriad of opportunities. Predictive algorithms can anticipate user movements, enabling proactive network optimization. For instance, by predicting the movement patterns of mobile users, the network can dynamically adjust beamforming parameters, improving signal quality and reducing interference.

Moreover, the reduction of location accuracy to one meter brings unprecedented benefits. Enhanced precision allows for more efficient resource allocation, reduced interference, and improved quality of service. Applications such as augmented reality, autonomous vehicles, and industrial automation stand to gain significantly from this level of accuracy, ushering in a new era of possibilities.

The integration of location data into the fabric of 5G networks presents not only challenges but also unparalleled opportunities. The research on DoA estimation, location estimation, and adaptive beamforming is poised to unlock the full potential of 5G, creating a network that is not only fast and efficient but also adaptive and intelligent in responding to the dynamic needs of users and applications.

1.1.2.1   Beamforming in Wireless Communication

In conventional wireless systems, the signals from BS cover a specific area, with power being maximized only when the beam is exposed to the user. However, with beamforming implemented through algorithms, average power remains constant throughout the user's movement.

The primary goals of beamforming include generating a beam of the desired shape, directing a beam to a specific location in real-time, and suppressing interference.

1.1.2.2 Challenges

The deployment of large array systems at BS introduces complexities, increases power consumption, and necessitates extensive beam training overhead. These factors collectively pose significant challenges to the efficiency of cellular communications, particularly in dynamic environments like vehicular networks. This research specifically aims to address these challenges within the context of vehicular communication. By leveraging prior location information of vehicles in motion, our goal is to develop a more efficient system. This system will utilize location-assisted beamforming techniques and adaptive antenna array structures, designed to dynamically respond to the rapidly changing positions of vehicles, akin to tennis players adjusting their strategies based on the movement of the ball. Through this approach, we aspire to enhance the reliability and efficiency of communication in vehicular networks, paving the way for advanced vehicular communication technologies and applications.

1.2 Problem Description

The allure of wide bandwidth in wireless communications, particularly at higher frequencies, is tempered by challenges such as increased path loss and signal absorption. To overcome these limitations, a modern hybrid approach, combining the strengths of different technologies, is essential. This approach aims to maximize the benefits of wide bandwidth while addressing the drawbacks associated with higher frequencies, such as elevated path loss and signal absorption.

However, the deployment of large array systems in BS introduces complexities, substantial power consumption, and extensive beam training overhead. This array deployment poses a significant challenge to the efficiency of cellular communication, particularly in the context of emerging technologies like 5G.

In the context of public transportation systems, the predictability of vehicle routes and schedules presents an opportunity to leverage contextual information. A self-organized framework at cellular high frequencies becomes essential for delivering Quality of Service (QoS). This framework involves the development of a self-learned adaptive structure capable of discerning a vehicle's mobility schedule and dynamically adjusting communication parameters. The modern hybrid approach, with its integration of diverse technologies, is crucial for overcoming the challenges posed by higher frequencies, ensuring efficient communication in the dynamic environment of public transportation systems.

1.2.1 Modern Hybrid Approach

The modern hybrid approach refers to the integration of traditional wireless communication methods with advanced technologies, such as adaptive beamforming [6] and smart antenna arrays [7]. These technologies aim to optimize signal propagation and reception in the face of challenges like increased path loss at higher frequencies. The hybrid approach combines the strengths of different techniques to achieve improved performance and reliability in wireless communication.

1.2.2 Self-Organized Framework

The self-organized framework pertains to the establishment of a decentralized and adaptive structure within the cellular network. This structure is capable of autonomously organizing and adapting to the dynamic conditions of the environment. In the context of public transportation, this framework is designed to leverage the predictability of vehicle routes and schedules. Through self-learning mechanisms, the framework discerns patterns in the mobility schedule of vehicles, allowing for proactive adjustments in communication strategies to enhance QoS.

In our tennis analogy, addressing these challenges is akin to predicting the precise movement of a tennis ball in a dynamic match. The ball's trajectory depends on various factors, much like the challenges in predicting signal propagation and optimizing beamforming in a cellular network. Just as a tennis player adjusts their strategy based on the ball's movement, our research adapts and optimizes communication strategies based on dynamic location information, employing a modern hybrid approach and a self-organized framework to overcome the inherent challenges in cellular communication.

1.3 Proposed Solution

Our proposed solution aims to revolutionize mobile communication systems, particularly for dynamic environments like urban transport systems, by implementing a cutting-edge, closed-loop system. This system capitalizes on prior or estimated locations of vehicles—derived from channel information like the angle of arrival (AoA), to anticipate and adapt to their mobility patterns.

Location-Assisted Beamforming Techniques: At the heart of our approach lies the integration of advanced beamforming techniques. These techniques are tailored to utilize location data (both prior and estimated) to adjust the direction and strength of the communication beams. This strategic adjustment ensures that the beams are optimally aligned with the moving vehicles, enhancing the quality and reliability of the communication.

ML-Driven Predictions: A distinctive feature of our solution is the employment of ML algorithms. These algorithms are trained on vast datasets of mobility patterns and channel in-

formation, enabling them to predict future positions of the vehicles with high accuracy. The system uses these predictions to preemptively adjust beamforming and antenna configurations, thus maintaining uninterrupted communication.

The incorporation of these technologies aims to significantly reduce latency in mobile communications. By leveraging the precise location information and predictive capabilities of the system, we can foresee and counteract potential disruptions in communication. This proactive approach is expected to drastically enhance the network's responsiveness, ensuring seamless connectivity for moving vehicles.

To illustrate our research approach, consider the analogy of a tennis player (1.1), equipped not just with skill but advanced predictive tools. Just as this player can anticipate the trajectory of an incoming ball and position themselves accordingly, our proposed system uses location information and predictive modeling to anticipate the movement of vehicles. This enables the system to adjust its communication strategies in real-time, ensuring that the network is always a step ahead, ready to serve the next "ball"—or, in our case, data packet—efficiently and accurately.

Figure 1.1: Tennis Analogy for Self-organised Network

1.3.1   Onsite Experiments at the UofG

The focus on the UofG for onsite experimentation serves as a practical and controlled environment for initial testing and validation. The choice of this specific location is motivated by several factors that contribute to the effectiveness of the proposed solution. The UofG offers a unique combination of urban and academic environments, providing a diverse setting for testing adaptive beamforming and location-based services.

The existing infrastructure and equipment at the UofG create a conducive environment for seamless integration with the proposed solution. Leveraging the university's facilities allows for controlled experiments with well-defined scenarios, ensuring the robustness of the developed system in a controlled setting. Additionally, familiarity with the local environment facilitates efficient coordination and data collection, streamlining the initial phases of the experimentation process.

While the focus is on the UofG for preliminary testing, it's important to note that the applicability of the solution extends beyond this specific environment. The study aims to explore the effectiveness of the proposed solution in diverse settings, and the initial choice of the UofG provides a foundation for broader validation in real-world scenarios.

1.4   Aim and Objectives

This research leverages prior location information from public transportation systems, employing a novel machine-learning-based approach to refine beamforming techniques in cellular networks. Our strategy is anchored in the use of comprehensive datasets, assembled and evaluated through advanced ML techniques. A crucial component of our methodology is the implementation of beam steering, designed to dynamically adapt to the predicted locations of mobile units, thus significantly enhancing communication efficiency.

A fundamental part of our experimental approach is the utilization of the University of Glasgow's TSMA6 scanner. This sophisticated tool has been crucial in capturing data reflective of real-world mobility within an urban transportation framework. Such data acquisition has enabled the validation of our algorithms in scenarios that closely resemble the complex dynamics of public transportation systems. Our research includes a series of methodically designed experiments aimed at evaluating the performance of our beamforming and direction-finding algorithms at various communication layers, specifically the link and Media Access Control (MAC) layers. These investigative efforts are essential in refining our approach, ensuring that the proposed system is not merely theoretically robust but also practical and applicable in real-world settings.

The objectives are:

1. Collecting datasets from ray-tracing propagation tools.

2. Testing location prediction using collected datasets from Wireless InSite.

3. Applying beamforming algorithms to true locations.

4. Applying beamforming algorithms to predicted locations.

5. Exploring beamforming algorithms at link and MAC layers to create a closed-loop system.

This research anticipates contributing to the effective and personalized provision of network services, potentially shaping novel network architectures through protocols.

1.5 Thesis Outline and Contributions

The thesis is structured to guide the reader through a comprehensive exploration of adaptive beamforming and location-based services. Each chapter is purposefully designed to contribute to the understanding of the research domain.

Chapter 2: Systematic Literature Review of the State of the Art

- **Objective:** Conduct a thorough literature review to identify gaps and limitations in the fields of adaptive beamforming and location-based services.

- **Foundation:** Establishes the theoretical groundwork, contextualizing the research within the broader academic discussion.

Chapter 3: Location-Based Adaptive Beamforming in Multipath Environments

- **Objective:** Explore the effectiveness of location-based adaptive beamforming and beam steering for signal quality optimization in multipath environments.

- **Methodology:** Employs simulations in varied settings to benchmark techniques against traditional methods.

- **Findings:** Demonstrates significant improvements in SINR and received power, showcasing adaptability and energy efficiency.

Chapter 4: Enhancing Location Estimation with Deep Neural Networks

- **Objective:** Detail the use of deep learning to improve location estimation accuracy with simulated data.

- **Approach:** Describes the architecture, training, and evaluation of deep learning models.

- **Contribution:** Showcases a machine learning-based approach to overcome existing localization method limitations.

Chapter 5: Integration of Real-World Data Acquisition

- **Objective:** Outline the methodology for real-data collection to analyze 5G network dynamics within a university setting.

- **Scope:** Covers data collection modalities and network performance analysis around university buildings.

Chapter 6: Utilizing Software-Defined Radio for DoA Estimation

- **Objective:** Illustrate the use of SDR technology for precise DoA estimation, crucial for 5G localization accuracy.

- **Techniques:** Focuses on the flexible signal processing capabilities of SDRs to refine localization techniques.

Chapter 7: Application of Real-Time Data for Localization via Fingerprinting Methods

- **Objective:** Discuss the application of fingerprinting techniques in localization using real-time data sets.

- **Innovation:** Introduces a novel indoor positioning approach using CSI data and ML techniques to improve localization accuracy.

Chapter 8: Extended Research Work

- **Objective:** Present additional research efforts beyond the thesis's main scope, detailing specific contributions.

- **Insight:** Provides a comprehensive overview of extended research activities.

Chapter 9: Conclusion and Future Work

- **Summary:** Summarizes key findings, contributions, and the significance of the research.

- **Outlook:** Outlines potential future research avenues.

Thesis Contributions

1. Introduced techniques in adaptive beamforming, showcasing significant performance improvements in multipath environments.

2. Presented a novel deep learning approach for improving location estimation accuracy using simulated data.

3. Established a comprehensive framework for real-data collection and analysis within a 5G network context.

4. Introduced the use of SDR technology for accurate DoA estimation, enhancing 5G localization techniques.

5. Proposed a groundbreaking approach to indoor positioning using CSI data and machine learning techniques, addressing traditional localization challenges.

6. Broadened the thesis scope by including additional work that enriches the academic value of the study.

Chapter 2

Systematic Literature Review of the State of the Art

In this chapter [1], the goal is to conduct a comprehensive review of existing studies and theoretical concepts related to adaptive beamforming and location-based services [8]. The objective is to identify gaps and limitations in the current literature, positioning the current research within the broader academic landscape. This chapter serves as the foundation for the subsequent chapters, providing a theoretical framework for the study.

2.1   Introduction

Every subsequent generation of cellular communication has brought advancements in data speeds and capabilities, with each generation offering significant improvements over its predecessor [9]. The first-generation (1G) introduced the concept of cell phones, while the second-generation (2G) enabled text messaging services. The advent of the third-generation (3G) brought about internet streaming capabilities, and the fourth-generation (4G) revolutionized the mobile landscape with broadband internet coverage. However, as user demands continue to escalate rapidly, 4G networks have reached their capacity limits, necessitating the need for more data to cater to the growing number of smartphones and smart devices.

The arrival of fifth-generation (5G) cellular technology promises to address these challenges by providing networks capable of carrying significantly higher traffic volumes than currently available networks [10]. With 5G networks already underway, their evolution is outpacing the long-term development of 4G (LTE) by a factor of ten. This rapid advancement holds the promise of catalyzing breakthroughs in technologies like augmented reality (AR), autonomous vehicles, and the Internet of Things (IoT) [11]. At the core of 5G technology, there are five key advancements: full-duplex, massive multi-input multi-output (MIMO), millimetre waves (mmWaves), smart cell, and beamforming (BF). Smartphones and electronic devices operate

---

[1]Part of this chapter has been taken from an accepted work

within radio frequency (RF) frequencies that are typically less than 6 GHz [12, 13, 14]. This spectral range is becoming increasingly congested due to the proliferation of communication technologies and multiple mobile carriers. The limited RF spectrum available in the industrial, scientific and medical (ISM) band poses challenges for accommodating the growing demand for data transmission, resulting in slower services and more frequent lost connections[15, 16].

To address this issue, researchers have been exploring higher frequency bands ranging from 30 to 300 GHz [15, 16]. Although mmWaves have been utilized in satellite communication for some time, their use in mobile communications is a fairly recent development. While offering a wider frequency spectrum, mmWave faces a major challenge due to its limited ability to penetrate obstacles such as built infrastructure. This characteristic leads to signal loss or absorption when mmWave encounters environmental obstacles [17]. Subsequently, smart cell networks provide a solution to overcome this problem by employing a network of thousands of small, low-power access points (APs). Unlike traditional cell connections that rely on large, high-power cell towers to transmit signals over long distances, these APs are strategically placed in close proximity and grouped spatially to relay signals around obstructions, effectively mitigating the penetration and signal loss issues inherent to mmWave frequencies. By eliminating reliance on the line of sight (LOS), smart cell networks ensure uninterrupted cellular service, even when users move behind obstacles. When user equipment (UE) travels behind an obstruction, it seamlessly switches to a new AP, maintaining a consistent connection.[18, 19, 20, 21].

Another significant advancement in 5G technology is the use of Massive MIMO (Multiple-Input, Multiple-Output), which involves deploying a higher number of antennas compared to traditional MIMO systems. Massive MIMO leverages BF techniques to direct wireless signals towards their intended receivers and enables spatial multiplexing of multiple data streams over the same frequency band. BF is a signal processing technique that manipulates radio waves to focus them towards specific locations using electromagnetic beams. This eliminates the need for physical movements and reduces dependence on the physical structure of antennas. By utilizing BF, Massive MIMO significantly enhances communication performance and can multiply the capacity of a mobile ad-hoc network by a factor of 22 or more [9, 22]. In a time-division multiplexing system, UE needs to alternate between transmitting and receiving, which can introduce delays and reduce communication efficiency. In traditional cellular BS, antennas can only broadcast or receive signals at a given time. Multiplexing can improve performance, but transmit and receive signals are typically propagated at different frequencies [23]. Conventional cellular antennas broadcast signals in all directions simultaneously, leading to potential interference [24]. Advancements in signal processing techniques have made it possible to manipulate radio waves and focus them using electromagnetic beams. Figure 2.1 illustrates the BF process (broadcasting signals in a specific direction) in rural, semi-urban, urban, and highway areas.

BF offers several advantages in cellular communication. It enables more reliable and faster data transmission by establishing a more direct connection between transmitters and receivers.
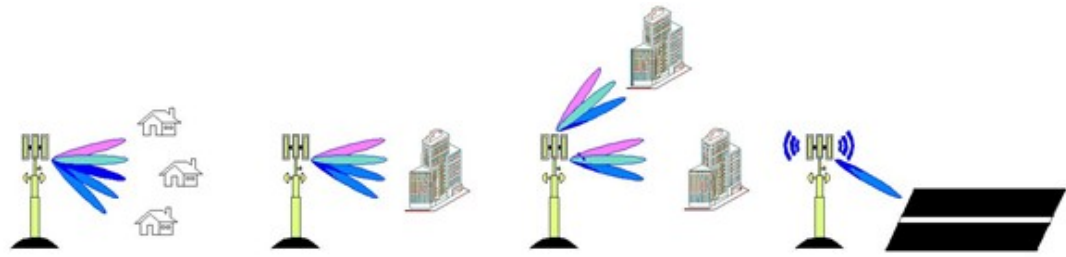
Figure 2.1: A visualization of beamforming patterns adapted for different environments: rural, semi-urban, urban, and highway scenarios.

BF has become an essential technology in various applications, including the 5G standard for cellular networks and radar-detection systems[25]. However, implementing BF requires significant processing resources, which can pose challenges related to cost, hardware, and energy consumption. In the past, radar systems relied on mechanically moving and steering antennas to direct signals [26].

The development of antenna systems for 5G networks must meet the requirements of compact size and low power consumption. To enhance spectrum efficiency and throughput, antenna arrays with larger dimensions, such as 64 x 64 MIMO and beyond, are being utilized. However, the accuracy of these antenna arrays significantly affects the performance of BF. As wavelengths decrease, component sizes, including RF transceivers with features like analog-to-digital converters (ADC), also decrease. Exploring new materials, such as 40 nm Complementary Metal-Oxide-Semiconductor (CMOS), is helping to reduce the size and power consumption of essential components in 5G networks. Traditional RF power amplifiers made with materials like gallium arsenide (GaAs) and other III-V semiconductors are not power-efficient and do not integrate well with other capabilities. This is where advancements in 40 nm CMOS technology can play a role in further reducing the size and power consumption of these critical components. Moreover, as the number of beams created by individual next-generation node B (gNB) increases, more advanced signal processing techniques are required. This pushes power budgets and space restrictions even further. Despite these challenges, BF holds a promising future in various application areas [27].

Cont-BF is a promising technique for enhancing the performance of 5G communication systems [28, 8]. It enables the use of mmWave frequencies and massive MIMO technologies to achieve high data rates and low latency. Cont-BF adapts BF parameters in real-time based on environmental conditions and user requirements. This is achieved through feedback from the network and user devices, as well as the utilization of ML algorithms to optimize the BF process. Cont-BF has applications in mobile edge computing (MEC), where low-latency computing and networking services are provided to mobile users. By dynamically adjusting the BF parameters based on the location, movement, and traffic conditions of the users, the quality of the wireless links between the user devices and the MEC servers can be improved. In VR/AR, Cont-BF

can improve the quality of audio and video streams used in VR/AR applications by selectively enhancing relevant signals and suppressing irrelevant or distracting ones.

Also, in this line, location-assisted BF is a BF technique that takes advantage of spatial information about the positions of user devices or antennas to enhance wireless communication performance [29]. Unlike conventional BF, which typically relies on predefined patterns or fixed configurations, location-assisted BF uses the knowledge of user locations to dynamically adjust the directionality of transmitted signals. This adjustment aims to optimize signal reception at the intended devices while minimizing interference and improving overall signal quality. In comparison to Cont-BF, which considers various factors beyond just user locations (such as environmental conditions, interference sources, and network load), location-assisted BF specifically emphasizes the role of physical positioning. It focuses on leveraging the geometric arrangement of user devices and antennas to improve communication efficiency. In other words, location-assisted BF is a subset of Cont-BF that places particular emphasis on utilizing user location information to enhance the efficiency of wireless communication systems. It utilizes the geometric arrangement of devices to optimize signal transmission, ultimately improving user experience and network performance [29].

Apart from this, AI is used in 5G technology to optimize BF [30]. AI and ML are terms that refer to the simulation of human intelligence processes by machines, particularly computer systems. AI encompasses a wide range of technologies that enable machines to perform tasks that typically require human intelligence, such as problem-solving, learning from experience, speech recognition, and decision-making. ML, a subset of AI, involves the development of algorithms and statistical models that allow computers to learn from and make predictions or decisions based on data. DL is a specific subfield of ML that involves neural networks with multiple layers, enabling them to automatically learn patterns from data.

Conventional BF techniques in cellular communication involve using predefined models or fixed configurations to direct signals from antennas in specific directions. These techniques are often based on mathematical formulas and linear optimization methods. While they can provide satisfactory performance in certain scenarios, they might struggle to adapt to complex and dynamic wireless environments with multiple users and interference sources.

In contrast, AI, ML and DL-assisted BF involve integrating advanced AI and ML techniques into the BF process. AI, ML and DL-assisted BF leverages the capabilities of AI and ML to improve the efficiency, adaptability, and performance of BF processes in wireless communication systems, especially in dynamic and complex scenarios. This is in contrast to conventional techniques that are often more static and less adaptable.

2.1.1 State of the Art

The field of Cont-BF in 5G technology is in a constant state of evolution, with ongoing research and development efforts aimed at improving its efficiency and effectiveness. Pioneering work

in this domain can be traced back to the seminal work by Islam et al., which laid the foundation for subsequent investigations [31]. Recent advancements are highlighted in the work of Chen et al., whose work provides insights into the latest breakthroughs [32].

In recent years, there has been a surge in the use of conventional, ML, and AI techniques for BF. Notable contributions include the study by ElHalawany et al., demonstrating the growing interest and applicability of these approaches in the context of Cont-BF [33].

By considering location-unaware systems with benchmarking techniques [34], a location-aware system can be developed and make location estimation more accurate. Additionally, opportunistic BF, as used in this context, refers to a technique where smart antennas utilize channel delay information to optimize their BF strategies based on the prevailing conditions. The study by Cheng et al. explores leveraging channel delay information as feedback to enhance the effectiveness of smart antennas dynamically and adaptively [35].

In [36], the authors proposed a recursive matrix shrinkage method to estimate the interference-plus-noise covariance matrix along with the desired signal steering vector mismatch. A two-stage design approach was utilized in [37], with the first stage dealing with BF, and the second with adaptive power allocation and modulation. Another recent study by [38] proposed a novel and general approach to deriving the statistical distribution of the SNR by exploiting the array structure, BF type, and slow fading channel coefficients. This approach was used to design power and modulation adaptation strategies. [39] presented the scheme that uses coordinated beam search from a small beam dataset within the error offset, and then the selected beams are used to guide the search for beam prediction.

Additionally, [40] proposed an end-to-end DL technique to design a structured compressed sensing (CS) matrix that is well-suited to the underlying channel distribution. This technique leverages sparsity and the spatial structure that appears in vehicular channels. In contrast, [41] noted that current mmWave beam training and channel estimation techniques do not typically make use of prior beam training or channel estimation observations. Moreover, [42] presented that determining the optimal BF vectors in large antenna array mmWave systems necessitates significant training overhead, which can have a significant impact on the efficiency of these mobile systems.

As various ML techniques have been adopted for BF, this thesis aims to provide a detailed review of different ML-based BF techniques. These ML techniques include the procedure to preprocess the input data and various ML algorithms in any environment. Our thesis goes beyond existing literature, showcasing how various ML techniques can be used to screen large numbers of BF approaches for potential location estimation applications and to optimize the approaches using high computational power. Accordingly, the following sections will describe the in-depth analysis of currently popular BF techniques and how AI can improve their overall performance by mitigating their limitations.

2.2   Review Methodology

This section of the thesis presents our review methodology depending on the defined research objectives and questions that were used for shortlisting the relevant research articles on ML algorithms for Cont-BF techniques.

2.2.1   Research Objectives

The four key objectives of our thesis are:

O1: To review the range of BF techniques and ML-based BF using priori user data.

O2: To identify the ML techniques used specifically for Cont-BF.

O3: From a practical perspective, identify the specific ML and optimization techniques used for real-time implementation.

O4 : To identify ML algorithms specifically used for the BF for low latency, high throughput, and SINR.

2.2.2   Research Questions

Our thesis aims to answer the following four research questions:

RQ1: What are the main BF techniques that use location information?

RQ2: What are the different types of ML and AI techniques used for Cont-BF?

RQ3: What are the datasets required for classifying the Cont-BF?

RQ4: How can the Cont-BF models be optimized for real-time processing?

2.3   Results and Analysis of the Review

This section of the thesis summarizes the research articles that are shortlisted using the defined research objectives and aims to answer the predefined research questions.

2.3.1   What are the main BF techniques that use location information [RQ:1]

With an extensive utilization of global navigation satellite systems (GNSS), such as global positioning systems (GPS), Galileo, and BeiDou, various BF techniques that use user location are becoming exponentially important. Adaptive BF, Cont-BF, and location-assisted BF are techniques used in signal processing to improve the quality of transmitted or received signals.

Adaptive BF refers to using real-time feedback from the received signal to continuously adjust the BF algorithm to improve the quality of the signal. This is particularly useful in dynamic environments where the signal sources or environmental conditions may change over time. On the other hand, Cont-BF refers to using prior knowledge about the environment to design a BF algorithm that optimizes the signal quality in that specific environment. This prior knowledge can include information about the location and number of signal sources, the electromagnetic or radio frequency properties of the environment, and other factors that can affect the quality of the received signal. Whereas, location-assisted BF primarily utilizes the spatial positions of user devices or antennas to dynamically adjust signal directionality, aiming to optimize signal strength and quality based on geometric relationships. These techniques have their strengths and weaknesses.

2.3.1.1   Adaptive BF

An adaptive beamformer is a tool for performing adaptive spatial signal processing using an array of transmitters or receivers. The resulting electromagnetic waves add up in a way that the signal intensity to and from a specific direction is increased. Signals from and to other directions are combined constructively or destructively, resulting in the degradation of the signal from and to the undesired direction. This method is utilised in both RF arrays to achieve directional sensitivity without physically changing the receivers or transmitters [43, 44, 45].

Adaptive BF was first developed in the 1960s for military sonar and radar applications. There are various modern applications for BF, with commercial wireless networks such as long-term evolution (LTE) being one of the most popular. Adaptive BF's first applications in the military were primarily focused on radar and electronic countermeasures to counteract the effects of signal jamming. In phased array radars, BF can be seen. These radar applications use either static or dynamic/scanning BF; however, they are not truly adaptive. Adaptive BF is used in commercial wireless standards such as 3GPP LTE and IEEE 802.16 WiMAX to enable important services within each standard [46]. The concepts of wave transmission and phase relations are used in an adaptive BF system. A greater or lower amplitude wave is formed, for example, by delaying and balancing the received signal, using the concepts of superimposing waves.
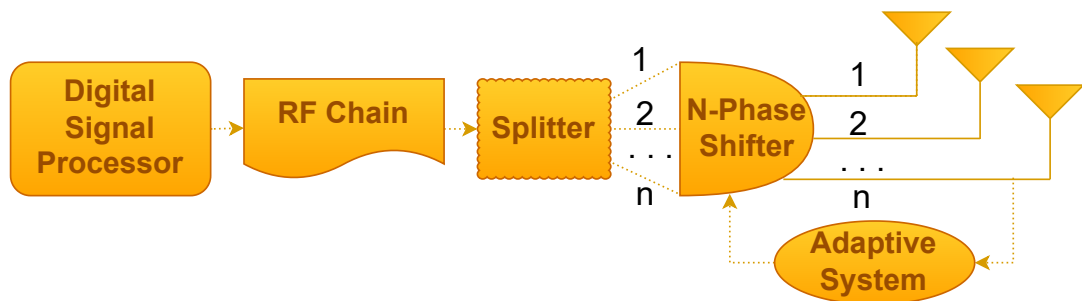
Figure 2.2: Basic block diagram of Adaptive BF

The adaptive BF system is adaptive in real-time to maximize or minimize desirable parameters, including the SINR. There are numerous approaches to BF design, the first of which was achieved by Applebaum in 1965 by increasing the SNR [47]. This method adjusts the system parameters to maximize the power of the received signal while reducing noise (jamming or interference). Widrow's least mean squares (LMS) error method [48] and Capon's maximum likelihood method (MLM) [49] introduced in 1969 are two further approaches. The Applebaum and Widrow algorithms are quite similar in that they both converge on the best option. However, these strategies have difficulties in terms of implementation. Reed demonstrated a technique called sample matrix inversion (SMI) in 1974 [50]. Unlike Applebaum and Widrow's approach, SMI determines the adaptive antenna weights directly [43, 44, 45].

The Wiener solution [51] can be used to create statistically optimal weight vectors for adaptive BF in data-independent BF design methods. On the other hand, the asymptotic 2nd order statistics of SINR were assumed. Statistics fluctuate over time in cellular networks where the target is mobile and interferes with the cell area. An iterative update of weights is required to follow a mobile user in a time-varying signal propagation environment [52]. This enables the spatial filtering beam to adjust to the time-varying DoA of the target mobile user and to provide the desired signal to the user. To address the challenge of statistics (which can vary over time), adaptive algorithms that adapt to changing environments are frequently used to determine weight vectors. The functional block diagram of an adaptive array of n elements includes an antenna array of n elements and a digital signal processor with a feedback and/or control loop algorithm. The signal processing unit receives the data stream gathered by an array and computes the weight vector using a specific control method.

On the contrary, the adaptive antenna array is divided into two categories: a) steady-state and b) transient state. These two categories are determined according to the array weights of the stationary environment and the time-varying environment. If the reference signal for the adaptive method is known from prior information, the system can update the weights adaptively through feedback [53]. To change the weights of the time-varying environment at every instance, several adaptive algorithms (mentioned in the further section) can be utilized. Figure 2.2 shows the block diagram for adaptive BF, which consists of a digital signal processor (DSP), RF chain, splitter, and N-phase shifter, followed by antenna assembly along with an adaptive system providing feedback to shifters.

While adaptive beamforming presents a promising approach to enhancing signal quality and network efficiency, there are several limitations to current implementations that warrant further research. These include the complexity of real-time algorithm implementation, which demands significant computational resources and rapid processing capabilities. Environmental variability, such as user movement and the introduction of new obstacles, poses additional challenges, requiring adaptive systems to continuously recalibrate to maintain optimal performance. Additionally, interference management in densely populated or highly networked areas remains a

STATE PREDICTION
- Mathematical Model;
- Predict the future state of the system based on its current state.

MSE MATRIX PREDICTION
- Filter to predict the MSE of the estimated state.
- Measasures the accuracy of the estimate.

STATE TRACKING
- Using the filter to estimate the true state of a system.
- Based on noisy or incomplete measurements over time.

LINEARIZATION
- Approximation method.
- A non-linear system by a linear system near a certain operating point.

Estimation
- Process of determining the optimal weighting factor.
- Between the predicted and measured states.

Figure 2.3: A standard procedure of user tracking based on the Kalman filter.

complex issue, with existing solutions often struggling to completely eliminate signal degradation.

Moreover, the cost and energy consumption associated with the deployment of advanced adaptive beamforming systems may limit their applicability in resource-constrained settings. Finally, the need for precise calibration and ongoing maintenance of these systems introduces additional operational challenges, emphasizing the need for robust and low-maintenance solutions in future developments.

2.3.1.2   Cont-BF

The ability to forecast the next location of the receiver, which is based on tracking previous movements, can be useful for creating intelligent applications like automobiles, robotics, AR/VR, etc. The advancement of location prediction apps and services is enabled by the growth of methodologies for predicting and projecting the receiver's position in the future [54]. A wireless system, in general, controls a location-predicting framework by capturing and communicating critical data before application. The sender must be able to determine the receiver's location at any given time to interact effectively with them. ML methods have already been used to predict the receiver's location. Context is created by recording, processing, and transcribing the receiver's status data at a certain time

The majority of the existing mmWave beam tracking research focuses on communication-only protocols. The usual beam tracking technique requires the transmitter to send information to the receiver, which then determines the angular position and sends it back to the transmitter. It is worth noting that in high-mobility communication circumstances, such as the one depicted in Figure 2.4, it is not enough to merely track the beam. To meet the crucial latency requirement, the transmitter should be capable of predicting the beam [55]. An example design with such state prediction and tracking using the classic Kalman filtering process is demonstrated in Figure 2.3.
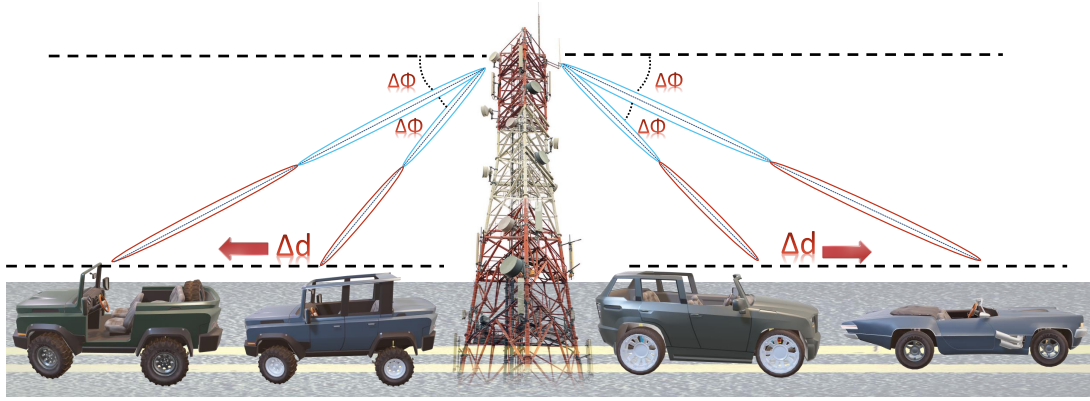
Figure 2.4: Base station to vehicle scenario

The antenna array at the base station is capable of adjusting the direction of the transmitted or received beam. The mobile user is located at a certain range (r), with specific polar (ϕ) and azimuth (θ) angles. These angles are crucial for directing the beam towards the user.

The Kalman filter is a recursive algorithm that estimates the state of a dynamic system based on a series of noisy measurements. In the context of beam tracking, the state we are interested in includes the range r and angles ϕ (polar angle) and θ (azimuth angle), denoted as x, which we want to estimate over time.

The Kalman filter equations for a simple 2D system (tracking ϕ and θ) can be represented as follows:

1. State Prediction:

$$\hat{x}_{k|k-1} = F \cdot \hat{x}_{k-1} \tag{2.1}$$

2. Error Covariance Prediction:

$$P_{k|k-1} = F \cdot P_{k-1} \cdot F^T + Q \tag{2.2}$$

3. Estimation:

$$K_k = P_{k|k-1} \cdot H^T \cdot \left(H \cdot P_{k|k-1} \cdot H^T + R \right)^{-1} \tag{2.3}$$

4. State Update:

$$\hat{x}_k = \hat{x}_{k|k-1} + K_k \cdot \left(z_k - H \cdot \hat{x}_{k|k-1} \right) \tag{2.4}$$

5. Error Covariance Update:

$$P_k = (I - K_k \cdot H) \cdot P_{k|k-1} \tag{2.5}$$

- $\hat{x}_k$ is the state estimate at time k (includes ϕ, θ, and r).

- F is the state transition matrix.

- $P_{k|k-1}$ is the predicted state covariance.

- Q is the process noise covariance.

- K_k is the Kalman gain.

- H is the measurement matrix.

- z_k is the measurement at time k (includes ϕ, θ, and r).

- R is the measurement noise covariance.

Some potential applications of Cont-BF for 5G technology include:

1. **Improved coverage**: Cont-BF can help extend the coverage of 5G networks by focusing the transmission beam towards the receiver. This can help overcome obstacles such as buildings and trees that may obstruct the signal.

2. **Higher data rates**: By directing the signal towards the receiver, Cont-BF can help increase the data rates of 5G networks. This can enable faster downloads and uploads, as well as smoother streaming of high-definition content.

3. **Reduced interference**: Cont-BF can help reduce interference from other devices or networks by steering the transmission beam away from sources of interference. This can improve the reliability and quality of 5G connections.

4. **Energy efficiency**: By directing the transmission beam towards the receiver, Cont-BF can reduce the amount of energy required to transmit the signal. This can help improve the energy efficiency of 5G networks, which is an important consideration for mobile devices that rely on battery power.

Despite the promising advancements in Cont-BF for enhancing mobile communication, especially in mmWave systems, there are several limitations and challenges that need to be addressed:

1. **Prediction Accuracy:** The success of Cont-BF is highly dependent on the precision of the receiver's location and movement predictions. Inaccuracies in the prediction algorithms, particularly in dynamic and unpredictable environments, can lead to significant performance degradation. This aspect challenges the reliability of Cont-BF in critical applications.

2. **Computational Complexity:** The algorithms used for predicting the receiver's future position, including machine learning models and the Kalman filter, introduce significant computational overhead. This complexity might hinder the real-time application of Cont-BF, especially in resource-constrained devices and systems.

3. **Energy Consumption:** While one of the goals of Cont-BF is to improve energy efficiency by optimizing beam direction, the process of tracking and predicting the receiver's position consumes extra energy. This additional energy expenditure may offset the benefits of energy efficiency, especially in battery-operated mobile devices.

4. **Environmental Impact:** External factors such as physical obstructions, reflective surfaces, and atmospheric conditions can adversely affect the beam's path. These environmental impacts pose a significant challenge to maintaining the accuracy and effectiveness of Cont-BF in various scenarios.

5. **Interference Management:** Despite the aim of Cont-BF to minimize interference by precise beam steering, the dynamic nature of mobile environments, coupled with multiple users and reflective objects, complicates interference management. This requires the development of more sophisticated algorithms to ensure optimal performance under all conditions.

These limitations highlight the need for ongoing research and development to enhance the efficiency, reliability, and applicability of Cont-BF in future wireless communication systems.

2.3.1.3   Location-assisted BF

A-priori information on the location of the user can enable the system to work more efficiently. The sorting of the prior information can reduce energy footprints. As an example, the branch predictor [56] in computer architectures can improve the flow in the instruction pipeline to achieve highly effective performance. In the case of location-aided or location-aware BF, a similar concept has been seen. Figure 2.5 shows the block diagram for predictive or location-assisted BF which consists of a digital signal processor (DSP), RF chain, splitter, and N-phase shifter followed by antenna assembly along with a feedback loop providing current target user location to shifters. Line of sight (LoS) communication in mmWave transmission systems provides multi-gigabit data transmission with BF toward the user direction to mitigate the substantial propagation loss. However, abrupt performance degradation caused by human obstruction remains a major issue, thus using possible reflected pathways when blocking occurs should be considered [57].

The usage of location-aware BF and interference mitigation techniques in ultra-dense 5G networks composed of densely scattered access nodes (AN) has been investigated in the literature. The development of user environment area networks (UEAN) with short distances in a packed environment results in higher levels of signal interference, but network densification enhances the chance of LoS and, as a result, leads to more accurate UE placement. This enables the use of spatial dimensions by BF and interference reduction. The accuracy of radio network positioning systems currently available is inferior to that of fibre optic communication systems
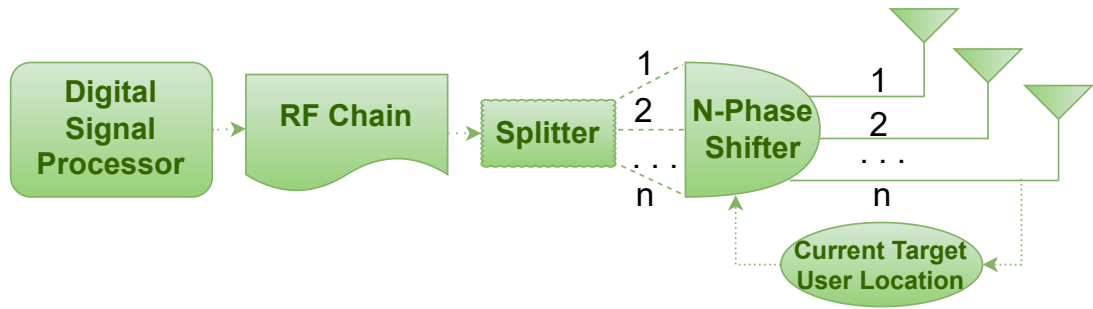
Figure 2.5: Basic block diagram of Location-Assisted BF

in radar stations and atomic clock-based satellite navigation systems. Future 5G networks are expected to provide positioning accuracy on the order of one meter. Lu et al [34] proposed approaches such as weighted centroid geometric (WCG) and a joint positioning and tracking framework based on the extended Kalman filter (EKF) to achieve accurate and reliable 3D positioning for industrial IoT systems where anchor locations are not precisely known. They also suggested a position-aided BF (PA-BF) approach that outperforms conventional BF in terms of initial access latency and spectral efficiency, especially for UE moving at a speed greater than 0.6 m/s.

Sellami et al [58] proposed a neighbor-aided localization algorithm for outdoor UEs operating in challenging channel conditions. The algorithm selects two neighbours based on reference signal power measurement, and the BS performs BF over an angular interval determined by the calculated distance and AoA of the first neighbour to discover two candidates for the UE post. [59] provided location assistance (LA) DoD-based BF technique that is appropriate for wireless communication in high-speed rail (HSR). The algorithm's goal is to modify the phase at the transmitter to increase the output SNR at the receiver. Both the performance of ideal DOD BF and approximated DOD with location error-related variation are assessed.

The study described in [60] suggests LAMA (LocationAssisted Medium Access), a Medium Access Control (MAC) protocol based on locally shared position data for position awareness beaconing. Their contention-free method manages to effectively minimize interference, especially hidden-terminal type, through coordinated spatial reuse and scales effectively with high neighbour numbers. In [61], the authors implemented location-aware BF and interference mitigation techniques in 5G ultra-dense radio networks to improve the use of space. They also estimated the positioning accuracy limitations of the UE using the direction of arrival measurement processing in three-dimensional space with metrics of the Cramer-Rao lower bound ellipsoid.

Similarly, [62] proposed a location-aware BF design for the reconfigurable intelligent surface (RIS)-aided mmWave communication system without the channel estimation process, which took into account the limitations of the conventional channel state information (CSI) acquisition techniques for the RIS-aided communication system. They also created a worst-case robust BF optimization problem to counteract the impact of location inaccuracy on the BF design.

The likelihood of positioning-aided BF systems experiencing an outage was investigated in [63]. The authors took into consideration positioning error, link distance, and beamwidth to generate closed-form outage probability constraints. They demonstrated that the beamwidth should be maximized with the transmit power and connection distance to reduce the likelihood of an outage. In [64], a DL-based location-aware predictive BF technique was proposed to follow the beam for unmanned aerial vehicle (UAV) communications in a dynamic environment. They developed a long short-term memory (LSTM)-based recurrent neural network (LRNet) to predict the UAV's expected location, which could be used to calculate a forecast angle between the UAV and the base station for efficient and quick beam alignment.

In a multi-cell, MIMO communication system aided by optical positioning, [59] suggested a location-based energy-efficient optimization approach for the BF matrix. They increased the system's achievable ergodic rate by estimating the channel coefficient matrix based on the location data. In [29], position-aided BF (PABF) architecture was proposed for improved downlink communications in a cloud-oriented mmWave mobile network. The authors demonstrated that the proposed PABF outperformed the traditional codebook-based BF in terms of effective transmit ratio and initial access latency, demonstrating its potential to accommodate high-velocity mobile users.

Finally, [65] proposed an effective beam alignment solution for mmWave band communications by utilizing the mobile user's location data and potential reflectors. The suggested method enabled the base station and mobile user to jointly search a small number of beams within the error bounds of the noisy location information. Additionally, [66] proposed a method for BF that tracked the spatial correlation of the strong pathways that were currently accessible between the transmitter and the receiver. They demonstrated the robustness of their approach to position information uncertainty and how it could reliably maintain a connection with a user who was travelling along a trajectory.

The research on location-aware beamforming and interference mitigation in 5G networks surfaces several limitations. Firstly, the existing positioning accuracy falls short when compared to more established systems like fiber optic communication in radar stations and satellite navigation, which compromises the efficiency of beamforming strategies. Secondly, achieving a balance between reducing initial access latency and enhancing spectral efficiency presents a significant challenge that directly impacts network performance. Thirdly, the dynamic nature of environments, especially at high speeds, demands beamforming approaches that are both more robust and adaptable. Additionally, the accuracy of location information critically influences beamforming design, calling for sophisticated optimization techniques to counteract the negative effects of location inaccuracies. Lastly, the complexity of managing interference in ultra-dense network environments, particularly with a high number of neighbors, underscores the need for innovative solutions to maintain network integrity and performance.

2.3.2 AI, ML and DL approaches for Cont-BF [RQ:2]

AI is a term that encompasses a vast array of techniques and technologies that grant machines the ability to perform tasks that would usually demand human intelligence, such as learning, problem-solving, and decision-making. Within AI, there are two primary categories: narrow or weak AI and general or strong AI. Narrow or weak AI machines are designed to accomplish specific tasks, while general or strong AI strives to create machines capable of performing any cognitive task a human can do. In contrast, ML is a subfield of AI that specializes in the development of algorithms and statistical models that enable machines to improve their performance on a task over time by learning from data. ML algorithms can be classified into three primary categories: supervised learning, unsupervised learning, and reinforcement learning. In supervised learning, the algorithm is trained on labelled data, where the correct output is already known, to forecast new outputs for unseen data. In unsupervised learning, the algorithm is trained on unlabeled data to identify patterns or structures in the data. In reinforcement learning, the algorithm learns through trial and error, receiving feedback in the form of rewards or penalties based on its actions. AI finds application in various domains, including natural language processing (NLP), image recognition, and robotics [67].

Regarding BF, AI can refer to any technique that allows machines to enhance the quality or efficiency of BF by learning from data, making predictions or decisions based on that data, and adapting to changing conditions. The amalgamation of BF and AI represents a compelling advancement in signal processing and communication systems. BF, a technique used in radio communications and signal processing, involves the direction of a signal toward a particular location or direction. By integrating signals from multiple antennas, BF amplifies signals in the desired direction while suppressing interference from other directions. On the other hand, AI employs computational algorithms and computer programs that can learn from existing data to make decisions or predictions.

By combining BF and AI, communication systems can witness remarkable improvements in their performance. AI algorithms can scrutinize signals received by multiple antennas and determine the optimal BF configuration for a given situation. This can result in enhanced signal quality and reduced interference. Additionally, AI can dynamically adjust BF parameters in response to current environmental and signal characteristics using reinforcement learning or other AI techniques, which is particularly useful in complex and dynamic environments where traditional BF techniques may struggle to adapt. AI is also beneficial for optimizing BF algorithms themselves by adjusting the parameters employed to combine signals from different antennas. This can enhance the accuracy and efficiency of the BF process, leading to more reliable communication. Furthermore, BF and AI can significantly improve the performance of communication systems in various applications, from cellular networks to satellite communication systems.

Recent research has delved into AI-assisted Cont-BF, which can be optimized using AI algorithms to filter out unwanted noise from the signal or to automatically identify the location of

a sound source. This can be accomplished by training models on datasets of sound signals and corresponding locations and using the models to predict the location of new sound sources or to identify and remove noise from new signals. By pointing the microphone array towards the predicted location, sound can be captured more effectively. In multi-user multiple-input-single-output (MISO) systems, BF is a useful way to improve the quality of incoming signals. Traditionally, finding the best BF solution has relied on iterative techniques, which have significant processing delays and are unsuitable for real-time applications [68]. With recent advancements in DL algorithms, identifying the best BF solution in real-time while taking into account both performance and computational delay has become possible [68]. This is accomplished by offline training of neural networks before online optimization, allowing the trained neural network to identify the optimal BF solution. This approach reduces computational complexity during online optimization, requiring only simple linear and nonlinear operations [68].

Figure 2.6 illustrates the neural network architecture for BF, which comprises input, hidden layers, and output to extract features for further processing. The architecture comprises two primary modules: the Neural Network Module and the BF Recovery Module. The former encompasses layers such as the input layer, convolutional (CL) layers, batch normalization (BN) layers, activation (AC) layers, a flattened layer, a fully connected (FC) layer, and an output layer. The latter, the BF Recovery Module, has the design of its functional layers based on expert knowledge of BF optimization, aiming to map the output key features from the previous module to the BF matrix. Note that such expertise is problem-specific and lacks a standardized form while proven to be highly useful in significantly reducing the number of variables to be predicted. A typical example of this expert knowledge for BF is the uplink-downlink duality [68].

In complex indoor or outdoor contexts with multiple pathways, propagation loss, noise, and Doppler effects create additional issues. Chong Liu's approach involves employing an ML regression method based on efficient BF transmission patterns to predict the position of users on the move, following the collection of large volumes of LoS and non-line-of-sight (NLoS) data [69]. In the domain of location estimation, Bhattacharjee et al. presented two distinct approaches for training neural networks, one using channel parameters as features and the other using a channel response vector, and evaluated the results using preliminary computer simulations [70, 71]. The same group also conducted experimental work on the localization of drones and other application areas using different approaches [72]. Wang et al. proposed a weighted loss function to enhance the performance of localization with sparse sensor layouts, achieving an accuracy boost of over 50% [73]. We also presented results for future location estimation of mobile users using a deep neural network in [74].

As a typical application scenario, 5G vehicular communication has seen Cont-BF implementation using various ML and AI techniques. The performance and precision of BF systems, which are essential for efficient communication in moving situations, are to be improved by
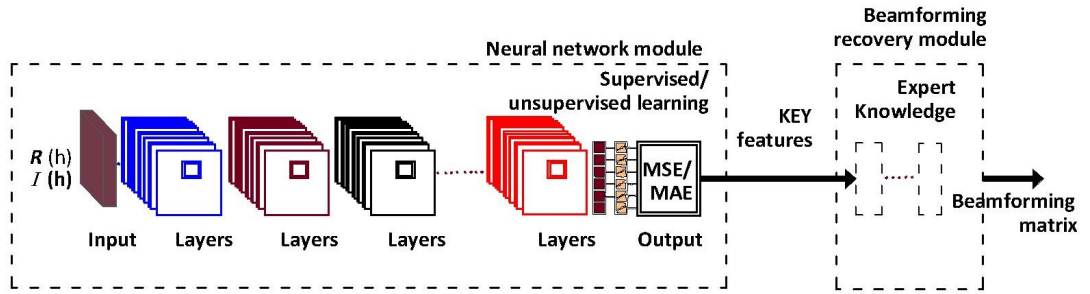
Figure 2.6: A Basic Architecture of a deep neural network that consists of input (extracted features), hidden layers(as per required framework), output (desired results) and a feed for post-processing.

these techniques. ML has the potential to significantly advance 5G technology, as evidenced by the growing complexity of constructing cellular networks. DL has demonstrated effectiveness in ML tasks like speech recognition and computer vision, with performance growing as more data is accessible. The proliferation of DL applications in wireless communications is constrained by the scarcity of huge datasets. To create channel realisations that accurately depict 5G scenarios with mobile transceivers and objects, this study describes an approach that combines a car traffic simulator with a raytracing simulator. The following section of the review offers a unique dataset along with various ML as well as AI techniques used for examining millimetre wave beam selection methods for car-to-infrastructure communication. The application of datasets produced with the suggested methodology is demonstrated by experiments including DL in classification, regression, and reinforcement learning problems [75]. Also, Table 2.1 shows the performance of different Cont-BF techniques based on results from various studies and Table 2.2 summarizes the advantages and disadvantages of different types of ML and AI techniques used in Cont-BF.

Table 2.1: Performance comparison of different Cont-BF techniques based on results from various sources

Technique Name	Description	Advantages	Limitations	Type of Data Required
Geometric-Based	Determines the location of the user using the arrival times of signals from multiple antennas	-Low computational cost	-Limited accuracy in indoor environments -Vulnerable to multipath fading	-Antenna array data -User location data
Channel State Information (CSI)-Based	Uses CSI data from multiple antennas to estimate the user's location	-High accuracy -Robustness to multipath fading	-Requires high-quality CSI data -Complex algorithms	-CSI data from multiple antennas -User location data
Hybrid-Based	Combines geometric and CSI-based techniques to improve and robustness	-High accuracy -Robustness to multipath fading and noise	-Requires complex algorithms -May have high computational cost	-Antenna array data -CSI data from multiple antennas -User location data
ML-Based	Uses ML algorithms to learn the relationship between antenna array data and user location	-High accuracy -Can adapt to changing environments	-Requires large amounts of training data -May have high computational cost during training	-Antenna array data -User location data for training
DL-Based	Uses DL algorithms to learn the relationship between antenna array data and user location	-High accuracy -Can adapt to changing environments -Can handle large amounts of data	-Requires even larger amounts of training data than ML-based techniques -May have high computational cost during training	-Antenna array data -User location data for training

2.3.2.1 DL

The extraction of valuable characteristics from input signals and the provision of more precise predictions have been accomplished using DL techniques like convolutional neural networks (CNNs) and recurrent neural networks (RNNs) [76].

For instance, Wang et al. used DL to simplify BF weight estimation in 5G systems [73]. They developed a channel model and trained convolutional neural networks on generated data. The networks predicted BF weights based on channel data, reducing complexity. Results show the potential of DL for digital and hybrid BF, and performance comparison with conventional techniques was presented [77]. Also, [78] proposed a method that aims to improve the performance of Random Forest, Multilayer Perceptron, and k-Nearest Neighbors classification models by increasing the amount of data through synthetic data inclusion. Their experimental results showed that the inclusion of synthetic data improved the macro F1 scores of the models. The Random Forest, Multilayer Perceptron, and k-Nearest Neighbors achieved macro F1 scores of 0.9341, 0.9241, and 0.9456, respectively, which are higher than those obtained with the original data only, thus indicating better performances.

Huang et al. [79] proposed a DL-based fast-BF design method for sum rate maximization under a total power constraint. The method was trained offline using a two-step training strategy. Simulation results demonstrated that the proposed method is fast while obtaining comparable performance to the state-of-the-art method. They derived a heuristic solution structure of the downlink BF through the virtual equivalent uplink channel based on the optimum MMSE receiver. BPNet is designed to perform the joint optimization of power allocation and virtual uplink BF (VUB) design and is trained offline using a two-step training strategy. A DL-enabled BF neural network (BFNN) is proposed, which can optimize the beamformer to attain better spectral efficiency. Simulation findings reveal that the proposed BFNN achieves significant performance gain and high robustness to imperfect CSI. The proposed BFNN greatly decreases the computational complexity compared to conventional BF algorithms. Spectral Efficiency, Performance Gain, Robustness To Imperfect CSI, and Computational Complexity (Measured In Floating Point Operations) are the main outcomes of BFNN [80].

Xia et al. [68] proposed a BF neural network (BNN) for the power minimization problem in multi-antenna communication systems. The BNN was based on convolutional neural networks and the exploitation of expert knowledge. It achieved satisfactory performance with a low computational delay. A deep fully convolutional neural network (CNN) was used for BF, providing considerable performance gains. The CNN was trained in a supervised manner, considering both uplink and downlink transmissions, with a loss function based on UE receiver performance. The neural network predicted the channel evolution between uplink and downlink slots and learned to handle inefficiencies and errors in the whole chain, including the actual BF phase [81]. A DL model is employed to learn how to use these signatures for predicting the BF vectors at the BS [42]. Additionally, [42] discussed a novel integrated ML and coordinated BF solution to support

highly mobile mmWave applications. The solution used a DL model to learn how to use signatures to predict the BF vectors at the BS. This rendered a comprehensive solution that supports highly mobile mmWave applications with reliable coverage, low latency, and negligible training overhead.

Hameed et al. [82] proposed a DL-based energy BF scheme for a multi-antennae wireless powered communication network (WPCN). We used offline training for the deep neural network (DNN) to provide a faster solution to the real-time resource allocation optimization problem. Simulation results showed that the proposed DNN scheme provided a fair approximation of the traditional sequential parametric convex approximation (SPCA) method with low computational and time complexity.

When exploring the application of Deep Learning (DL) techniques in beamforming, it is crucial to consider several limitations that can impact the effectiveness and practicality of these approaches. DL models heavily rely on extensive and high-quality datasets for training, posing a challenge when faced with limited or biased data that may hinder generalization and real-world performance. Additionally, the inherent complexity of deep neural networks often results in black-box models, making it difficult to interpret the decision-making process and potentially reducing trust in the beamforming outcomes. The computational demands of training DL models for beamforming can be significant, requiring substantial processing power and time, which may limit their deployment in resource-constrained environments. Overfitting, a common issue with DL models, can lead to suboptimal performance on unseen data, emphasizing the need for robustness to varying channel conditions and environmental factors. Ensuring the quality and representativeness of training data is essential for effective DL-based beamforming, as noisy or incomplete datasets can compromise performance. Transferability of DL models across different scenarios and environments presents a challenge, highlighting the importance of adaptability in diverse deployment settings. Moreover, handling interference sources effectively remains a critical aspect where DL models may encounter difficulties, impacting overall beamforming system performance. By acknowledging and addressing these limitations, researchers can enhance the reliability, efficiency, and applicability of DL-based beamforming solutions in practical wireless communication systems.

2.3.2.2 Supervised Learning:

Different kinds of RF environments have been classified and predicted using supervised learning methods like the support vector machine (SVM) and decision trees. A modified SVM technique is proposed for 3D MIMO BF in 5G networks. The Advanced Encryption Standard algorithm is employed for more security, and interference is reduced in two stages. The suggested ML-3DIM method outperforms existing methods in terms of throughput, SINR, and SNR by up to 20%, 30%, and 35%, respectively, according to simulation results [83]. [84] investigated the ML-based BF design in two-user MISO interference channels. It proposed an ML structure

that takes transmit power and channel vectors as input and then recommends two users' choices between MRT and ZF as output. The numerical results showed that proposed ML-based BF design found the best BF combination and achieved a sum rate of more than 99.9% of the best BF combination.

Ramon et al. [85] introduced an SVM-based approach for linear array processing and BF. It showed how the new minimization approach can be applied to the problem of linear BF with BER performances of the adopted LS and SVM for various noise levels ranging from 0 to 15 dB.

ML BF approach based on the k-nearest neighbors (k-NN) approximation has been considered, which was trained to generate the appropriate BF configurations according to the spatial distribution of throughput demand. Performance was evaluated statistically via a system-level simulator that executes Monte Carlo simulations in parallel. The ML-assisted BF framework achieved up to 5 Mbits/J and 36 bps/Hz in terms of energy efficiency (EE) and spectral efficiency (SE), respectively, with reduced hardware and algorithmic complexity [86]. BeamMaP was a BF-based ML model for positioning in massive MIMO systems [87]. Simulation results showed that BeamMaP achieved Reduced Root-Mean-Squared Estimation Error (RMSE) performance with an increasing volume of training data. BeamMaP was more efficient and steady in the positioning system compared with k-NN and SVM [87].

Singh et al. [88] discussed an ML method for BF at the receiver side antennas for deploying LOS communication in satellite communication (Satcom). It described how the antenna array weights are pre-calculated for a number of beam directions and kept as a database. The signal weights that were calculated for each array element by using their progressive measured phase difference were due to the arriving signal, which was given as input to a linear regression ML model, and the DoA of the signal is predicted. A method for determining an appropriate precoder based on knowledge of the user's location was proposed. The proposed method involved a neural network with a specific structure based on random Fourier features, allowing us to learn functions containing high spatial frequencies. The proposed method was able to handle both LOS and NLoS channels [89].

2.3.2.3   Unsupervised Learning

Unsupervised learning methods like clustering and principal component analysis (PCA) have been used to spot trends and put related data points in one category. For instance, [90] proposes a BF algorithm for fifth-generation and later communication systems. The approach combines the benefits of conventional optimization-based BF techniques with DL-based techniques. To create the initial BF, a novel architecture is proposed, and performance is increased by building a deep unfolding module. The entire algorithm is unsupervised and trained, and simulation results demonstrate enhanced performance and reduced computing complexity when compared to current approaches.

Hojatian et al. [91] proposed a novel unsupervised learning approach to design the hybrid BF for any subarray structure while supporting quantized phase shifters and noisy CSI. No BF codebook was required, and the neural network was trained to take into account the phase-shifter quantization. Simulation results showed that the proposed DL solutions can achieve higher sum rates than existing methods.

2.3.2.4   Reinforcement Learning (RL)

Cont-BF system performance has been enhanced using reinforcement learning techniques like Q-learning and policy gradient methods [92]. For instance, to make network design and maintenance more straightforward, a brand-new intelligent algorithm for massive MIMO BF performance optimisation is proposed in this research. To produce accurate user mobility patterns, pertinent antenna designs, and an estimate of the effectiveness of the generated antenna diagrams, the system uses three neural networks that apply a deep adversarial reinforcement learning workflow. This method has the advantage of learning independently and without requiring big training datasets [93].

Sun et al. investigated the use of deep reinforcement learning to predict coordinated BF strategy in an ultra-dense network and found that the optimal solution is a balanced combination of selfish and altruistic BF [94]. The BF vectors were obtained efficiently through the learned balancing coefficients. RL-based algorithm for cognitive BF was proposed for multi-target detection in massive MIMO (MMIMO) cognitive radars (MMIMO CR). The proposed RL-based algorithm outperformed the conventional omnidirectional approach with equal power allocation in terms of target detection performance. The performance improvement was even more remarkable under environmentally harsh conditions such as low SNR, heavy-tailed disturbance and rapidly changing scenarios [95].

Raj et al. [96] proposed a blind beam alignment method based on RF fingerprints of UE obtained from BS. They used deep reinforcement learning on a multiple-base station cellular environment with multiple mobile users. Achieved a data rate of up to four times the data rate of the traditional method without any overheads. [97] proposed a novel multiagent reinforcement learning (MARL) formulation for codebook-based BF control. It took advantage of the inherently distributed structure in a wirelessly powered network and laid the groundwork for fully locally computed beam control algorithms. A cognitive BF algorithm based on the RL framework is proposed for colocated MIMO radars. The proposed RL-based BF algorithm is able to iteratively sense the unknown environment and synthesize a set of transmitted waveforms tailored to the acquired knowledge. The performance of the proposed RL-based BF algorithm is assessed in terms of probability of detection (P_D) [98].

Nasim et al. [99] proposed an RL approach called the combinatorial multi-armed bandit (CMAB) framework to maximize the overall network throughput for multi-vehicular communications. They proposed an adaptive combinatorial Thompson sampling algorithm, namely adap-

tive CTS, and a sequential Thompson sampling (TS) algorithm for the appropriate selection of simultaneous beams in a high-mobility vehicular environment. Simulation results showed that both of their proposed strategies approach the optimal achievable rate achieved by the genie-aided solution.

The results discuss the application of machine learning and deep learning techniques in the context of millimeter wave technology, particularly focusing on antenna design and beamforming. These technologies offer advantages such as flexibility, high bandwidth, and improved system performance. Machine learning algorithms are utilized to enhance the design and operation of millimeter wave antennas, enabling more efficient wireless communication systems. The research highlights the use of reinforcement learning algorithms for spatial beam selection, hybrid beamforming architectures, and the optimization of beam patterns. Despite the advancements in utilizing deep learning for antenna design, challenges related to data security, system vulnerability, and training complexity remain prevalent in these systems [100].

Table 2.2: Table summarizing the different types of ML and AI techniques used in Cont-BF

Technique Name	Description	Advantages	Limitations
Support Vector Machines (SVM)	Supervised learning algorithm that learns a decision boundary between classes	-Can handle high-dimensional data -Effective in binary classification tasks	-May overfit with noisy or imbalanced data
Random Forest (RF)	Ensemble learning method that combines multiple decision trees to improve performance	-Can handle high-dimensional data, -Can handle missing or noisy data -Can provide feature importance measures	-May overfit with noisy or imbalanced data
Convolutional Neural Networks (CNN)	Neural network architecture that uses convolutional layers to extract features from input data	-Highly effective for image and signal processing tasks -Can learn complex spatial patterns	-May require large amounts of training data -Maybe computationally expensive
Recurrent Neural Networks (RNN)	Neural network architecture that can process sequential data by maintaining a memory of past inputs	-Effective for time-series data and natural language processing tasks -Can handle variable-length inputs	-May be prone to vanishing or exploding gradients -May require large amounts of training data
Reinforcement Learning (RL)	Learning paradigm in which an agent learns to make decisions through trial and error in an environment	-Can adapt to changing environments -Can handle complex decision-making tasks	-May require significant computational resources -May require careful tuning of hyperparameters

2.3.2.5 Hybrid Learning

Cont-BF system performance has also been improved using hybrid methods that incorporate several ML and AI techniques, such as deep reinforcement learning. To address the hybrid BF issue

in huge MIMO systems, deep reinforcement learning is suggested. The suggested techniques reduce computing complexity while achieving spectral efficiency performance that is close to ideal [101]. Hybrid BF, combining digital baseband precoders and analog RF phase shifters, is an effective technique for mmWave communications and massive multiple-in-multiple-out (MIMO) systems. ML techniques can be used to improve the achievable spectral efficiency of hybrid BF systems. The proposed two-step algorithm can attain almost the same efficiency as that can be achieved by fully digital architectures [102].

Aljumail et al. [103] described the design of ML-based hybrid BF for multiple users in systems that use mmWaves and massive MIMO architectures. The simulation results showed that the ML-based hybrid BF architecture can achieve the same spectral efficiency (bits/sec/Hz) as the fully digital BF designs with negligible error for both single-user and multi-user Massive-MIMO scenarios. [104] proposed a novel RSSI-based unsupervised DL method to design the hybrid BF in massive MIMO systems. They proposed a method to design the synchronization signal (SS) in initial access (IA) and a method to design the codebook for the analog precoder. They showed that the proposed method not only greatly increases the spectral efficiency, especially in frequency-division duplex (FDD) communication, by using partial CSI feedback, but also has a near-optimal sum rate and outperforms other state-of-the-art full-CSI solutions.

Deep neural networks (DNNs) can be used to approximate the singular value decomposition (SVD) and design hybrid beamformers. DNN-based hybrid BF improved rates by up to 50–70% compared to conventional hybrid BF algorithms and achieved a 10–30% gain in rates compared with the state-of-the-art ML-aided hybrid BF algorithms. The proposed approach had low time complexity and memory requirements [105].

The research on hybrid beamforming (BF) systems utilizing machine learning (ML) and artificial intelligence (AI) techniques for massive MIMO and mmWave communications reveals promising advancements yet encounters limitations. Key challenges include the computational complexity and the efficiency trade-off, reliance on channel state information (CSI), and the performance under multi-user scenarios. Although these methods, as cited in various studies, aim to achieve spectral efficiency close to fully digital BF systems with reduced complexity, the balance between practicality and optimal performance remains a significant hurdle. Furthermore, the dependency on CSI, especially in dynamic environments, introduces additional complexity regarding feedback and accuracy. The adaptability of these ML and AI-driven approaches to diverse and unpredictable network conditions also raises concerns about their scalability and real-world applicability.

2.3.3   Datasets for Cont-BF Classification [RQ:3]

Researchers often need datasets that contain location data, RF signals, and other pertinent elements to identify Cont-BF approaches. The following are a few examples of datasets that have been applied in earlier research:

2.3.3.1 Vehicular Networks Dataset (VeND)

The University of California, Los Angeles (UCLA) created this dataset [106], which includes observations from a vehicular network testbed. The dataset contains data about the cars and their movements in addition to details about the wireless channel, such as the SNR and the channel impulse response (CIR) [107].

[108] presented a realistic synthetic dataset, covering 24 hours of car traffic in a $400 - km^2$ region around the city of Koln, in Germany. The dataset captures both the macroscopic and microscopic dynamics of road traffic over a large urban region. Incomplete representations of vehicular mobility may result in over-optimistic network connectivity and protocol performance.

2.3.3.2 5G-VICTORI

is a project financed by the European Union that aims to create 5G technologies for a range of applications, including vehicular communication. With regard to vehicular communication, the project has created a number of datasets, including assessments of the radio frequency (RF) channel and network performance in practical settings [109].

Bassbouss et al. [110] discussed how the new 5G network technology would impact the digitalization of various industries, including modern railway transportation. The Future Railway Mobile Communication System (FRMCS) service requirements and system principles were well-mapped to 5G concepts, but deployment paradigms needed to be established to prove their effectiveness. The 5G-VICTORI project aimed to deliver a complete 5G solution for railway environments and FRMCS services, and this work discussed the key performance indicators and technical requirements for an experimental deployment in an operational railway environment in Greece.

2.3.3.3 5G-EmPOWER

This EU project aims to develop 5G technology for a range of applications, including vehicular communication. With regard to vehicular communication, the project has created a number of datasets, including assessments of the RF channel and network performance in practical settings [111].

3GPP is embracing the concept of Control-User Plane Separation (a cornerstone concept in software-defined network (SDN) in the 5G core and the Radio Access Network (RAN). An open-source SDN platform for heterogeneous 5G RANs has been introduced, which builds on an open protocol that abstracts the technology-dependent aspects of the radio access elements. The effectiveness of the platform has been assessed through three reference use cases: active network slicing, mobility management, and load-balancing [111].

2.3.3.4   ns-3

The Network Simulator 3 (ns-3) is an open-source network simulator that is useful for simulating and modelling vehicular communication in 5G networks. In addition to mobility models for simulating the movement of vehicles, NS-3 has various built-in modules for modelling the wireless channel [112].

Perrone et al. [113] presented a framework for the ns-3 network simulator for capturing data from inside an experiment, subjecting it to mathematical transformations, and ultimately marshalling it into various output formats. The application of this functionality is illustrated and analyzed via a study of common use cases. The design presented provides lessons transferrable to other platforms.

2.3.3.5   Connected automobiles and Cities

The National Renewable Energy Laboratory (NREL) created this dataset, which contains information from a field investigation of connected automobiles in a smart city setting. The dataset contains details about, among other things, network performance, traffic flow, and vehicle trajectories[114].

In [115], big data from the cellular network of the Vodafone Italy Telco operator can be used to compute mobility patterns for smart cities. Five innovative mobility patterns have been experimentally validated in a real industrial setting and for the Milan metropolitan city. These mobility patterns can be used by policymakers to improve mobility in a city, or by Navigation Systems and Journey Planners to provide final users with accurate travel plans.

2.3.3.6   DeepSense6G

DeepSense 6G is a collection of data that includes different types of sensing and communication information, such as wireless communication, GPS, images, LiDAR, and radar. This data was gathered in real-life wireless environments and represents the world's first large-scale dataset of this kind. The dataset contains over one million samples of this multi-modal sensing-communication data and was collected in over 30 different scenarios to target various applications. The collection of data was done at several indoor and outdoor locations with high diversity and during different times of the day and weather conditions. Additionally, there are tens of thousands of data samples that have been labelled both manually and automatically.

Also in [116], the DeepSense 6G dataset is a large-scale dataset based on real-world measurements of co-existing multi-modal sensing and communication data. The DeepSense dataset structure, adopted testbeds, data collection and processing methodology, deployment scenarios, and example applications are detailed in the work. The work aims to facilitate the adoption and reproducibility of multi-modal sensing and communication datasets. The researchers ([117]) had a 400 GB dataset containing hundreds of thousands of WiFi transmissions collected "in the

wild" with different SNR conditions and over different days. They also had a dataset of transmissions collected using their software-defined radio testbed, and a synthetic dataset of LTE transmissions under controlled SNR conditions.

2.3.3.7 SUMO

The Simulation of Urban MObility (SUMO) is an open-source traffic simulation software that allows modelling and simulating traffic flow in urban areas. It can simulate individual vehicles, pedestrians, public transportation, and various road networks. SUMO has a variety of applications, including traffic planning, intelligent transportation systems, and autonomous driving. A synthetic dataset generator was developed to support research activities in mobile wireless networks. The generator uses traces from the SUMO simulator and matches them with empirical radio signal quality and diverse traffic models. A dataset was created in an urban scenario in the city of Berlin with more than 6h of duration, containing more than 40000 UEs served by 21 cells [118].

2.3.4 Miscellaneous Datasets

2.3.4.1 5G3E Dataset

[119] introduced the 5G3E dataset, designed to contain thousands of time series related to the observation of multiple resources involved in 5G network operation. This dataset was specifically created to support 5G network automation, encompassing a variety of collected features ranging from radio front-end metrics to physical server operating system and network function metrics. The testbed associated with the dataset was deployed to facilitate the generation of traffic, starting from real traffic traces of a commercial network operator.

2.3.4.2 5G Trace Dataset

Another dataset is the 5G trace dataset from a significant Irish mobile operator introduced by [120]. This work presented a 5G trace dataset collected from a major Irish mobile operator. The dataset was generated from two mobility patterns (static and car) and across two application patterns (video streaming and file download). The dataset was composed of client-side cellular key performance indicators (KPIs) comprised of channel-related metrics, context-related metrics, cell-related metrics, and throughput information. Additionally, The authors provided a 5G large-scale multi-cell ns-3 simulation framework to supplement our real-time 5G production network dataset. This framework allowed other researchers to investigate the interaction between users connected to the same cell through the generation of their synthetic datasets.

2.3.4.3 SPEC5G Dataset

[121] curated SPEC5G, the first publicly accessible 5G dataset for natural language processing (NLP) research. The dataset contains 134 million words in 3,547,587 phrases taken from 13 online websites and 13094 cellular network specs. The authors utilized this dataset for security-related text categorization and summarization by utilizing large-scale pre-trained language models. For protocol testing, pertinent security-related attributes were also extracted using text classification techniques. Additionally, [122] presented a novel mobility dataset generation method for 5G networks based on users' GPS trajectory data. It aggregated the user's GPS trajectories and modeled his location history by a mobility graph representing the cell BS he passed through. The generated dataset contained the mobility graph records of 128 users. The user mobility dataset for 5G networks based on GPS geolocation is valuable for predicting user mobility patterns.

2.3.4.4 Labelled Dataset for 5G Network

In another study, [123] discussed a methodology for collecting a labelled dataset for a 5G network. It described how to build a 5G testbed and use it to collect data. This data can then be used to construct a 5G-based labelled dataset. A 5G testbed was built to observe 5G network features by replaying the collected data. A specialized network collector system was implemented to collect 5G edge network traffic data. A re-collecting methodology using the proposed 5G testbed and network collector can be used to construct a 5G-based labelled dataset for supervised learning methods.

2.3.4.5 5G Users Measurement Campaign

Also, [124] utilized the results from a publicly available measurement campaign of 5G users and analyzed various figures of merit. The findings indicated that the downlink and uplink rates for static and mobile users can be represented by either a lognormal or a generalized Pareto distribution. Moreover, the time spent in the same cell by a mobile (driving) user was observed to be best captured by a generalized Pareto distribution. Additionally, the prediction of the number of active users in the cell was found to be feasible.

2.3.4.6 5G Tracker

Furthermore, [125] discussed 5G Tracker, a crowdsourced platform that includes an Android app to record passive and active measurements tailored to 5G networks and research. It has been used for over 8 months and has collected over 4 million data points. The platform is useful for building the first-of-a-kind, interactive 5G coverage mapping application. 5G Tracker is a crowdsourced platform to enable research using commercial 5G services. 5G performance is affected by several user-side contextual factors, such as user mobility level, orientation, weather,

location dynamics, and environmental features. 5G Tracker has been used to collect over 4 million data points, consuming over 50 TB of cellular data across multiple 5G carriers in the U.S.

2.3.4.7 Mobile Edge Computing in 5G

Moreover, bringing computational and storage technologies closer to end users with strategically deployed and opportunistic processing and storage resources, mobile edge computing in the 5G network was developed by [126] as a very attractive computation architecture. This work used data mining and statistical methods to analyze Baidu website data. The analysis results gave suggestions to improve the design and development of 5G services. Data mining and statistical analysis of Baidu cloud services in the 5G network revealed that clustering, outlier detection, prediction, and statistical methods can be used to evaluate smart city services. The analysis results provided insights into the design and development of 5G services (API website). The findings suggested that mobile edge computing in 5G networks can be used to improve the performance of smart city services.

2.3.4.8 5G+ Industrial Internet

Finally, [127] discussed a project to collect "three-level" edge layer data from equipment manufacturers, equipment users, and spare parts manufacturers. The goal was to establish a unified data standard and help companies build general services around equipment data. 5G+ Industrial Internet is used to collect data from three levels of edge layers: spare parts manufacturers, equipment manufacturers, and equipment users. Data is assimilated and unified into a single standard. A large-scale and shallow informatization project of incremental equipment is implemented in the Yangtze River Delta in a short period of time.

Table 2.3: Table listing datasets related to User Location

Dataset Name	Source	Characteristics
IEEE 802.11n Channel Measurement	IEEE 802.11n working group	Channel state information (CSI) from multiple antennas
KTH Localization Dataset	KTH Royal Institute of Technology	Received signal strength (RSS) and AoA from multiple antennas Ground truth location data
CSI-Hotel Dataset	University of California, Santa Barbara	CSI data from multiple antennas in an indoor environment
DeepMIMO Dataset	Arizona State University	Synthetic data generated by a ray-tracing tool for a variety of scenarios, including urban and indoor environments
iNEMO Dataset	STMicroelectronics	Acceleration, magnetic field, and angular velocity data, along with ground truth location data

Also, Table 2.3 lists some 5G data sets consisting of channel state information (CSI), phase, received power, etc. that can be used for user localization.

2.3.5 Optimization techniques for Cont-BF [RQ:4]

While using AI-based techniques, system optimization is a crucial step. AI-based Cont-BF models can be optimised using various strategies to ensure real-time processing. One method to accelerate computations is through hardware acceleration techniques like GPU processing. Additionally, pre-trained models or reducing the number of parameters in the model design can be used to optimize the model. To decrease the model size and boost computational effectiveness, techniques like pruning, quantization, and knowledge distillation can be applied. Improving the feature extraction and input data pre-processing phases can also help with real-time processing. Creating specialised algorithms and optimisation strategies adapted for certain hardware and deployment conditions can also enhance the performance of Cont-BF models.

Figure 2.7 shows some of the possible ways to optimise Cont-BF models for real-time processing, which are explained in detail below:

2.3.5.1 Model simplification:

Simplifying the model architecture, such as reducing the number of layers or the number of neurons in each layer, can improve computational efficiency and reduce processing time. For instance, the research suggests a strategy that uses ML and hardware performance counter data to optimise power and performance for GPU-based systems. The model can accurately detect power-performance bottlenecks and provide optimization techniques for a variety of sophisticated compute and memory access patterns. The model, which has been validated on NVIDIA Fermi C2075 and M2090 GPUs as well as the Keeneland supercomputer at Georgia Tech, is more reliable and accurate than existing GPU power models [128].

2.3.5.2 Hardware acceleration:

Dedicated hardware, such as graphics processing units (GPUs), field-programmable gate arrays, or application-specific integrated circuits, etc., can speed up the processing of Cont-BF models by performing parallel computations. To determine the direction of incoming signals, BF is a signal processing technique that combines signals from a number of receivers. Although it overcomes noise interference, adaptive BF (ABF) is computationally expensive. In current GPUs, ABF can be implemented in parallel. ABF can be parallelized on an NVIDIA GPU using the author's method, which has a lower throughput than the serial implementation but is still able to be improved [129].
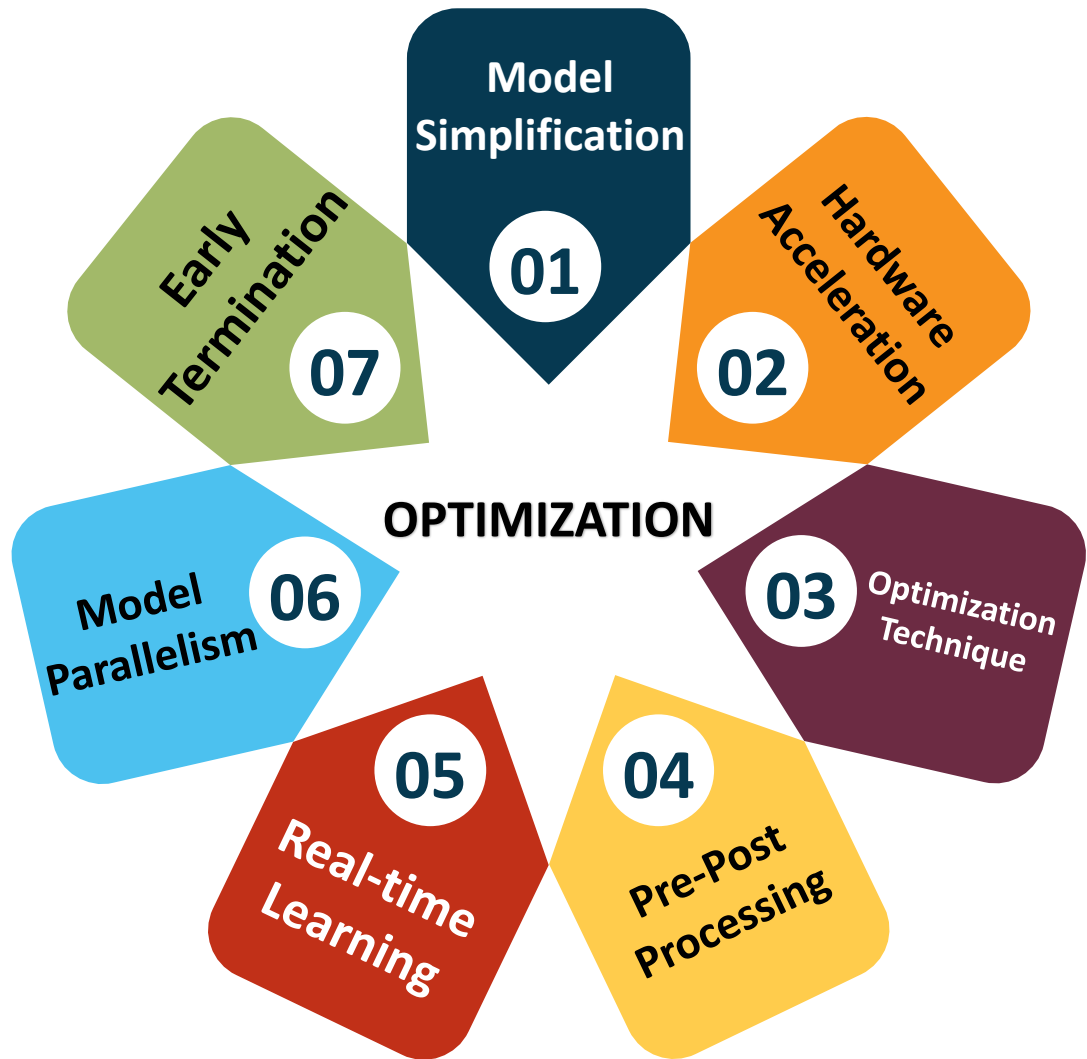
Figure 2.7: Optimization Techniques for Cont-BF

2.3.5.3 Optimization techniques:

Various optimization techniques, such as weight pruning, quantization, and knowledge distillation, can be applied to Cont-BF models to reduce their computational complexity and memory footprint without significant loss in accuracy. This research [130] explores the use of the deep neural network (DNN) model as the teacher to train recurrent neural networks (RNNs), specifically long short-term memory (LSTM), for automated voice recognition (ASR). The method successfully trains RNNs without the use of additional learning methods, even with a small amount of training data.

2.3.5.4 Preprocessing and postprocessing:

Preprocessing the input data to reduce its dimensionality or complexity, and postprocessing the output data to refine the results or reduce noise can help improve the performance and effi-

ciency of Cont-BF models. With the use of DL, a low-complexity precoding design approach for multiuser MIMO systems is suggested in [131]. The suggested method uses methods such as input dimensionality reduction, network pruning, and recovery module compression to produce a performance that is comparable to the conventional WMMSE algorithm with relatively little computational cost.

2.3.5.5   Real-time learning:

Using online or incremental learning algorithms instead of offline or batch learning can enable Cont-BF models to adapt to changing conditions in real-time and reduce the need for frequent retraining. In [132], two adaptive learning approaches such as ADAM and RAL are proposed for the real-time detection of network assaults in Internet network traffic. These methods achieve excellent detection accuracy even in the presence of idea drifts by dynamically learning from and adapting to non-stationary data streams while lowering the demand for labelled data.

2.3.5.6   Model parallelism:

Breaking the model into smaller sub-models and processing them in parallel can improve the overall processing speed of Cont-BF models. This can be done using techniques such as data parallelism or model parallelism. With a focus on model and data parallelization, [133] addresses distributed ML architecture and topology. It analyses ML algorithms and offers parallelization suggestions. The specific needs and demands of communications networks, such as resource allocation and trade-offs between privacy and security, are not addressed.

2.3.5.7   Early termination:

Stopping the model's processing early when a certain threshold is reached can reduce unnecessary computation, especially in cases where the output has already converged. [134] promotes early pausing before convergence to prevent overfitting and suggests the use of cross-validation to detect overfitting during neural network training. The study uses multi-layer perceptrons with resilient backpropagation (RPROP) training to assess the effectiveness and efficiency of 14 distinct automatic stopping criteria from three classes for a variety of activities. The findings indicate that slower stopping criteria slightly improve generalisation, although training time often increases by a factor of four.

The choice of optimization techniques will depend on the specific requirements of the application and the constraints of the hardware platform. A combination of these techniques can be used to achieve the best balance between performance and efficiency for the real-time processing of Cont-BF models.

In this chapter, we delved into the state-of-the-art methodologies demonstrating the critical role of location information in optimizing beamforming strategies, particularly through the ap-

plication of artificial intelligence (AI) techniques. We discussed how leveraging user location data can significantly refine adaptive beamforming (BF) processes, enhancing the overall performance of wireless networks. Moreover, we explored the integration of deep learning (DL) into BF strategies, showcasing its potential to address the challenges posed by dynamic environments, network heterogeneity, and varying user mobility patterns. This examination sets a foundation for future research aimed at advancing the implementation and effectiveness of AI-enhanced beamforming in real-world scenarios, underpinning the ongoing evolution of mobile communication systems.

Chapter 3

Location-Based Adaptive Beamforming

This work report delves into exploring location-based adaptive beamforming and beam steering within the realm of mobile communication in multipath environments, aiming to advance beyond conventional methodologies. In the contemporary landscape of heightened reliance on mobile communication, optimizing signal quality stands as a paramount concern. Through extensive simulations conducted in diverse settings, encompassing both open spaces and a digital twin of a university campus, we scrutinized the efficacy of these innovative techniques in comparison to traditional methods. The results are compelling, showcasing notable improvements of up to 40% in SINR and up to 30% in received power in open space scenarios. The virtualized university campus scenario witnessed even more substantial enhancements, with SINR and received power improvements reaching up to 50% and 40%, respectively. Crucially, these groundbreaking strategies exhibit adaptability to user mobility while emphasizing energy efficiency. However, it is imperative to recognize the study's limitations, including its dependence on precise location information and susceptibility to interference from neighboring cells and users.

3.1 Introduction

As wireless communication technologies rapidly evolve, the imperative for innovative solutions becomes crucial to address the escalating demands of users, the dynamism of environments, and the diversity of communication devices [135]. Emerging 6G communication systems, characterized by their promise of high data rates and ultra-low latency, necessitate efficient spectrum utilization and sophisticated adaptive beamforming techniques [136]. This research is dedicated to exploring the application of advanced beamforming techniques, namely,MRT and ZF, in the context of location-based adaptive beamforming and beam steering.

   MRT and ZF are pivotal in directing beams optimally for power distribution among users and minimizing interference, respectively, thereby enhancing overall system performance [137, 138]. These techniques play a critical role in overcoming challenges such as multipath propaga-

tion, dynamic user mobility, and the complexities of urban environments, thereby improving signal quality and reducing interference [139, 140]. Our investigation employs simulations within a virtualized University of Glasgow campus (referred to as a digital twin) and open spaces to assess the efficacy of MRT and ZF techniques. The overarching goal is to enhance SINR and received power, with a focus on the practical ramifications for mobile communication scenarios in the real world.

This study endeavors to bolster the reliability of wireless communication systems, particularly under challenging propagation conditions. By employing adaptive beamforming, where beam patterns dynamically adjust based on user locations, we aim to address the hurdles of signal attenuation, multipath fading, and interference. This approach not only enhances SINR and resource efficiency but also aligns seamlessly with dynamic user movements, ensuring highly responsive and reliable communication networks.

3.2 Related Work

Adaptive beamforming and location-based communication within wireless systems have been the subjects of significant research, yielding seminal contributions aimed at enhancing system efficiency and reliability.

Fundamental to this area, MRT maximizes signal power at the receiver by intelligently weighting signals from multiple antennas, while ZF beamforming focuses on eliminating interference by directing the beam toward the intended user [137, 138]. Noteworthy advancements such as Minimum Mean Square Error (MMSE) and Regularized Zero Forcing (RZF) have emerged, offering a balance between signal quality and interference mitigation [141, 142].

The integration of geographical information has been shown to optimize adaptive beamforming in dynamic scenarios, with Onrubia et al. utilizing Global Navigation Satellite System (GNSS) coordinates for real-time beam steering [143]. Kela et al. have extended the application of location-based beamforming to urban environments, tackling the challenges introduced by structures and multipath propagation [144].

The utilization of digital twins, as demonstrated by Tao et al.'s virtualization of the University of Glasgow campus, offers realistic environments for simulating communication systems, bridging the gap between theoretical studies and practical implementations [145]. Despite the foundational work laid by existing literature, there remains a gap in comprehensive evaluations of adaptive beamforming and location-based communication under authentic, real-world conditions. This study seeks to bridge that gap by assessing the performance of advanced beamforming techniques in dynamic and complex mobile communication environments.

Key contributions of this research include:

1. Employing a digital twin provides a realistic setting for evaluating location-based adaptive beamforming.

2. The incorporation of precise geolocation data enables effective beam steering based on user locations.

3. This research takes into account real-world complexities, such as multipath propagation and weather conditions, for a comprehensive evaluation.

4. By applying MRT and ZF techniques, this study aims to enhance signal quality through beam steering while simultaneously mitigating interference.

3.3   Methodology

This chapter elucidates the methodology underlying our investigation into the implementation and effectiveness ofMRT and ZF beamforming techniques (Figure 3.1). Utilizing a sophisticated system model, alongside simulations within a digital twin ([146]) of the University of Glasgow campus, this study aims to enhance our understanding of adaptive beamforming's impact on signal integrity and network performance in urban environments.
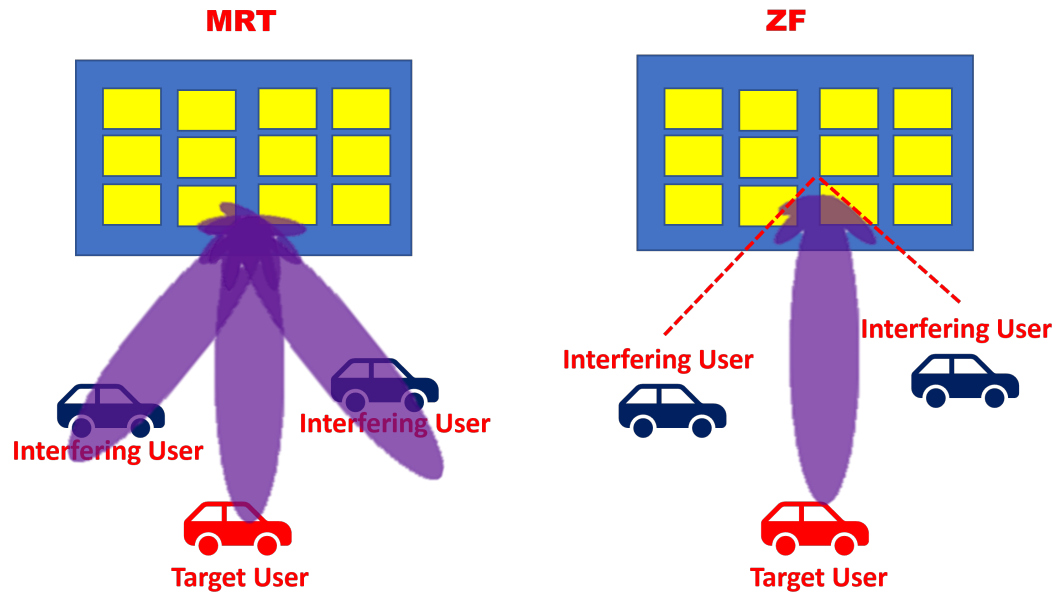
Figure 3.1: Description of MRT and ZF beamforming techniques.

3.3.1   System Model

Our model primarily focuses on the downlink scenario, where the base station serves multiple users by transmitting signals directly tailored to each user's channel conditions while mitigating interference to others. This scenario necessitates a comprehensive understanding of the downlink channel matrix representation and sophisticated power allocation strategies to optimize system performance. We utilized two key beamforming techniques:

MRT([137]): A beamforming technique that optimizes power distribution across UE by directing beams towards all user antennas, thereby maximizing signal gain for each user. The weighting vector w_k for user k is defined as:

$$\mathbf{w}_k = \frac{\mathbf{h}_k}{|\mathbf{h}_k|}\sqrt{p_k} \tag{3.1}$$

where h_k represents the channel vector from the transmitter to user k, and p_k denotes the power allocated to user k.

ZF([138]): This technique aims to minimize inter-user interference by carefully shaping the transmitted beam toward intended receivers while nullifying potential interference, enhancing system performance. The beamforming matrix W is given by:

$$\mathbf{W} = \mathbf{H}(\mathbf{H}\mathbf{H})^{-1}\Lambda^{-1}\sqrt{\mathbf{P}} \tag{3.2}$$

where H is the channel matrix, Λ is a diagonal matrix with regularization parameters, and P represents the power allocation matrix.

To evaluate the performance of our proposed schemes, we calculated the SINR for each user in the system. The SINR accounts for both the desired signal and interference from other users, along with background noise. It is calculated as follows:

$$\text{SINR}_k = \frac{|\mathbf{g}_k\mathbf{w}_k|^2}{\sum_{i \neq k}^{K}|\mathbf{g}_k\mathbf{w}_i|^2 + \sigma^2} \tag{3.3}$$

where g_k is the channel gain vector for user k, and σ^2 is the noise power.

3.3.2   Simulation Setups and Proposed Solution

To evaluate the efficacy of location-based beamforming techniques within complex multipath environments, we deployed simulations within a virtualized representation of the University of Glasgow (UofG) campus. This simulation, known as a digital twin, replicates the actual campus layout and architecture, offering an authentic backdrop for our analyses [145].

Multipath environments are characterized by the propagation phenomenon where transmitted signals reach the receiving antenna through multiple paths. These paths can result from reflections, diffraction, and scattering off surfaces such as buildings, vehicles, and other obstacles. Multipath can lead to interference and fading, posing significant challenges for signal integrity and network performance. A digital twin of an urban campus like UofG provides an ideal scenario to study these effects due to its inherent structural complexity.

The choice of a 16x16 Multiple Input Multiple Output (MIMO) antenna array for open space scenarios is strategic. This configuration balances the complexity and performance trade-offs, offering substantial beamforming gains and spatial multiplexing capabilities without the

prohibitive computational overhead associated with larger arrays. The 16x16 array enables fine-grained beam steering and signal focusing, essential for mitigating multipath effects and enhancing signal reception in cluttered urban environments.

Regarding the antenna array's orientation and element spacing:

Orientation: The antennas are typically oriented to maximize coverage and signal quality, considering the environmental layout and expected user positions.

Element Spacing: The element spacing within the antenna array is often set to half the wavelength ($\lambda/2$) of the carrier frequency to prevent grating lobes and ensure a uniform radiation pattern. For a carrier frequency of 3.75 GHz, this results in spacing that supports both beamforming effectiveness and spatial resolution.

The selection of 16-QAM (Quadrature Amplitude Modulation) as the modulation scheme strikes a balance between spectral efficiency and resilience to noise and interference. While higher-order modulation schemes like 64-QAM or 256-QAM offer greater data rates by packing more bits into each symbol, they are also more susceptible to errors in challenging multipath conditions due to their tighter constellation spacing. 16-QAM is chosen as a compromise, providing a fourfold increase in data rate over QPSK (Quadrature Phase Shift Keying) while still maintaining a level of robustness suitable for the expected urban multipath environment.

Proposed Algorithm: To systematically assess the performance of MRT and ZF beamforming, we implement a structured simulation algorithm. This algorithm incorporates real-world elements such as line-of-sight calculations, advanced ray tracing, and environmental effects like buildings and terrain into the simulation process, offering a nuanced view of beamforming efficacy in complex urban settings.

The algorithm, outlined in Algorithm 1, encompasses several critical steps from initializing the simulation environment with accurate geospatial data to calculating received power under various weather conditions and with beam steering techniques. This comprehensive approach ensures a thorough evaluation of how adaptive beamforming can improve communication reliability and quality in dynamic urban environments.

Through this detailed methodology, combining a rigorous system model with sophisticated simulations, our research aims to contribute valuable insights into the design and optimization of future wireless communication systems, particularly in the context of burgeoning 6G technologies.

3.4   Results

This section delves into the simulation outcomes for location-based adaptive beamforming and beam steering within multipath scenarios. We benchmark these outcomes against a control scenario termed "open space," which is characterized by an environment devoid of significant obstructions that influence signal propagation. Our analysis leverages key performance indica-

---

Algorithm 1 Proposed Algoritm

Load the site viewer with the building map.
Set up a small cell transmitter (tx) with specific parameters.
Display the transmitter.
Set up a ray-tracing propagation model with concrete buildings and terrain.
Initialize an empty array *P_gu*.
Set locations for small cell receivers (rx).
for each receiver in the list **do**
    Set up a receiver at the specified location.
    Calculate line-of-sight between transmitter (tx) and receiver.
    Set up another receiver at a different location.
    Create a composite model with additional gas and rain effects.
    Perform ray tracing between transmitter and receivers in different weather conditions.
    Calculate received power considering weather effects.
    Configure antenna properties for beam steering.
    Perform ray tracing with beam steering.
    Calculate and display received power with beam steering.
    Generate coverage data for the transmitter in different weather conditions.
    Update the *P_gu* array with the coverage data.
end for

---

tors (KPIs) such as SINR, Received Power, and Energy Efficiency to assess the efficacy of our proposed schemes.

The primary motivation for employing location-based beamforming and steering techniques arises from the need to enhance communication link quality in complex environments. Such environments, exemplified by a digital twin of a university campus, present unique challenges due to multiple signal paths and potential obstructions. By dynamically adjusting the beam's direction based on the receiver's location, the proposed schemes aim to optimize signal quality (SINR) and strength, thereby ensuring robust wireless communication.

3.4.1 Proposed Scheme

The proposed schemes encompass advanced implementations ofMRT and Zero-Forcing (ZF) beamforming techniques. These implementations are uniquely optimized through the integration of location information, enabling adaptive beam steering that significantly reduces interference and improves signal reception quality. Through these techniques, our analysis demonstrates that the proposed schemes are highly effective in navigating the challenges posed by multipath and obstruction-laden environments.

3.4.1.1 User Mobility and Energy Efficiency

The resilience of the proposed schemes against user mobility was also put to the test, with results indicating an admirable adaptation to dynamic user movements, maintaining high SINR

and received power levels with minimal interference. Table 3.1 encapsulates these findings, offering a comparative glimpse at the mean values of received signal power, interference power, and SINR for both MRT and ZF techniques.

Table 3.1: Performance Table

Scenario	Parameters	MRT	ZF
Digital Twin	Received Power (dBm)	-47.0	-61.1
	Received Interference Power (dBm)	-45.9	-10.0
	SINR (dB)	-3.0	17.0
Open Space	Received Power (dBm)	-54.0	-69.1
	Received Interference Power (dBm)	-53.9	-10.0
	SINR (dB)	-3.9	15

Moreover, the exploration into the trade-off between performance and energy efficiency unveiled that the proposed schemes not only achieve remarkable performance metrics but also enhance energy efficiency by up to 20% in comparison to scenarios without beam steering. The efficiency metrics were derived using a formula documented in [147].

Despite the pronounced benefits, the dependency on precise location information emerges as a limitation, prompting future research directions towards developing more robust location estimation methodologies. Additionally, the schemes' susceptibility to interference from adjacent cells underscores another area for future exploration, particularly in devising effective interference management strategies.

3.4.2 Detailed Insights into Open Space and GU Campus Scenarios

3.4.2.1 Open Space

Within the bounds of an open area, our approach harnesses an antenna with a robust 50-meter coverage capability, meticulously oriented to accommodate users in both line-of-sight (LOS) and non-line-of-sight (NLOS) conditions. The application of sophisticated beamforming methods, inclusive of position-to-angular conversion and the MUSIC algorithm, is showcased in Figures 3.2, 3.3, and 3.4. These figures illuminate the precision in location estimation, a pivotal factor in optimizing the beam's direction towards the desired user while mitigating potential interference. Our analysis reveals that through MRT and ZFBF, signal coverage is significantly enhanced, even in scenarios populated with interfering users, as depicted in Figure 3.7 for MRT, and Figure 3.8 for ZFBF. These methodologies' prowess in ensuring consistent and reliable communication is demonstrated, emphasizing their ability to maintain signal integrity.
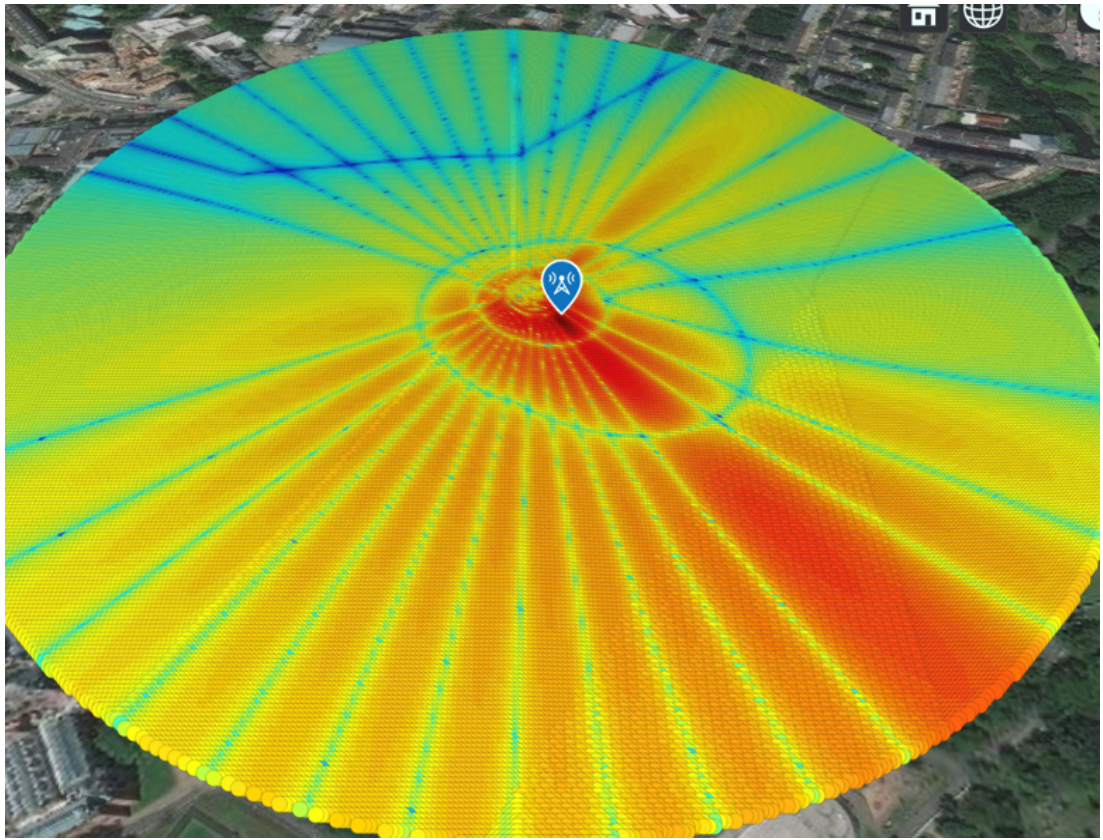
Figure 3.2: Beam coverage area of the base station placed on JWS rooftop of the University of Glasgow in the presence of the target user.
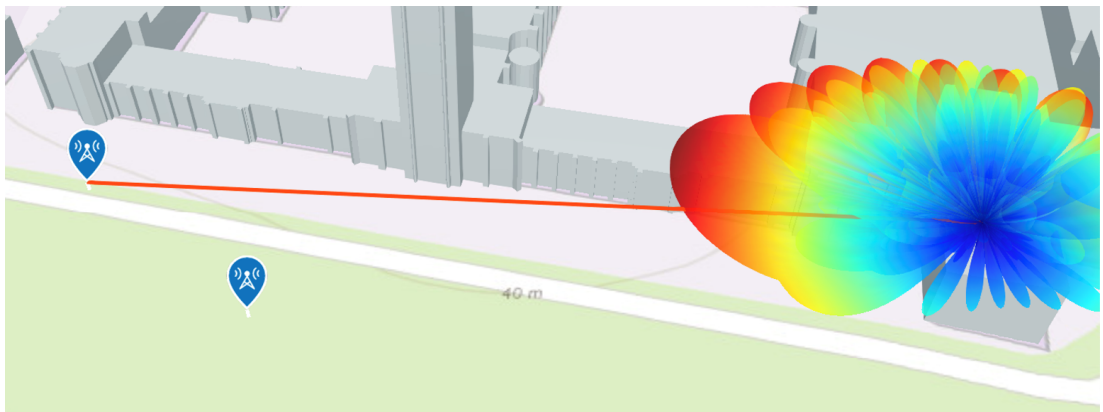
Figure 3.3: Beam propagation from the base station to the target user in LOS.

3.4.2.2   GU Campus Scenario

Transitioning to the complex environment of the GU Campus, the simulation employs a 16x16 Uniform Rectangular Array (URA) antenna, strategically oriented and utilizing three-dimensional ray tracing to craft a realistic channel model. This model is vital for adapting beamforming weights in response to dynamic target movements, encapsulated in Figures, 3.10, and 3.9. The simulations undertaken within this virtual campus environment reveal the nuanced challenges of urban beamforming, from the necessity of precise channel information to the computational
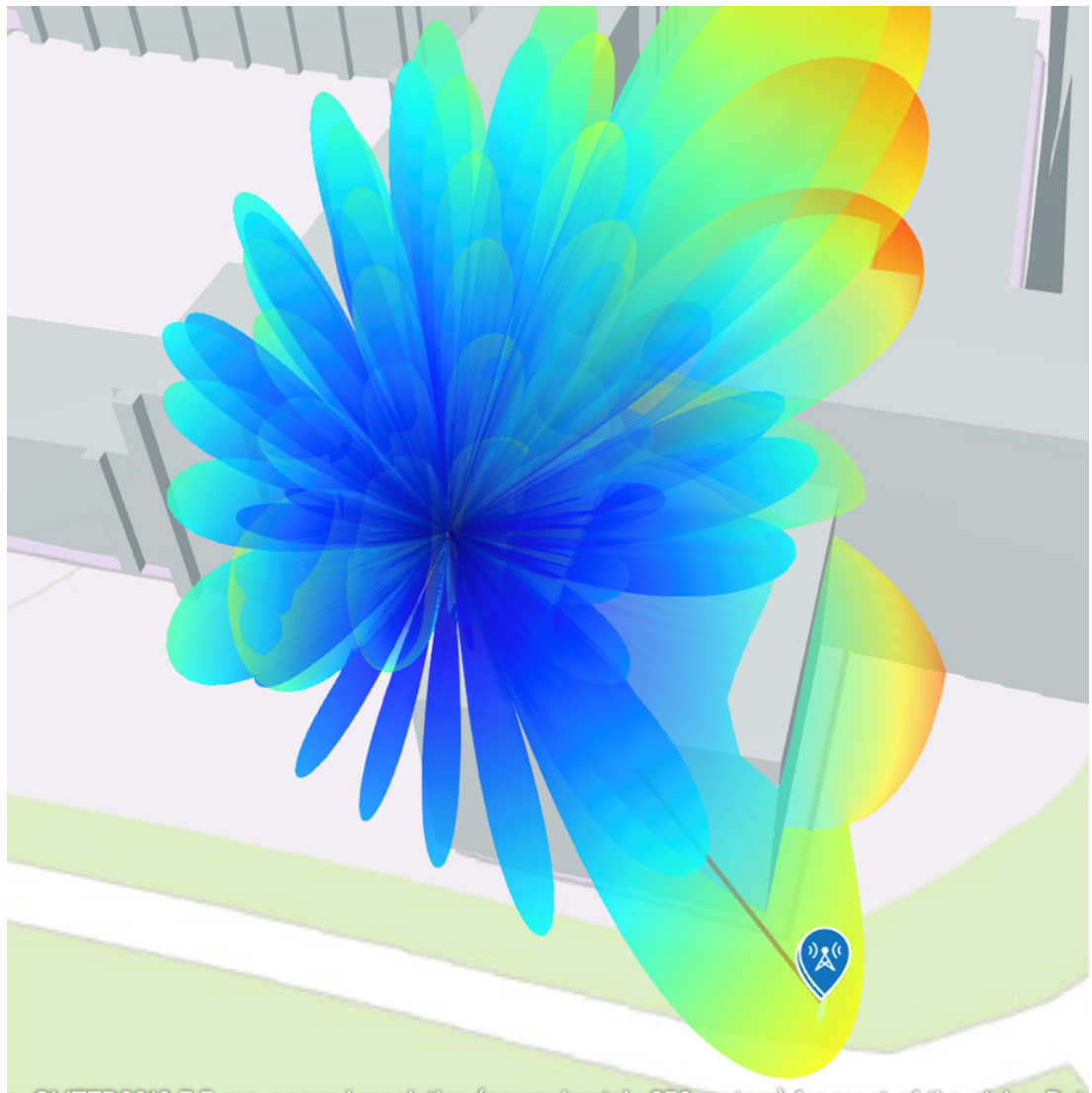
Figure 3.4: Beam pointing towards the target user in NLOS.
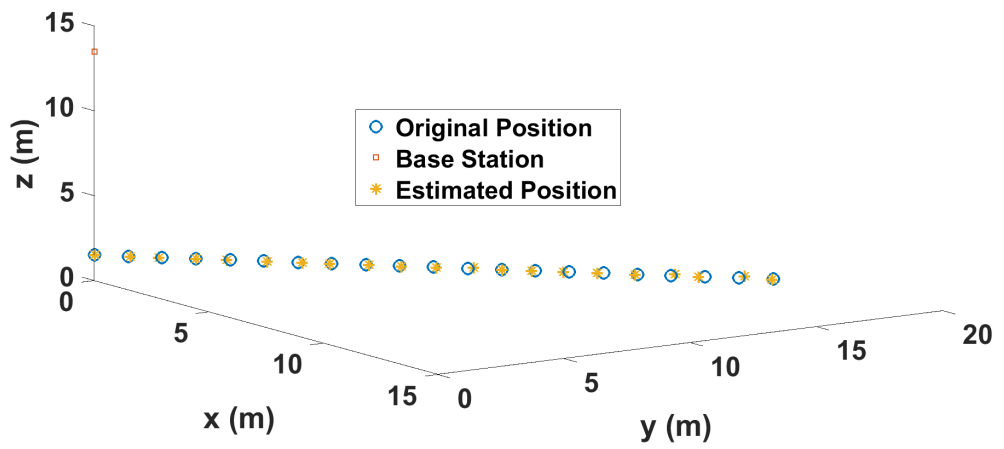
Figure 3.5: Location estimation using MRT and ZF BF.
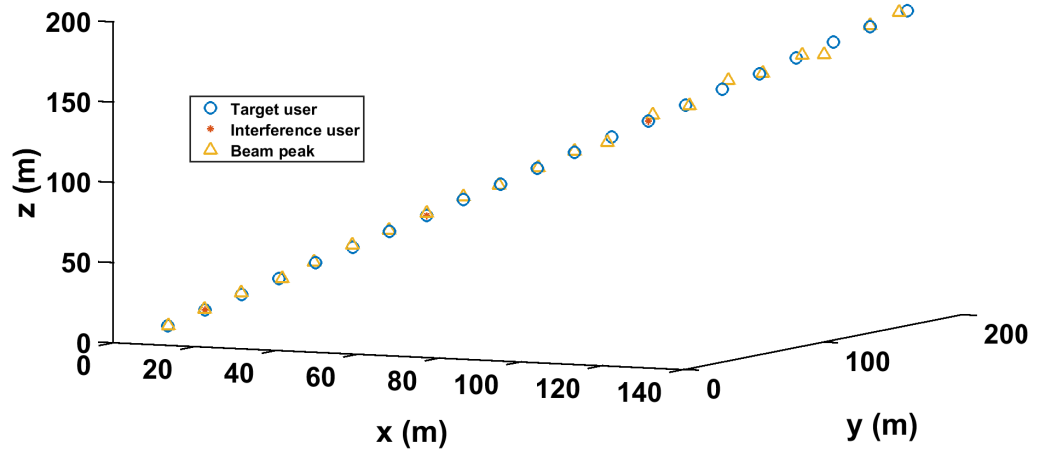
Figure 3.6: Beam pointing towards the target user when MRT BF is used with a single user moving at a constant speed.
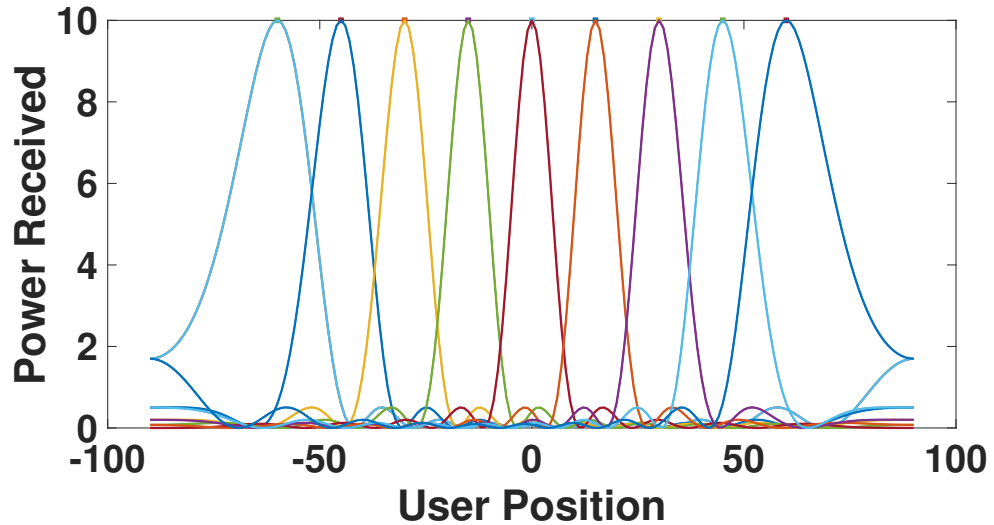
Figure 3.7: Beam pointing towards the target user when MRT BF is used with interfering users.

intensity required for simulating realistic multipath scenarios. Notably, the adaptability of ZF in nullifying signals towards interfering users exemplifies the advanced capabilities of current beamforming techniques to maintain high-quality communication paths in the face of urban complexities, as illustrated in the movement and radiation pattern coverage in Figures 3.10 and 3.9.

In summary, the results section provides a thorough examination of the methodologies' effectiveness in enhancing wireless communication networks' performance through advanced beamforming techniques. The findings not only underscore significant improvements in key performance metrics but also chart potential avenues for future research aimed at overcoming the identified limitations.
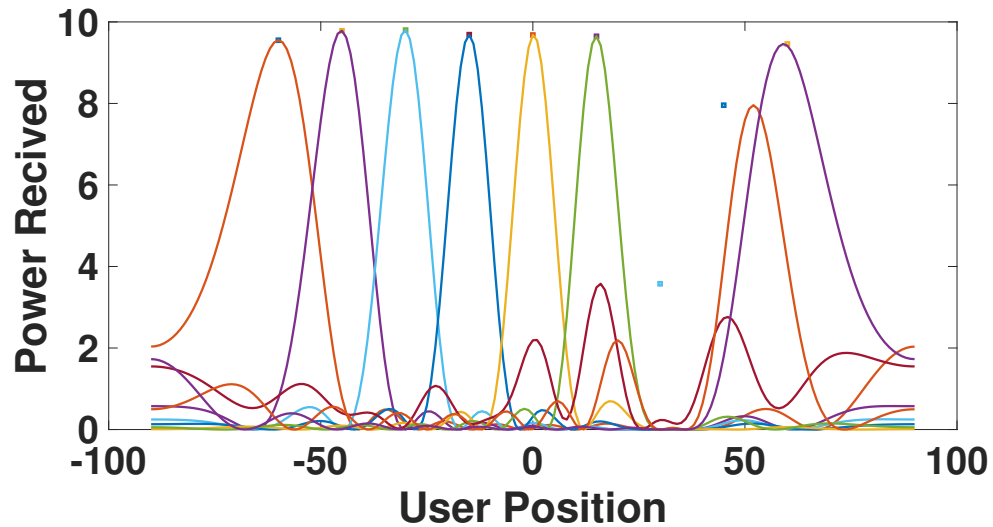
Figure 3.8: Beam pointing towards the target user when ZF BF is used with interfering users.
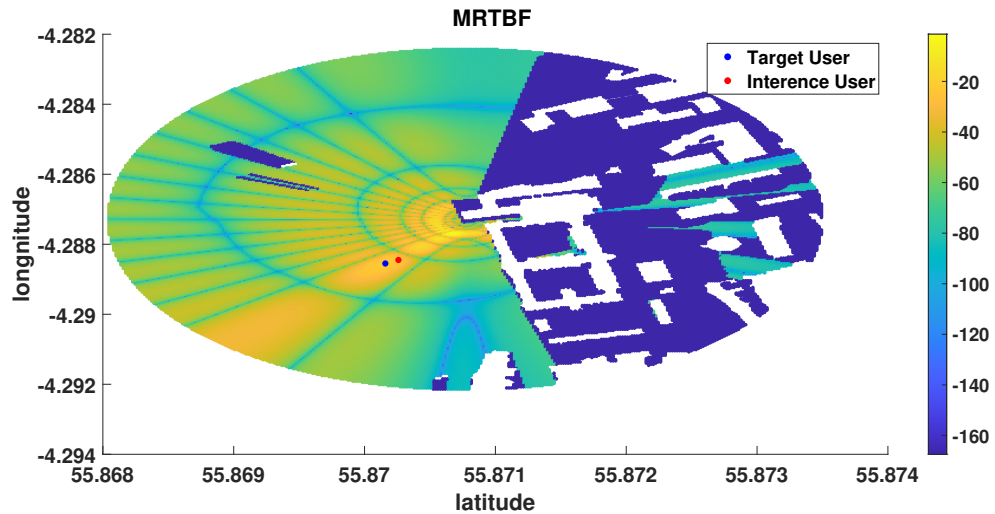
Figure 3.9: Beam pointing towards target user when MRT BF is used.

3.4.3 Conclusion

The comparative analysis presented underscores the significant performance and energy efficiency benefits offered by the proposed location-based beamforming and steering schemes. While the reliance on accurate location information and potential interference from neighboring cells present challenges, these limitations offer avenues for future research, including the development of robust location estimation techniques and interference management strategies. Overall, the findings advocate for the continued exploration and refinement of location-based adaptive beamforming techniques as a means to enhance wireless communication in complex environments.
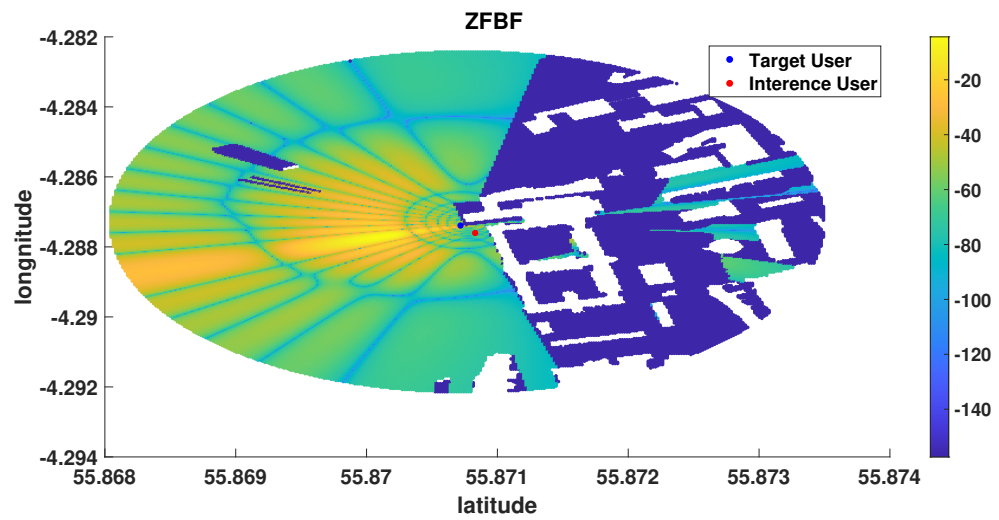
Figure 3.10: Beam pointing towards target user when ZF BF is used.

Chapter 4

Enhancing Location Estimation with DNN

This chapter focuses on the application of simulated data [1] through deep neural networks for location estimation. The primary objective is to describe the architecture, training process, and evaluation metrics employed to enhance location accuracy. By delving into the intricacies of the DL approach, the chapter aims to showcase the effectiveness of simulated data in improving location estimation. This chapter introduces machine learning (ML)-based approach aimed at overcoming the limitations observed in existing localization methods, notably those identified in the works of Anjinappa et al. [148] and Bhattacherjee et al. [70]. We detail the process of transforming channel characteristics and positional data derived from a ray-tracing model into a format conducive for training a Deep Neural Network (DNN) on the Base Station (BS) side. The methodology emphasizes the calculation of Multipath Components (MPCs) and the impact of varying the number of MPCs on localization accuracy.

The key contributions of this study are as follows:

- **Machine Learning-Enhanced Localization:** We introduce a novel approach that leverages machine learning (ML) to significantly enhance the localization process in wireless communication networks. Our method reduces run-time complexity while maintaining high accuracy in determining UE positions within the network.

- **Improved Localization Performance:** We demonstrate how ML techniques, when provided with sufficient training data, can effectively overcome the limitations of previous localization methods. By utilizing ML features, we enhance the precision of location estimation, particularly in complex indoor and outdoor environments.

- **Practical Application in 5G Networks:** Our research addresses the demands of 5G networks, where efficient and accurate localization is crucial for enabling advanced features and services. By proposing a machine-learning-based solution, we contribute to the practical implementation of 5G applications.

---

[1]Data Tool and Data extraction process is described in appendix

- **Potential for Future Developments:** We lay the foundation for further advancements in localization techniques by exploring the promise of ML in this context. This study opens the door to continued research and innovation in the field of wireless communication.

4.0.1 Methodology

In this section, we elucidate the transformation of channel features and position information, provided by the ray-tracing model, into input features and output labels for training a DNN on the base station side. Our approach will be compared with existing methods, particularly the proposals of ([148]) and ([70]).

As depicted in Fig. 4.1, the green dot signifies the location of the BS, while the red line traces the trajectory of the UE. Our study takes place in the UofG environment, involving a BS and mobile UE. The BS remains stationary, while we consider a random trajectory for the UE. Both the BS and the UE employ single and multi-element directional antennas, operating at various frequencies, allowing us to explore single input single output (SISO), single input multi output (SIMO), multi input single output (MISO), and multi input multi output (MIMO) scenarios. To configure the localization algorithm, we conducted multipath component (MPC) calculations.
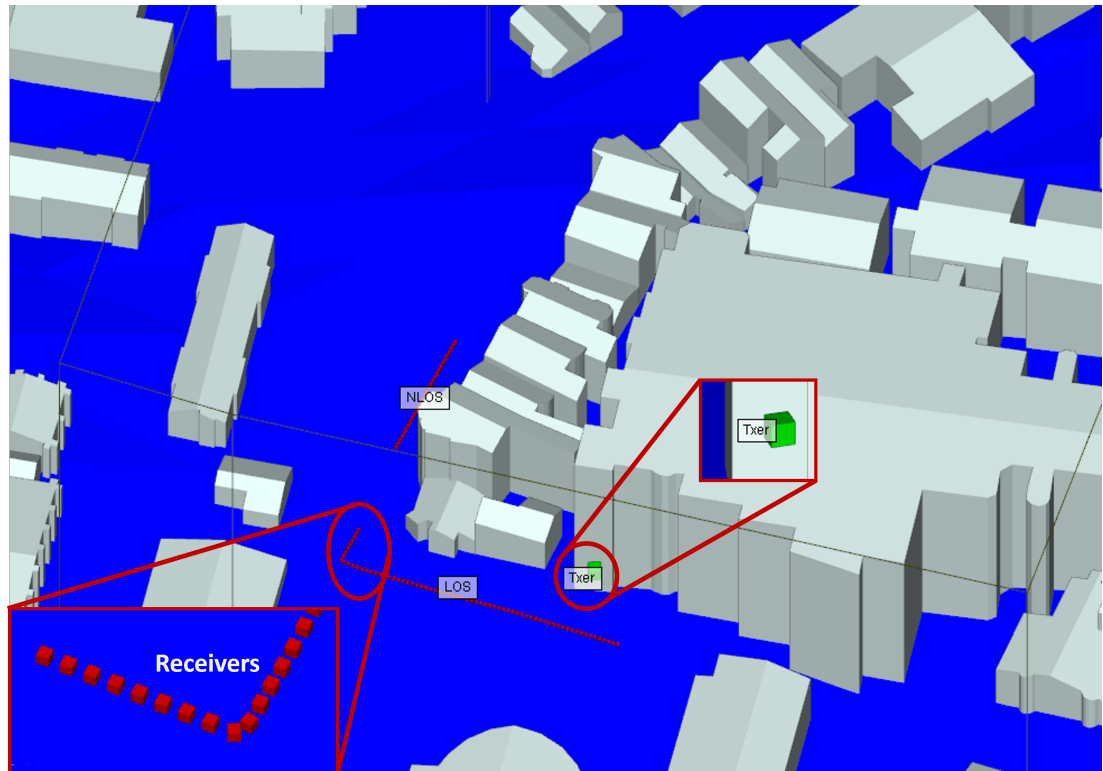
Figure 4.1: UofG scenario for angular and temporal correlation.

4.0.2 MPCs Calculation and Localisation Accuracy

The propagation environment between the transmitter and receiver is pivotal in determining localization accuracy. We define this environment through the channel impulse response, adopting the model from Anjinappa et al. [148]:

$$h(t, \tau, \psi, \theta) = \sum_{k=1}^{\tilde{K}(t)} \rho_k e^{-j\phi_k} \delta(\tau - \tau_k) \delta(\psi - \psi_k) \delta(\theta - \theta_k) \tag{1}$$

This equation serves as the cornerstone for analyzing the multipath effects within a wireless communication system, thereby enhancing the localization techniques through machine learning (ML). Each term in the equation is meticulously designed to represent different aspects of the signal's propagation and interaction with the environment:

- $h(t, \tau, \psi, \theta)$ encapsulates the total multipath environment effect on the transmitted signal, presenting a complex relationship between time, delay, and angles of arrival and departure.

- $\sum_{k=1}^{\tilde{K}(t)}$ aggregates the contributions from all significant multipath components ($\tilde{K}(t)$), which dynamically change over time, reflecting the non-static nature of the environment.

- **Amplitude and Phase (AnP) term** ($\rho_k e^{-j\phi_k}$) distinguishes each multipath component's amplitude (ρ_k) and phase shift ($e^{-j\phi_k}$), which are crucial for understanding signal behavior due to material interactions and propagation delays.

- The **ToA**, **Angle of Arrival (AOA)**, and **Angle of Departure (AOD)** terms are integral for precise localization, indicating the path's arrival time, and its direction at the receiver and transmitter, respectively.

A pivotal aspect of our study is the adaptability in the number of MPCs ($\tilde{K}(t)$) used for localization, which contrasts with the fixed numbers typically employed in prior research. Our methodology dynamically selects the optimal subset of MPCs, informed by a comprehensive analysis of the propagation environment and the specific characteristics of the University of Glasgow (UofG) scenario. This adaptability not only enhances localization accuracy but also demonstrates the model's robustness across various conditions.

Our experimental analysis spans several communication paradigms, including SISO, SIMO, MISO, and MIMO configurations, with a default of 25 paths considered for MPCs. However, this number is not rigid; our approach evaluates and selects the most effective combination of MPCs based on the scenario, thus ensuring the independence of localization accuracy from a fixed number of MPCs. The empirical evidence showcases our approach's efficacy, revealing a consistent relationship between the flexible number of MPCs and enhanced localization precision, particularly within the dynamic and complex UofG scenario.

This flexibility and the subsequent results underscore our contribution to the field of wireless communication, highlighting the potential of ML in advancing localization techniques within varying and unpredictable environments.

To comprehensively evaluate the system's performance across different frequencies, we conducted simulations at six distinct frequency bands: 0.9 GHz, 1.8 GHz, 2.1 GHz, 5 GHz, 5.9 GHz, and 28 GHz. The selection of these frequencies aligns with the investigation conducted by [148]. The study involves the University of Glasgow environment, employing a stationary BS and a UE following a random trajectory. Both single and multi-element directional antennas are used to explore SISO, SIMO, MISO, and MIMO scenarios.

The MPCs calculation procedure considers diverse scenarios, shapes, and data types, encompassing DoA, ToA, and RSSI. Figure 4.2 illustrates the number of MPCs as a function of the multipath component threshold (MPCT) for both Line-of-Sight (LoS) and Non-Line-of-Sight (NLoS) trajectories. The results consistently reveal a constant relationship, underscoring the importance of the independence of the number of MPCs for localization accuracy in the specific scenario, across the investigated frequency bands.
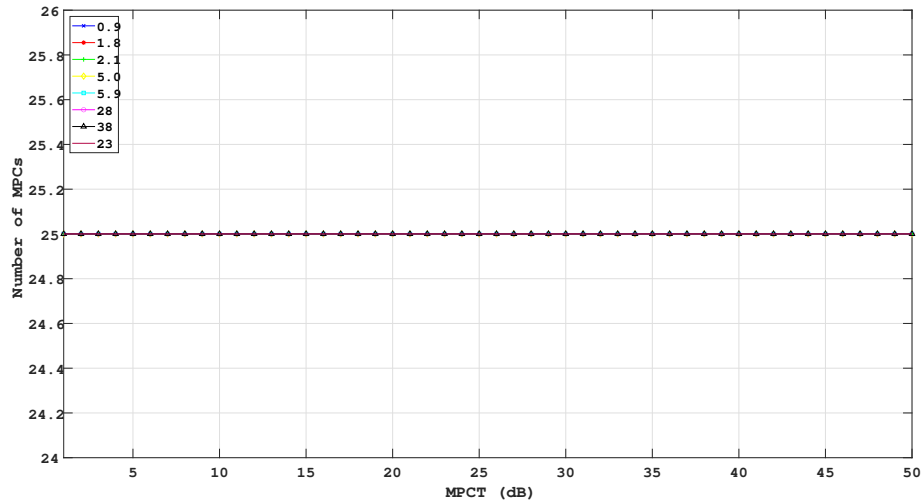
Figure 4.2: Number of MPCs as a function of MPCT for LOS and NLOS trajectory.

Key multipath channel statistics across different frequency bands corresponding to the same vehicular trajectory are provided in Figure 4.1, offering insights into how the V2X propagation behavior is coupled across sub-6 GHz and mmWave bands. Figure 4 plots the average number of (MPCs) as a function of the multipath component threshold (MPCT) at eight frequency bands for both the LoS and NLoS (Figure 4.2) scenarios, respectively. The average number of MPCs remains constant with the MPCT threshold, indicating that, according to the scenario, 25 MPCs can be used, in contrast to what the literature ([148]) (Figure 4.3) suggests i.e., 3 MPCs only. Out of these, the best one will be selected to train the neural network.

After comparing the results with the literature [148] (Figure 4.3), a significant change in the
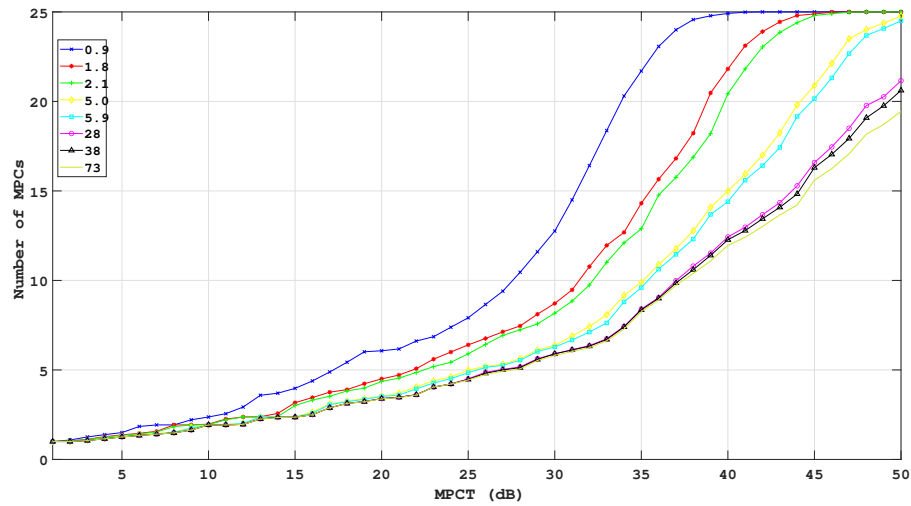
Figure 4.3: Number of MPCs as a function of MPCT for LOS and NLOS trajectory. [[148]]
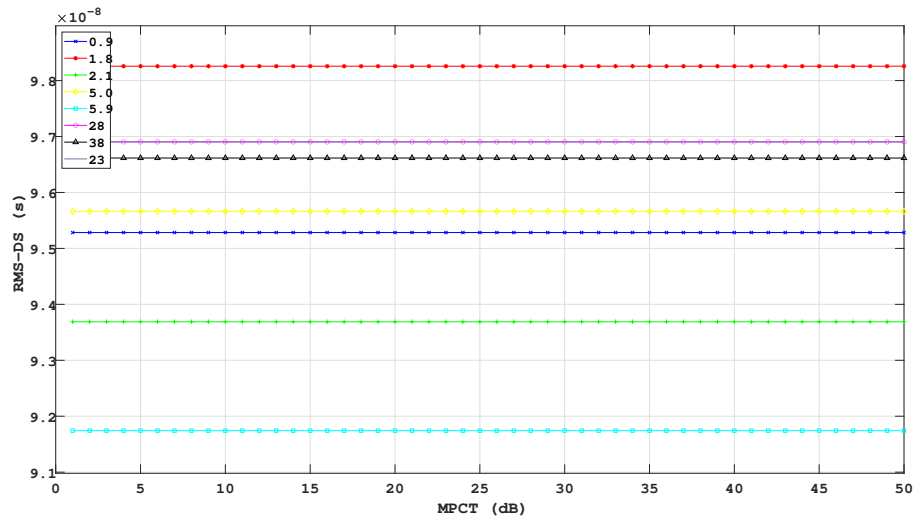
Figure 4.4: RMS-DS as a function of MPCT for LOS and NLOS trajectory.

results is observed when the dominant paths are set to 25 instead of 250. The reason behind this could be the scenario, the number of paths assigned, and the values attained for DoA, DoD, RSSI, and ToA. In short, multiple paths can be used instead of just 3, as the literature ([148]) claims for location estimation.

After that, the concluded MPCs value is implemented in the localisation algorithm to estimate the location information. This work was inspired by Localization with DNN using mmWave Ray Tracing Simulations by [70]. Two different methods were usd by [70] to train a neural network are proposed, one using channel parameters (features) and another using a channel response vector and comparing their performances using preliminary computer simulations. The former approach produces high localization accuracy has been used in this study:
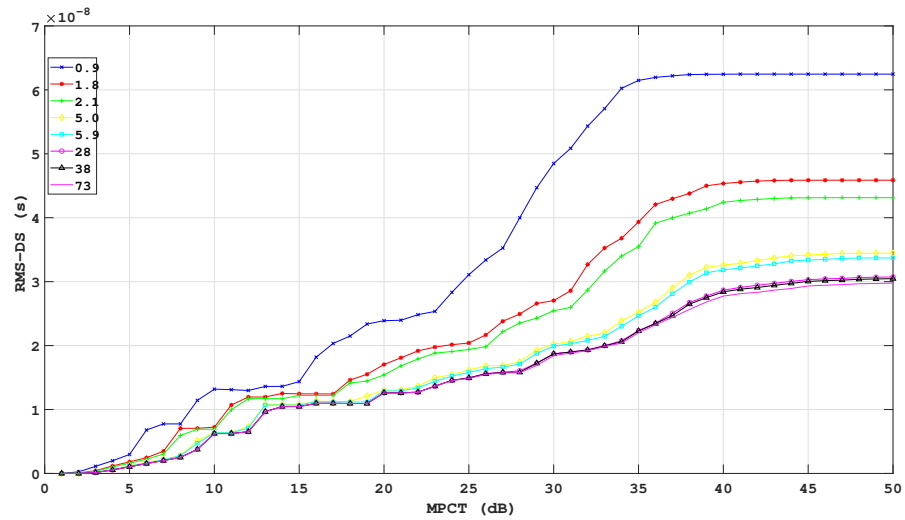
Figure 4.5: RMS-DS as a function of MPCT for LOS and NLOS trajectory.
[[148]]

Figure 4.6: Ray tracing scenario in the Gilmorehill campus of the University of Glasgow, Glasgow, UK.

considering that all users have a fixed number of MPCs, this method relies on the number of MPCs. On the other hand, the latter approach is independent of the MPCs, but it performs relatively poorly compared to the first approach. So, the former approach is tried for high localization accuracy. Given a ray tracing simulation, a DNN is used to predict the location of a UE through supervised learning. Channel parameters like DoA, ToA, and RSSI are used. The combination of DoA, ToA, and RSSI has been used and found the optimized parameters. Then the DNN consists of input i.e., ToA, DoA, and RSSI, which gets optimized and consists of two hidden layers and output in the form of x, and y coordinates. A fixed number of MPCs i.e., 25
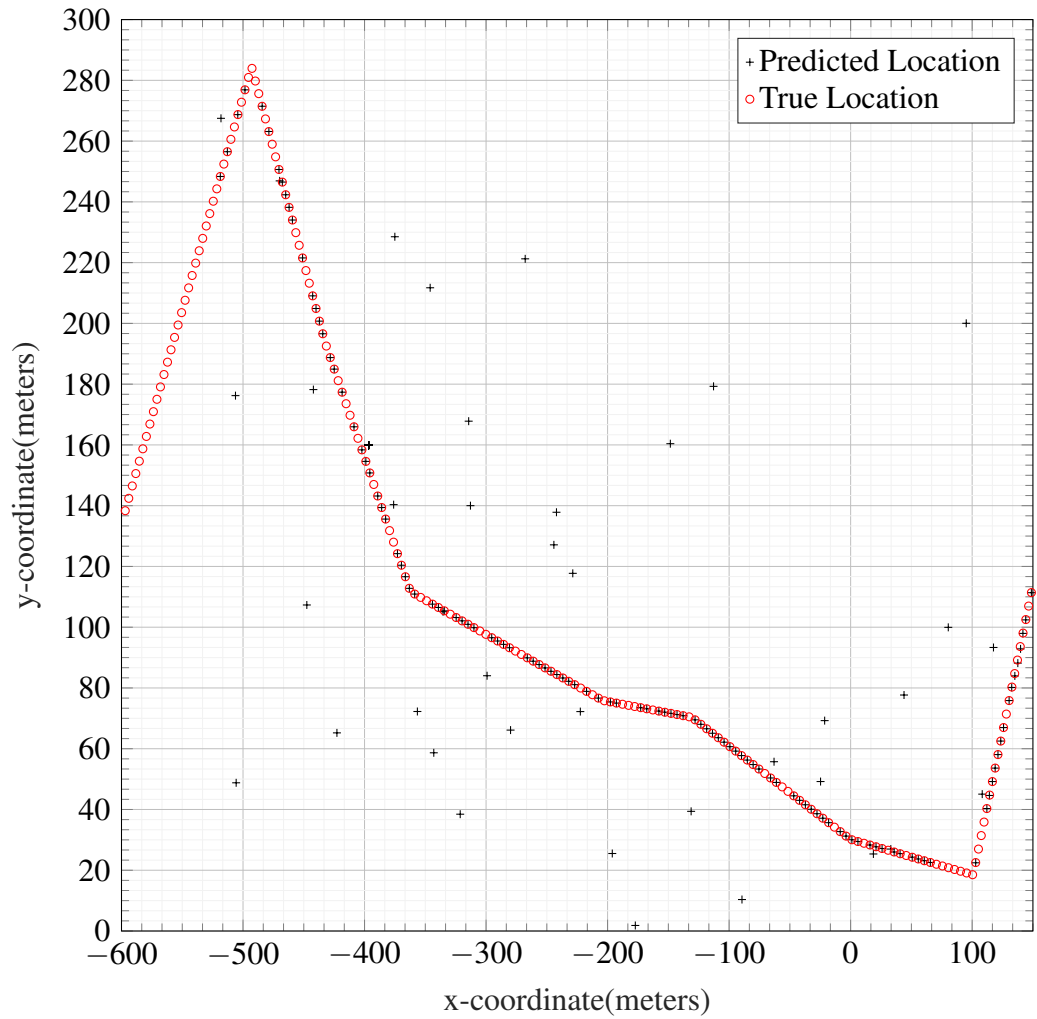
Figure 4.7: The predicted locations with respect to the true locations when using DoA, DoD, RSS and ToA.
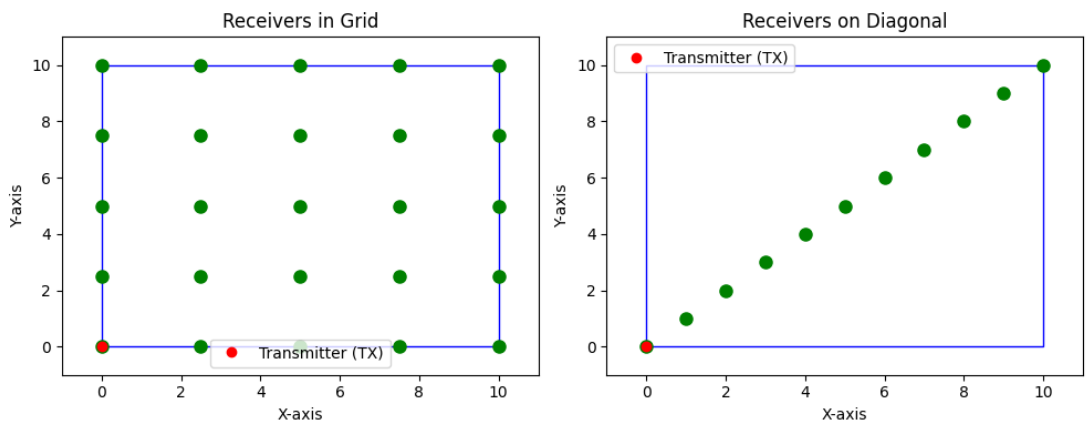
Figure 4.8: Illustration of the open area scenario with transmitters and receivers in grid and route configurations.

is used for each user.
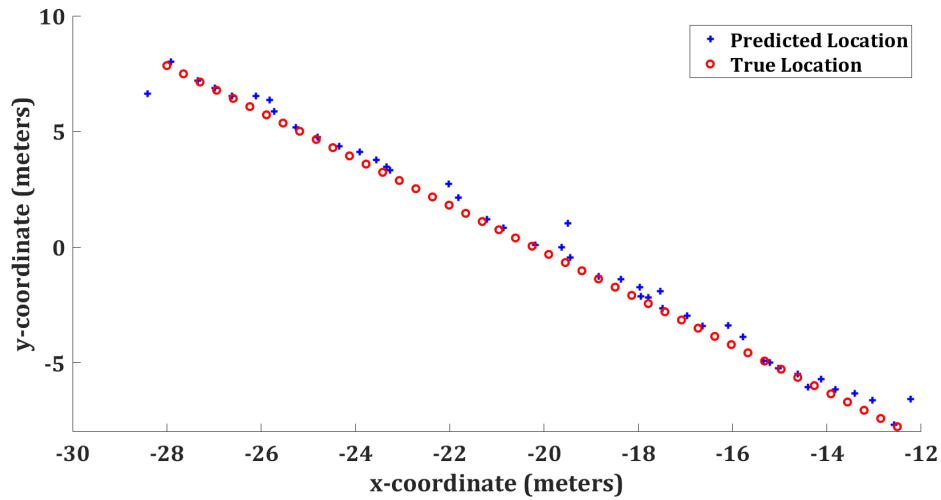
Figure 4.9: Location estimation for a route.
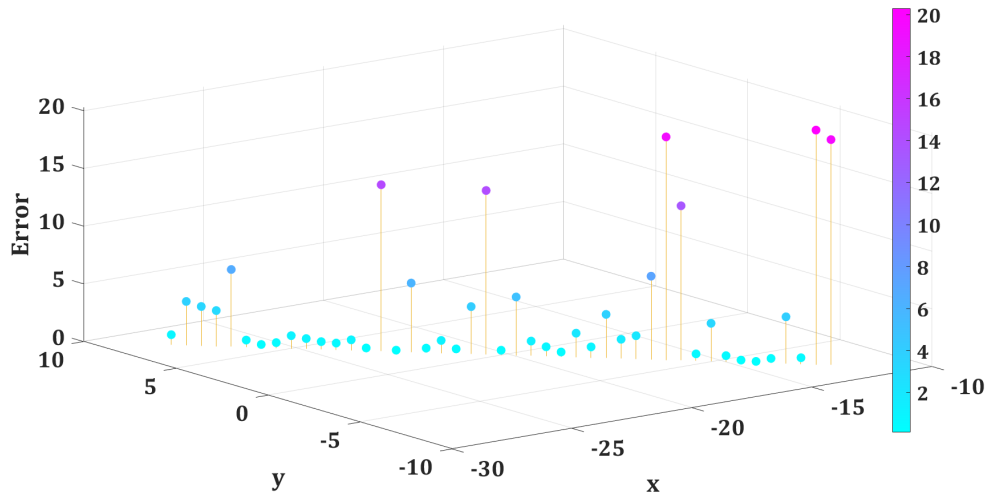
Figure 4.10: Error between the true location and estimated location for a route.

4.0.3 DNN Model for Localization

To optimize the channel characteristics for DNN input, a meticulous feature transformation process is employed. This process involves the extraction of significant features such as Angle of Arrival (AoA), ToA, and Received Signal Strength Indicator (RSSI) from the raw channel data. These features undergo preprocessing to enhance the model's learning efficiency, including normalization to scale the data and feature selection techniques to identify and retain the most informative attributes. This preprocessing step is critical for reducing dimensionality and improving the DNN's prediction accuracy.

In this section, we delve into the training of the DNN model to estimate user locations based on raw channel parameters observed at the BS, as provided by the ray tracing tool. These parameters encompass AoA, ToA, and RSS. The number of model inputs depends on the chosen number of MPCs and the features considered. In our configuration, we set the number of MPCs
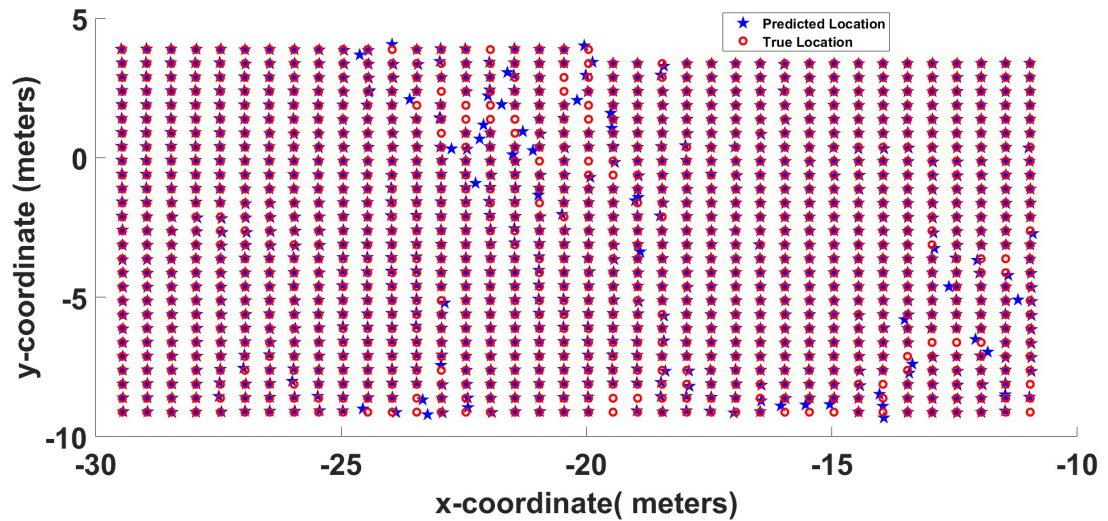
Figure 4.11: Location estimation for a grid.
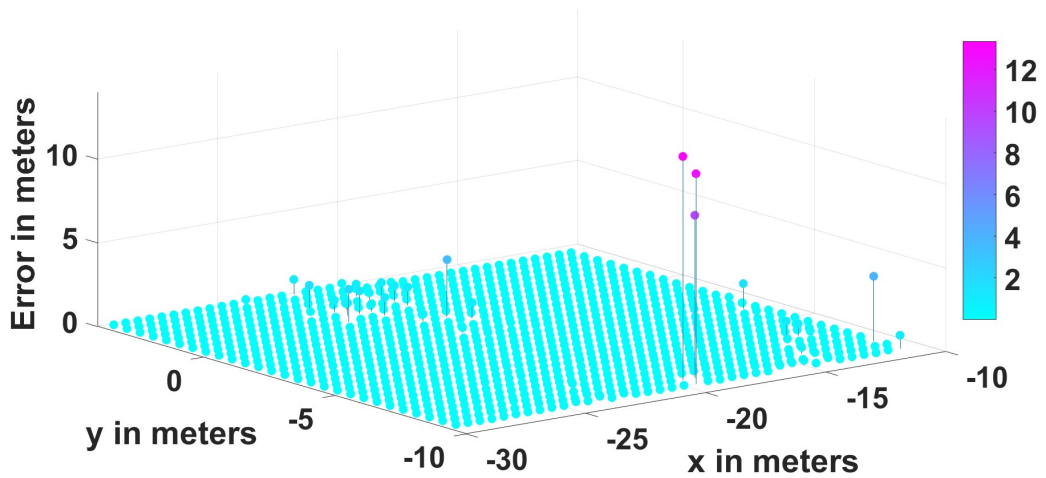
Figure 4.12: Error between the true location and estimated location.

to 25 and included three channel parameters.

4.0.4 Input Features

The number of input features varies depending on the combination of parameters, and it is equal to the product of the number of MPCs and the number of features chosen. We carefully select and normalize these feature combinations for optimal model performance.

4.0.5 Output Labels

The DNN is designed to output the UE's location as Cartesian coordinates, specifically the (x, y) positions. This decision is predicated on the model's application in urban environments where variations in elevation (z-coordinate) are constant and can be reasonably approximated. By

focusing on two-dimensional localization, the model complexity is reduced without significantly compromising the accuracy for the intended use-case scenarios. This approach facilitates a more straightforward interpretation of the results while maintaining the model's applicability across a range of urban settings.

4.0.6   DNN Architecture and Hyper-parameters

The DNN architecture is crafted, featuring an input layer, two hidden layers, and an output layer. The hidden layers comprise 128 and 64 nodes, respectively, and utilize ReLU (Rectified Linear Unit) activation functions to introduce non-linearity into the model. A dropout layer with a rate of 0.5 is introduced between the hidden layers to mitigate overfitting. The output layer employs a linear activation function, suitable for continuous value prediction. This architecture was selected through iterative testing, balancing model complexity with computational efficiency to ensure high localization accuracy. Bayesian optimization serves as the cornerstone for hyper-parameter tuning, facilitating an efficient search through the hyper-parameter space. Parameters such as the learning rate, number of epochs, and batch size are subject to optimization, with the objective function aimed at minimizing the validation loss. The search space is predefined with reasonable bounds for each parameter, ensuring the exploration is both comprehensive and focused. This process significantly contributes to refining the model's performance, striking an optimal balance between accuracy and training efficiency. To evaluate the model's performance, Root Mean Square Error (RMSE) is employed as the primary metric for assessing localization accuracy. This metric provides a clear measure of the average deviation between the predicted and actual UE positions. Model validation is conducted through a stratified train-test split, ensuring a representative distribution of data across both sets. This approach, coupled with cross-validation techniques, ensures the model's robustness and generalizability to unseen data, affirming its reliability for practical applications.

4.1   Experimental Results

To assess the efficacy of our machine learning-enhanced localization technique, we embarked on a series of experiments across two distinctly different scenarios: an open scenario and a scenario specific to the University of Glasgow (GU). These environments were selected to reflect the diverse challenges beamforming faces in 5G wireless communication networks, emphasizing the necessity for precise localization of UE by base stations (BS). The accuracy of such localization is paramount, as it directly influences the effectiveness of beam direction.

The open scenario provided a broad, unobstructed environment to evaluate the influence of multi-path components (MPCs) and various environmental geometries on our localization algorithm. This setting allowed us to dissect the propagation paths and channel responses under different conditions, thereby gauging the adaptability and resilience of our approach.

Conversely, the GU scenario presented a more intricate environment, replete with unique architectural and urban characteristics. This setting served as a litmus test for the practical applicability of our machine learning-based methodology in real-world, dynamic, and complex wireless networks.

4.1.1   Simulation Setup for MPCs Calculation

In this section, we detail the simulation setup for MPCs calculation and present key insights derived from our experiments. Leveraging a DNN-based approach, we employed ML to streamline location estimation in the context of vehicle-to-infrastructure channels across sub-6 GHz and mmWave bands. The MATLAB Bayesian-optimized DNN toolbox facilitated the processing of channel parameters, considering angular and temporal correlations. Our simulations, specific to the University of Glasgow campus, departed from previous experiments, offering a nuanced exploration.

Fig. A.4 provides an overview of the scenario, with receivers capturing a total of 25 MPCs for each vehicle location along the route. Notably, our experiments challenged conventional wisdom by exploring the flexibility in the number of MPCs used for location estimation, contrasting with prior suggestions of using only three paths for neural network training. Our findings unveiled the adaptability of our algorithm to different scenarios, advocating for a more inclusive approach to MPCs selection.

The exploration of the MPCT demonstrated its impact on channel statistics. Surprisingly, our results indicated the effective utilization of various MPCT values, debunking the notion of a fixed threshold. By adopting a range of MPCT values in our data processing, we showcased the algorithm's adaptability and automatic optimization. Furthermore, our experiments illuminated the consistency of channel statistics, such as RMS-DS, across MPCT values, affirming the robustness of our approach. In summary, our findings challenge established practices and underscore the algorithm's resilience in diverse scenarios.

4.1.2   Context and Methods

Location estimation's fundamental role in enabling efficient beamforming guided our exploration of channel parameters, including AoA, DoA, DoD, RSSI, ToA, and Delay. Different path types, including LoS and NLoS, were scrutinized. The incorporation of MPCs into the localization algorithm, comparing two approaches—one based on channel parameters and the other on a channel response vector—highlighted the former's superior performance.

4.1.3   DNN-Based Localization Algorithm

Our experiments aimed to minimize the mean error between known and estimated outputs for x and y coordinates. The following pseudocode 2 was used to perform the location estimation:

Algorithm 2 Proposed location estimation

    Data processing
    Input Raw dataset
    Initialize an accumulator $\mathbb{A}$ for processed data
    Calculate the number of raw data entries
    for Each raw data entry **do**
        Extract DoA, ToA, and Location
        Extract features (e.g., Delay, Azimuth, RSS)
        Store the set of features & location in $\mathbb{A}$
        Save $\mathbb{A}$
        Train & test neural network
        Load the Training dataset from $\mathbb{A}$
        Initialize neural network hyperparameters
        Optimize hyperparameters with Bayesian optimization
        Train Neural Network with optimized hyperparameters
        Load Testing dataset from $\mathbb{A}$
        Test trained neural network on Testing dataset
        Visualize predicted locations against ground truths.
    end for

4.1.4   Simulation Scenarios and Results

Simulations in open scenarios, depicted in Fig. 4.8, unfolded in grid and route configurations. Location estimation results for route and grid receivers, along with error analysis, are visualized in Fig. 4.9, Fig. 4.10, Fig. 4.11, Fig. 4.12. The figures offer valuable insights into the accuracy of location estimations in diverse scenarios. The exploration of MPCs variations and canonical shapes enriched our understanding of propagation paths and channel responses, challenging traditional practices.

    Our experiments underscore the importance of path number and placement for localization, challenging established norms. Visual representations accompany these findings, providing context and clarity to our results.

4.1.5   Simulation Context

Situated at the Gilmorehill campus, the small cell scenario operated at a carrier frequency of 3.75 GHz. The setup included a set of receivers capturing vehicle movement along defined routes at different speeds. The simulation parameters incorporated MIMO directional array antennas,

transmitter power, down-tilt and receiver sensitivity. Simulations were executed using Wireless InSite® MIMO version 3.3 on a high-performance computing platform.

4.1.6 Simulation Results

Fig. 4.13 visually presents predicted UE locations with respect to true locations, utilizing DoA, DoD, RSSI, and ToA. The results demonstrate the efficacy of the algorithm, achieving approximately 97% coverage in NLoS areas. The study illuminates the potential of high-accuracy localization for both LoS and NLoS scenarios using advanced antenna systems.
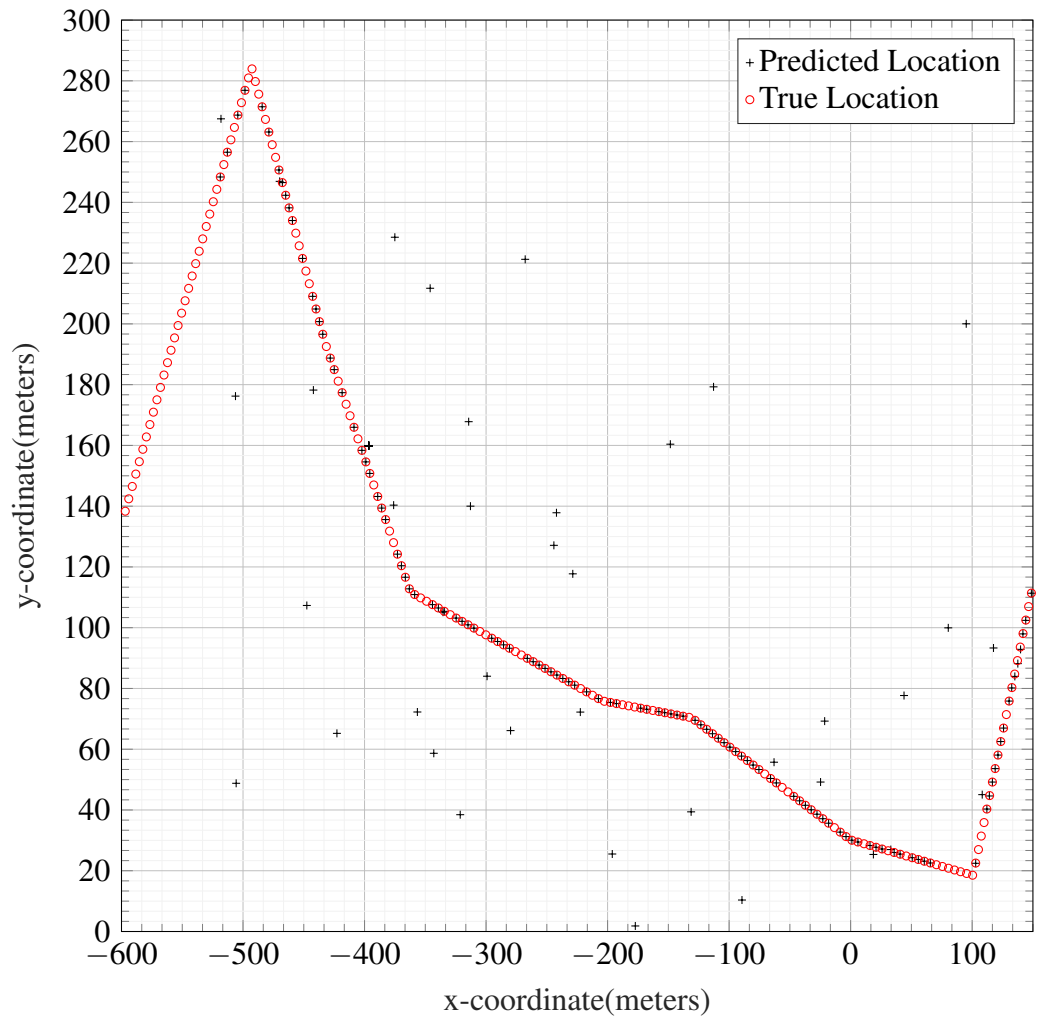
Figure 4.13: The predicted locations with respect to the true locations when using DoA, DoD, RSS and ToA.

Alt Text: Comparative analysis showing predicted versus true locations in a localization experiment, highlighting the accuracy of using DoA, Direction of Departure (DoD), Received Signal Strength (RSS), and ToA in determining UE positions.

4.2 Conclusion

In this work, we present a novel method for improving wireless network localization through the use of ML algorithms. To build a DNN on the base station (BS) side, our methodology used channel features and location data obtained from a ray-tracing model as input features and output labels. Our experiments' findings provide insight into the complex effects of various environmental configurations and scenarios on the precise localization prediction of UE, especially when datasets based on DoA, ToA, and RSSI are used. The study demonstrated the efficacy of utilizing MIMO antennas in addressing (NLoS) areas, resulting in a notable enhancement in the precision of UE location predictions. Our work marks a significant contribution to the evolving landscape of ML-driven localization in wireless networks. As technologies such as 5G and beyond continue to advance, our findings provide valuable insights into the potential for enhancing network performance by integrating ML-based localization techniques.

Chapter 5

Integration of Real-World Data Acquisition

This chapter aims to elucidate the transition from simulated data collection to actual data acquisition using the in-house setup, specifically leveraging the capabilities of the TSMA 6 scanner at the University of Glasgow. It underscores the methodology adopted for gathering real-time data through various modalities, including pedestrian movement, vehicular mobility, and robotic maneuvering, to understand and analyze the dynamics of 5G network performance within and around the JWS and JMS buildings of the university.

5.1   Introduction to TSMA6 in Real-World Data Collection

The TSMA6 scanner emerges as a cornerstone in this venture, facilitating the intricate process of capturing and analyzing the radio frequency (RF) spectrum in real-time. This state-of-the-art device is adept at scanning and dissecting the RF spectrum, providing invaluable insights into the spectral environment crucial for the development and refinement of wireless communication systems.

5.1.1   Understanding TSMA6

The TSMA6 is engineered to offer a wide frequency range, covering the spectrum from low-frequency bands used in IoT devices to the higher frequencies pertinent to 5G cellular and Wi-Fi networks. Its high sensitivity allows for the detection of weak signals, a critical attribute for analyzing signal strength across various scenarios. The real-time spectrum analysis capability of the TSMA6 ensures instantaneous monitoring and visualization of the RF spectrum, offering a dynamic view of the radio environment. The modular architecture of the scanner accommodates diverse antenna options and additional modules, enhancing its versatility and application in specialized measurements.

5.1.2 TSMA6's Role in Real-Time Data Generation

In the context of real-time data generation at the University of Glasgow, the TSMA6 scanner is instrumental in:

Concurrent Signal Capture: Operating alongside the in-house data generation setup, it captures signals in real-time, facilitating a comprehensive dataset that includes a wide array of signal information.

Enhanced Frequency Coverage: The inclusion of TSMA6 extends the frequency coverage, enabling the study of communication scenarios across diverse frequency bands.

Improved Spectrum Awareness: The real-time spectrum analysis capabilities of the TSMA6 augment the overall spectrum awareness, providing detailed insights into frequency occupancy, signal strengths, and interference patterns.

5.2 Data Collection Methodology

Leveraging the TSMA6 scanner and the QualiPoc interface, the data collection process extends to various modalities including walking, driving, and the deployment of robots to mimic different real-world scenarios such shown in Figure 5.1. The primary focus is on gathering critical parameters like RSRP (Reference Signal Received Power), TOA (Time of Arrival), and DOA (Direction of Arrival), essential for the localization algorithm. The dataset looks as shown in Figure 5.3.

Figure 5.1: Real-time data collection at UofG.

Figure 5.2: TSMA6 scanner and QualiPoc.

```
[DESCRIPTION]
Timestamp [hh:mm:ss]
GPS\Position\Latitude [°] : [1]
GPS\Position\Longitude [°] : [1]
GPS\Position\Altitude [m] : [1]
GPS\Position\Distance (GPS) (obsolete) [m] : [1]
GPS\Speed Info\Speed [km/h] : [1]
GPS\Speed Info\Heading [°] : [1]
5G NR Scan\Template Signals\Top N ToA(PPS) [<Auto>@630680[3]\Mbr 1] [ms] : [1]
5G NR Scan\Template Signals\Top N RSSI [<Auto>@630680[3]\Mbr 1] [dBm] : [1]
5G NR Scan\Template Signals\Top N ToA(CIR) [<Auto>@630680[3]\Mbr 1] [ms] : [1]
5G NR Scan\Template Signals\Top N SS-SINR [<Auto>@630680[3]\Mbr 1] [dB] : [1]
5G NR Scan\Template Signals\Top N SS-RSRP [<Auto>@630680[3]\Mbr 1] [dBm] : [1]

[DATA]
Timestamp [hh:mm:ss]    GPS\Position\Latitude [°] : [1] GPS\Position\Longitude [°] : [1]        GPS\Position\Altitude [m] : [1] GPS\Position\Distance (GPS)
11:56:28       47.471828       19.062922       190.02  0       0.04    212.41  ?       ?       ?       ?       ?
11:56:29       47.471697       19.062931       173.19  14.54   0.05    212.41  ?       ?       ?       7.97    ?
11:56:29       47.471697       19.062931       173.19  14.54   0.05    212.41  ?       ?       ?       ?       -85.39
11:56:29       47.471671       19.062933       169.78  17.49   0.05    212.41  ?       -71.99  6.89786549      ?       ?
11:56:29       47.471669       19.062933       169.56  17.68   0.06    212.41  ?       ?       ?       11.45   ?
11:56:29       47.471669       19.062933       169.56  17.68   0.06    212.41  ?       ?       ?       ?       -85.32
11:56:30       47.471643       19.062935       166.17  20.61   0.06    212.41  ?       -75.06  6.89786617      ?       ?
11:56:30       47.471641       19.062935       165.95  20.8    0.06    212.41  ?       ?       ?       14.53   ?
11:56:30       47.471641       19.062935       165.95  20.8    0.06    212.41  ?       ?       ?       ?       -85.53
11:56:30       47.471615       19.062937       162.55  23.73   0.06    212.41  ?       -79.01  6.8978625       ?       ?
11:56:30       47.471613       19.062937       162.34  23.92   0.06    212.41  ?       ?       ?       14.08   ?
11:56:30       47.471613       19.062937       162.34  23.92   0.06    212.41  ?       ?       ?       ?       -85.74
11:56:30       47.471587       19.062939       158.94  26.85   0.06    212.41  ?       -78.93  6.89786745      ?       ?
11:56:30       47.471585       19.062939       158.72  27.04   0.07    212.41  ?       ?       ?       14.26   ?
11:56:30       47.471585       19.062939       158.72  27.04   0.07    212.41  ?       ?       ?       ?       -85.35
11:56:30       47.471559       19.062941       155.31  29.99   0.07    212.41  ?       -77.26  6.89787073      ?       ?
11:56:30       47.471557       19.062941       155.09  30.18   0.07    212.41  ?       ?       ?       14.09   ?
```

Figure 5.3: Dataset from UofG campus (example).

5.2.1 Experimental Setup and Data Acquisition

The TSMA6 scanner, equipped with an RF antenna, a GPS module, and interfaced with the QualiPoc application on a 5G-enabled smartphone, forms the core of our data collection setup. The process facilitated the extraction of parameters critical to the localization algorithm, with RSRP values and TOA data being particularly emphasized. These parameters were collected in
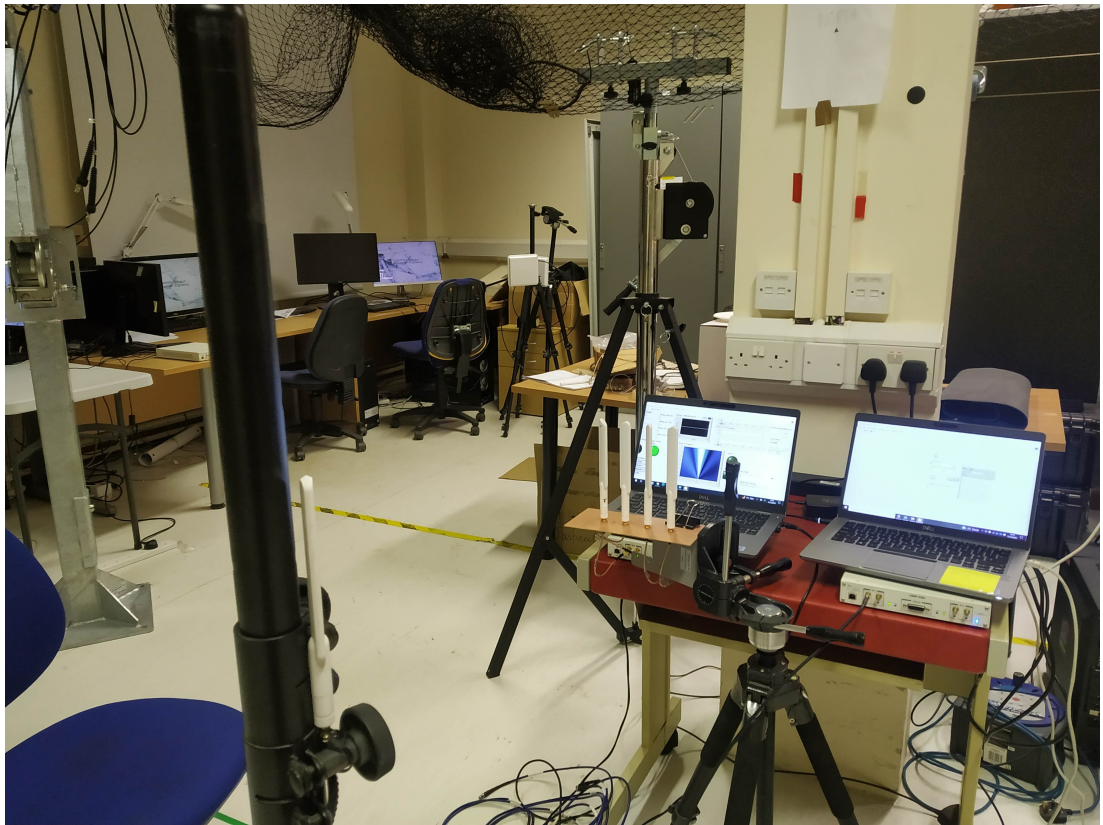
Figure 5.4: DoA setup schematic.

various settings around the JWS and JMS buildings, leveraging the 5G antennas installed both inside and outside these structures to capture a diverse set of data reflective of different user environments and mobility patterns. Figure 5.1 illustrates the real-time data collection setup at the UofG.

5.2.2 Addressing Limitations and Advancements

Despite the comprehensive capabilities of the TSMA6 scanner, it lacks the provision of DOA information directly. To circumvent this, a dedicated DOA setup, involving Universal Software Radio Peripherals (USRPs) and an antenna array system, is under development. This initiative aims to complement the data gathered through the TSMA6, enriching the dataset with accurate DOA measurements critical for refining the localization accuracy.

5.2.3 Impact and Implications

The deployment of the TSMA6 scanner for real-time data collection at the University of Glasgow represents a significant step forward in the practical examination and analysis of 5G network performance. The data gathered from this real-world setting is instrumental in validating the simulated models and enhancing the accuracy of localization algorithms. Moreover, this

initiative highlights the importance of incorporating sophisticated tools like the TSMA6 in the realm of wireless communication research, paving the way for innovative solutions in the optimization and deployment of 5G networks.

Chapter 6

Utilizing Software-Defined Radio for DoA Estimation

The quest for enhancing localization accuracy in wireless networks necessitates precise estimation of the DoA of signals. To address the limitations encountered with conventional data collection methods, particularly the inability of TSMA6 to provide DoA information, we turned our focus towards Software-Defined Radio (SDR) technology. SDR offers a flexible and innovative approach to signal processing, allowing for the dynamic adaptation of software to modify the radio system's behavior. This chapter delineates our journey in harnessing the capabilities of SDRs, specifically the BladeRF and the X300/X310 models, to achieve accurate DoA estimation essential for refining localization techniques in 5G networks.

6.0.1 Introduction

Software Defined Radio (SDR) is a term employed to describe radio systems where the bulk of their functions are executed through software, diverging from the prevalent hardware-centric approach observed in many recent Radio Frequency (RF) applications. An exemplary depiction of an ideal SDR is illustrated in Figure 6.1. In this conceptual framework, the RF Front End is streamlined, comprising solely a power amplifier and a high-speed Analog to Digital Converter (ADC). Consequently, the remaining tasks concerning the physical layer, including tasks like modulation, synchronization, and encoding, are undertaken through the application of Digital Signal Processing (DSP) techniques [149].

SDR systems are anticipated to operate across a broad frequency spectrum and fulfill a range of functions similar to those achievable through dedicated hardware implementations. For instance, employing a cost-effective SDR unit to tune into a local FM radio station or to intercept an Orthogonal Frequency Division Multiplexing (OFDM) signal utilizing Quadrature Amplitude Modulation (QAM) modulation in the 2.4 GHz band are among the prevalent and versatile applications of SDR systems.
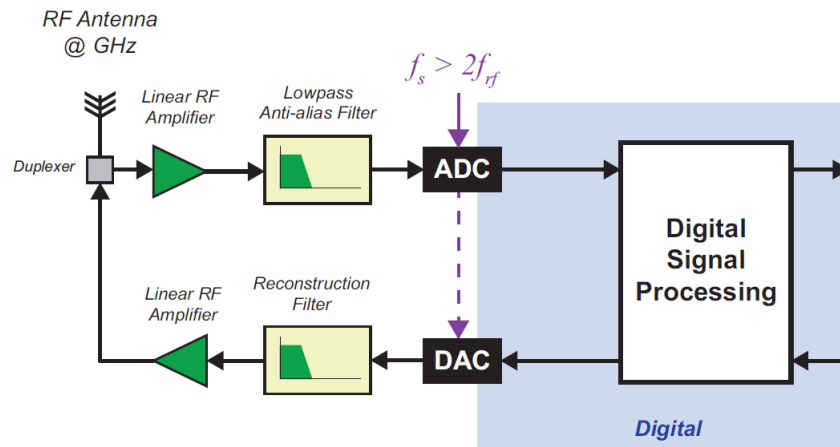
Figure 6.1: Ideal SDR block diagram. [149]

6.0.2 Hardware and Flexibility

6.0.2.1 Model-Based Design and Hardware in the Loop

In contrast to traditional radio units that rely on specialized hardware to process specific incoming signals, SDR hardware possesses a generic quality, enabling it to handle data across various frequencies and modulation schemes. This versatility is often facilitated by incorporating a Field Programmable Gate Array (FPGA) within the SDR radio. FPGAs within the domain of Digital Signal Processing (DSP) offer higher processing speeds and efficiency compared to microcontrollers. This advantage is attributed to the presence of dedicated DSP slices within the silicon, fostering faster processing suitable for RF applications, alongside the availability of tools for designing and simulating RF systems.

High-Level Synthesis (HLS) systems, such as MATLAB/Simulink, Python, or SystemC, serve to model an RF system, simulate it for proper tuning and debugging, and subsequently generate Hardware Description Language (HDL) code to program the physical hardware in line with the model. This design process is known as Model-Based Design. HLS software may also incorporate specific tools to expedite the implementation of particular hardware or software processes, further streamlining the model generation process.

Another prevalent design methodology is the Hardware in the Loop (HIL) approach. Similar to Model-Based Design, HIL employs high-level modeling software like MATLAB/Simulink or GNU Radio to craft an algorithmic representation of the system, incorporating the SDR as an integral component of the model. However, HIL diverges from Model-Based Design in that it doesn't involve generating custom HDL to run on the FPGA. Instead, it employs the SDR as a signal source and sink, allowing the computer to execute the intended algorithm. HIL models are relatively quicker for testing and validation compared to Model-Based Design, and they are also easier to create since subsystems aren't compiled into HDL. However, a performance trade-off emerges, as the algorithm isn't entirely executed in hardware.

6.0.2.2   Transceiver Architectures

A crucial phase within Software Defined Radios (SDRs) is the Analog-to-Digital (AD) and Digital-to-Analog (DA) conversion architecture. This architecture comprises three distinct methods to acquire or generate signals.

The Heterodyne architecture, the oldest among the trio, entails a physical downconverter achieved through a mixer and a local oscillator (LO). This technique shifts the received broad-spectrum signal to the baseband, facilitating sampling by the Analog-to-Digital Converter (ADC). Conversely, in cases where a signal is generated, the architecture shifts the signal to a higher frequency using the Digital-to-Analog Converter (DAC).

The direct conversion architecture, also recognized as Zero-Intermediate Frequency (Zero-IF), augments bandwidth efficiency by incorporating a second Heterodyne converter. The LO signal for this second converter is phase-shifted by $90°$. This configuration facilitates the generation of two independent data streams - the In-Phase and Quadrature (IQ) signals.

Lastly, the Direct Sampling architecture accomplishes signal conversion between the broadband and baseband domains through software. This approach is the most demanding, demanding Analog-to-Digital Converter (ADC) and Digital-to-Analog Converter (DAC) units with sampling rates in the hundreds to thousands of megahertz range. Nevertheless, this method delivers unparalleled flexibility, as the signal can be conveniently manipulated even during up-conversion processes.

The Direct Conversion architecture is widely adopted by a significant portion of SDRs available on the market. This architecture boasts compatibility with various signal types, like AM, FM, PSK, and QAM. Notably, many SDRs are designed with RF front-ends integrated into a single integrated circuit (IC). These ICs consolidate essential components such as a power amplifier, mixer, RF filter, and analog-to-digital converter (ADC) or digital-to-analog converter (DAC). This integration is augmented with a data interface, rendering it suitable for utilization alongside a range of microcontrollers. Notably, numerous ICs of this nature also encompass multiple coherent transmit (TX) and receive (RX) channels, all of which can be driven by a single local oscillator (LO). Noteworthy manufacturers in the domain of transceiver ICs include Lime Microsystems and Analog Devices.

6.0.3   Available Software-Defined Radio Units

A diverse array of SDR units are readily available for purchase today, catering to a broad spectrum of research, industrial, educational, and hobbyist applications. Prominent manufacturers like Ettus Research and National Instruments dominate the SDR market, offering feature-rich devices tailored for advanced research and industrial utilization. These devices typically encompass a host of attributes, including full-duplex capability, high-performance Field Programmable Gate Arrays (FPGAs), extensive frequency coverage (including mm-wave support), wide base-

(a) Heterodyne receiver

(b) Direct conversion receiver

(c) Direct sampling receiver
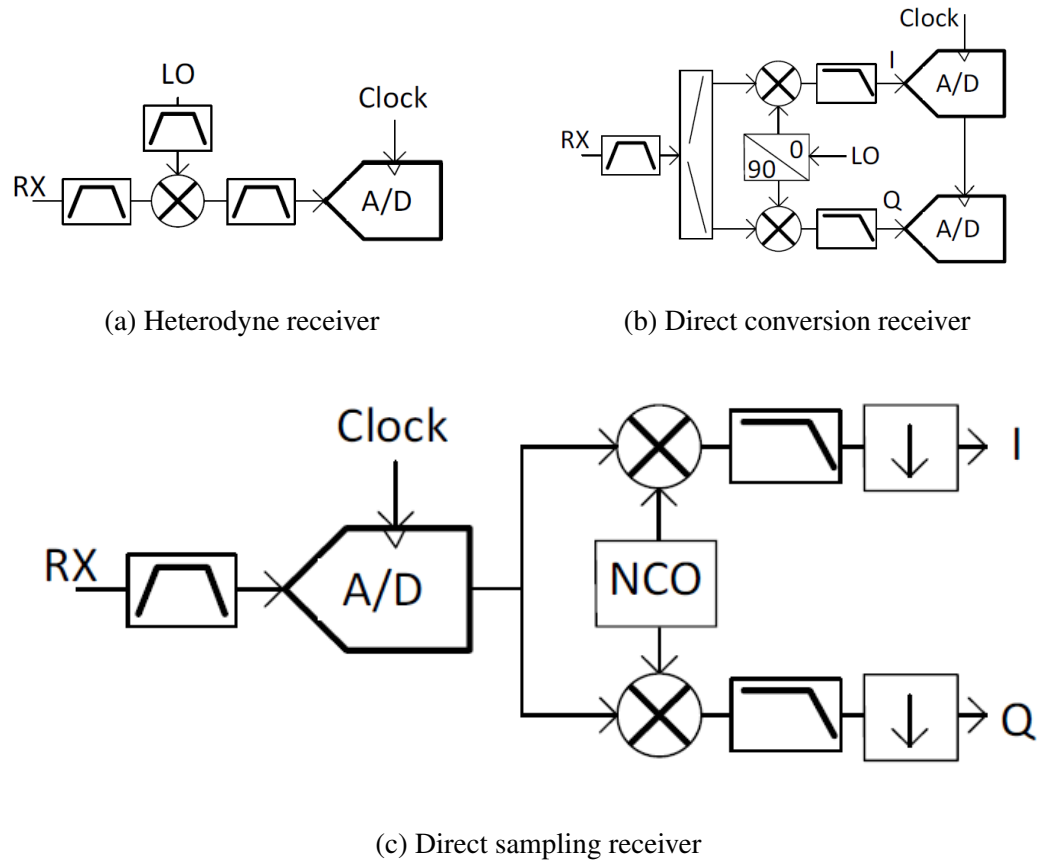
Figure 6.2: Receiver Architectures. [150]

band bandwidth, Multiple-Input Multiple-Output (MIMO) capabilities, and compatibility with established development tools.

Concurrently, there exists a range of SDR units designed with students, hobbyists, and budget-conscious engineers in mind. These platforms cater to individuals who might not have the financial means to invest in devices from the aforementioned manufacturers. Devices like RTL-SDR, LimeSDR, HackRF, BladeRF, and PlutoSDR exemplify this budget-friendly category. Notably, most of these devices are borne out of open-source initiatives, except for the PlutoSDR, which is backed by Analog Devices. These devices come with varying degrees of capability and compatibility, often representing community-driven efforts. Analog Devices, for instance, supports the development and production of the PlutoSDR, which is primarily intended to aid students in acquiring hands-on experience with digital communication systems.

6.1 Beamforming in Software-Defined Radio

SDR present an ideal platform for implementing beamforming, primarily because the technology's antenna array configuration, rather than its signal processing capability, is the key requirement. SDRs, especially those available commercially, are equipped with the hardware necessary
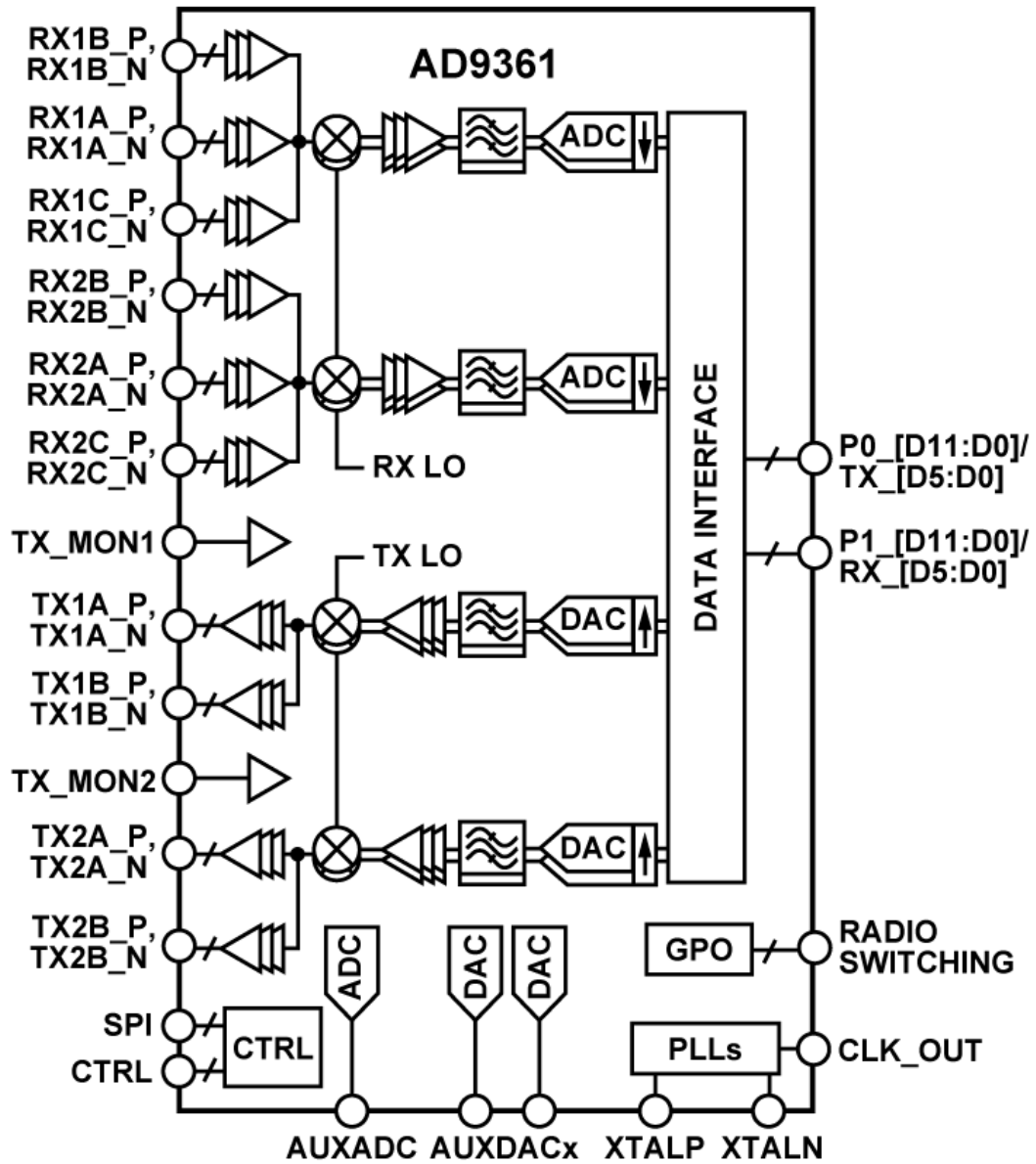
Figure 6.3: Block diagram of the AD9361 RF transceiver. [150]

SDR	Ettus B210	Hack RF	RTL-SDR	LimeSDR	PlutoSDR	BladeRF 2
Max Freq	6 GHz	6 GHz	1.7 GHz	3.8 GHz	3.8 GHz	6 GHz
Interfacing	USB3.0	USB2.0	USB 2.0	USB3.0	USB 2.0	USB3.0
Sample Depth	12-bit	8-bit	8-bit	12-bit	12-bit	
Duplex	Full	Half	N/A	Full	Full	
MIMO	2x2	1x1	0x1	2x2	1x1	2x2
TX Power	10 dBm	15 dBm	N/A	10 dBm	7 dBm	8 dBm

Table 6.1: SDR comparison table [151, 152, 153]

to manage multiple antennas, making digital beamforming the most practical approach. Implementations leveraging SDRs, such as those detailed in [154, 155], have utilized specialized hardware to streamline the setup of multiple SDR units. In these cases, LabVIEW facilitated the control and monitoring of the antenna array, demonstrating the potential of advanced SDR equipment. It's important to note, however, that replicating these configurations with budget-friendly SDRs can require more effort, expertise, and sometimes hardware tweaks. Digital beamforming can be susceptible to various non-ideal conditions like correlation errors, mixer frequency deviations, and unsynchronized oscillators. These factors demand careful consideration during the design process [156]. Fortunately, many such challenges have been addressed by SDR manufacturers. Yet, synchronization remains a pivotal concern for SDR-based beamforming systems.

6.1.1 Coherence and Synchronisation

Achieving successful digital beamforming necessitates either coherence or pseudo-coherence between the transmitter and receiver, ensuring a consistent phase relationship across channels. Additionally, the analog-to-digital converters (ADCs) and digital-to-analog converters (DACs) across channels must have precisely aligned sampling clocks.

A straightforward method for phase synchronization involves distributing a local oscillator (LO) signal to each SDR. However, this can introduce noise that adversely affects beamforming performance. An alternative is to maintain individual LOs for each SDR, using a low-frequency trigger signal to keep the LOs aligned without needing a pristine signal source.

6.1.2 Interfacing

The need for data transfer from multiple antennas significantly increases the interfacing bandwidth requirement from the SDR to the processor. For example, a four-element antenna array, each sampled at 10 MSPS with 32-bit IQ samples, demands a throughput of 1.28 Gbps, far exceeding the capabilities of USB 2.0 and necessitating faster protocols like USB 3.0 or Ethernet. The actual throughput achievable is highly dependent on the protocol and frame size. Designers can adjust sample rates, and SDRs vary in bit depths, offering flexibility to meet different throughput needs.

6.1.3 Transceiver Architecture

SDRs typically utilize external transceiver ICs with a Direct-Conversion architecture, limiting signal processing to the baseband and favoring phase-shift beamforming. This approach converts time delays into phase shifts within the signal's I and Q components but has limitations, such as a constrained steering angle and potential for non-ideal radiation patterns. Conversely, more versatile architectures allow for true time-delay beamforming, which is adaptable even in

broadband spectrums and avoids the steering angle limitations inherent in phase-shift beamforming. Despite its advantages, true time-delay beamforming demands picosecond-level sampling rates, challenging for budget ADCs and DACs.

SDR technology offers a promising avenue for beamforming applications, provided challenges like synchronization and interfacing bandwidth are adequately addressed. While each beamforming technique has its limitations, the flexibility of SDRs allows for innovative solutions that can meet the demands of various applications.

6.2   DOA Setup using SDRs

In this chapter, we delve deeper into the practical implementation of our research, bridging the gap between the theoretical underpinnings of beamforming discussed in Section 6.1 and its real-world application. While the previous section laid the foundation for understanding beamforming concepts, this chapter focuses on the "why" and "what" aspects of our research.

The primary goals of our work encompassed not only the technical implementation but also the rationale behind it. Our research aimed to address critical questions such as:

- **Why Beamforming?**: Beamforming techniques offer the promise of enhancing signal reception and transmission, particularly in wireless communication systems. The ability to direct signals precisely to or from specific locations has far-reaching implications for improving system performance, reducing interference, and enabling new applications.

- **What Are the Challenges?**: Implementing beamforming in real-world scenarios poses numerous challenges, including hardware integration, data acquisition, signal processing, and localization. Identifying and overcoming these challenges were integral aspects of our research.

With these questions in mind, our investigation encompassed two distinct tests to assess the accuracy of the DoA estimation. The first approach involved utilizing USRP in conjunction with LabVIEW. The second approach leveraged MATLAB in tandem with the BladeRF platform. These tests aimed to scrutinize the effectiveness of DOA estimation methodologies under varying conditions.

Furthermore, our exploration extended to localization techniques, wherein Channel State Information (CSI) data was employed. Through the integration of USRPs and LabVIEW, real-time data collection was facilitated, enabling the processing of location estimation using ML algorithms. This multifaceted investigation sought to ascertain the viability and precision of localization techniques through the fusion of sophisticated hardware, software, and ML methodologies.

6.2.1   DOA Set-up using MATLAB and BladeRF

A comprehensive simulation model of a downlink end-to-end communication system was crafted to assess the efficacy of the implemented beamforming algorithm in both the transmitter and

receiver components. The primary objective of this section entailed crafting a functional beamforming model that seamlessly caters to both transmitting (TX) and receiving (RX) arrays. In pursuit of this aim, the Hardware-in-the-Loop (HIL) approach emerged as an appealing strategy due to its potential to reuse the subsystems of the simulation within the HIL model, necessitating only minor adjustments.

6.2.1.1   Implementation and Testing

For the realization of this simulation, Simulink emerged as the chosen platform due to its adeptness in accommodating a wide array of algorithms and models pertinent to digital communications. Additionally, Simulink supports HIL workflows, thereby harmonizing well with various SDR.

Throughout the developmental process, numerous iterations of the end-to-end simulation were conceived, each progressively enriched with additional features and embedded with real-world impairments and characteristics. The creation and refinement of the simulation and its constituent subsystems occurred in tandem, subsequently undergoing rigorous testing within diverse models.

The culmination of these iterative efforts yielded a finalized simulation model characterized by several crucial subsystems. A visual representation of the ultimate model is showcased in Figure 6.4, encapsulating the intricate interactions and interdependencies within the simulated downlink end-to-end communication system.

The simulation incorporates the following crucial subsystems, each contributing to the overall functionality of the system (Figures 6.4 and 6.5):

- UE's movement pattern

- Modulator at the base station

- Receiver at the user's equipment

- TX beamformer at the base station

- RX beamformer at the UE

- Wireless channel

Analogous to the subsystems, a MATLAB script was devised to facilitate the management of parameters within these system blocks. The script serves the dual purpose of automating parameter modifications and linking them with relevant equations associated with each subsystem. It's worth noting that given the focus on the downlink scenario, the Base Station (BS) Modulator subsystem is colloquially referred to as the Modulator, and the UE Receiver subsystem is referred to as the Receiver since only a single instance of each is present within the model.
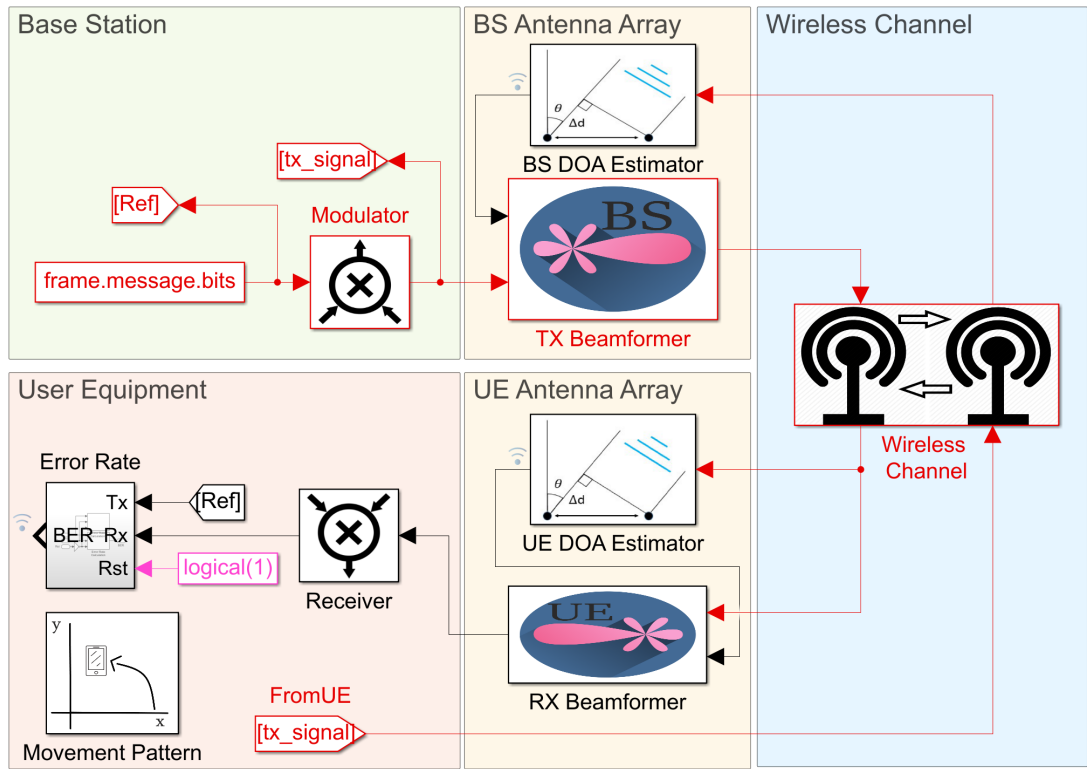
Figure 6.4: Simulink model for the UE tracking simulation.
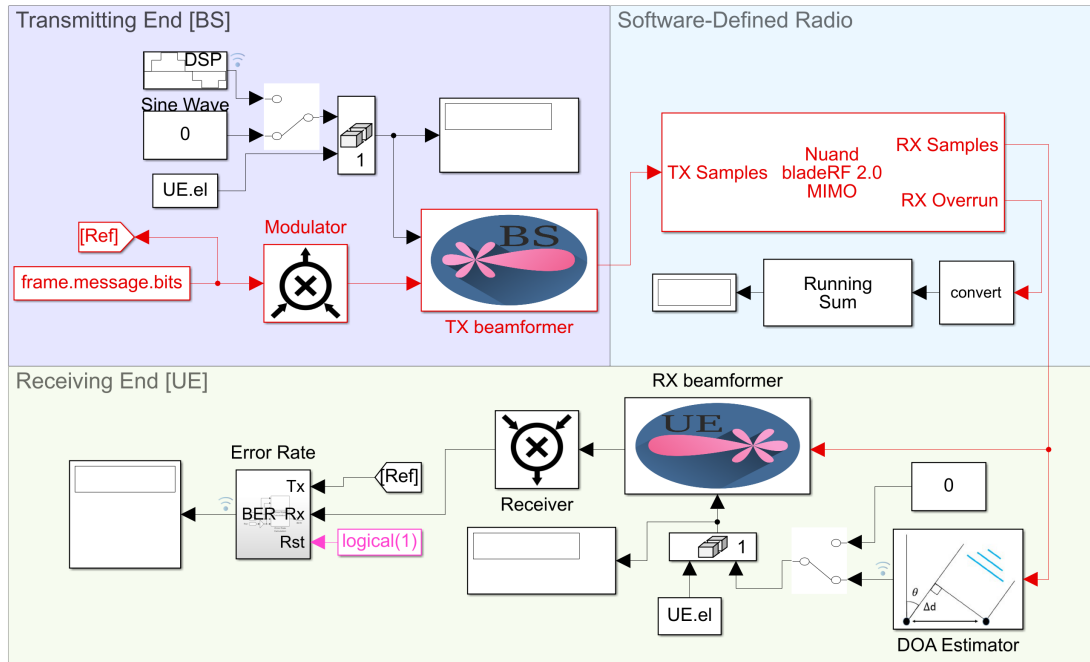
Figure 6.5: Simulink model for the HIL demonstration.

6.2.1.2 Hardware Implementation

The hardware implementation involves the utilization of BladeRF and a setup featuring two sets of dual antennas. This configuration enables wireless communication and UE tracking. The

core hardware components include two BladeRF devices, each equipped with two transmit (TX) antennas and two receive (RX) antennas. The connection is established using USB to USB-C cables. Additionally, a board with markings indicating antenna separation distances has been integrated and optimized for the frequency range spanning 1 to 6 GHz.
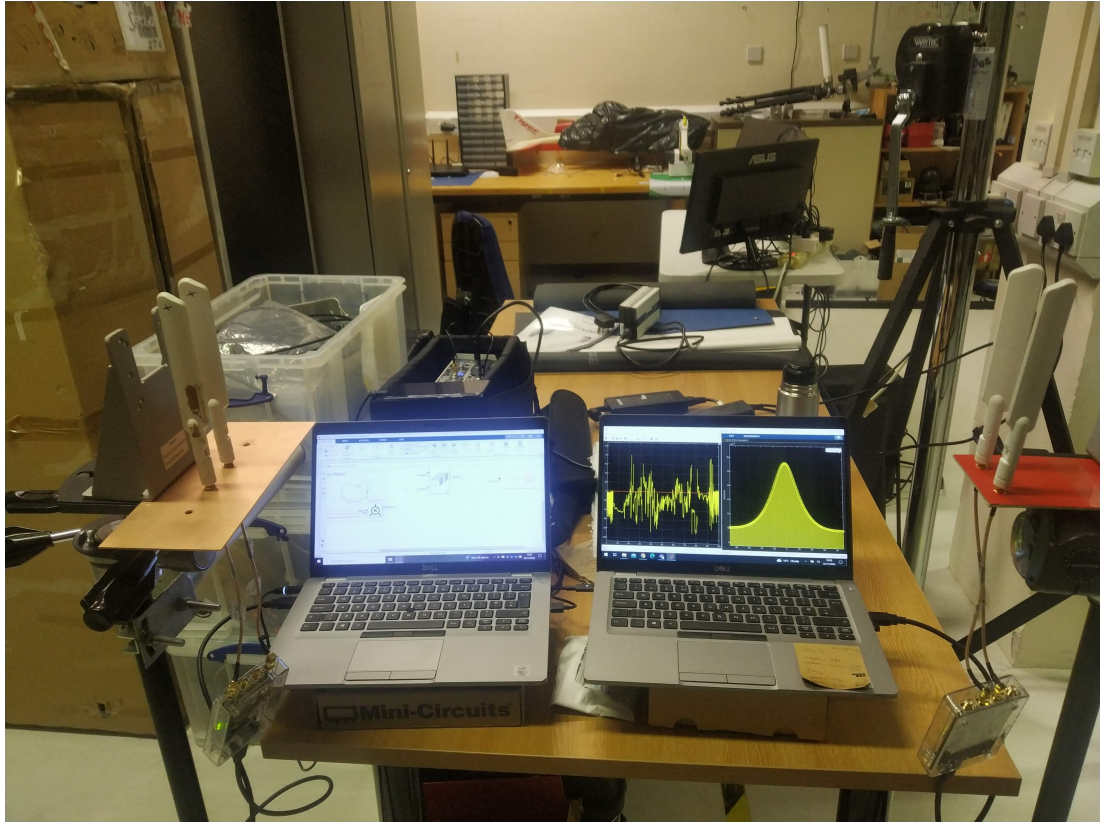
Figure 6.6: BladeRF Beam tracking setup.

6.2.1.3   Data Collection

Data collection in our research was facilitated through the use of a custom PowerShell script. This script was crafted to automate critical tasks essential for acquiring the necessary data from our hardware setup, thereby enabling further analysis and evaluation of our directional beam-forming system.

The purpose of the PowerShell script was twofold:

6.2.1.4   Signal Acquisition

The script was responsible for initiating and controlling the USRP in our hardware setup. It triggered the data acquisition process, capturing radio signals and relevant parameters required for subsequent analysis. This ensured a streamlined and consistent data collection process.

6.2.1.5   Data Organization

In addition to signal capture, the script played a vital role in organizing and storing the acquired data in an orderly fashion. This included labelling data sets, timestamps, and relevant metadata, which were instrumental in conducting comprehensive evaluations and comparisons.

By employing this custom PowerShell script, we not only simplified the data collection process but also ensured data integrity and consistency, laying a robust foundation for our research analysis.
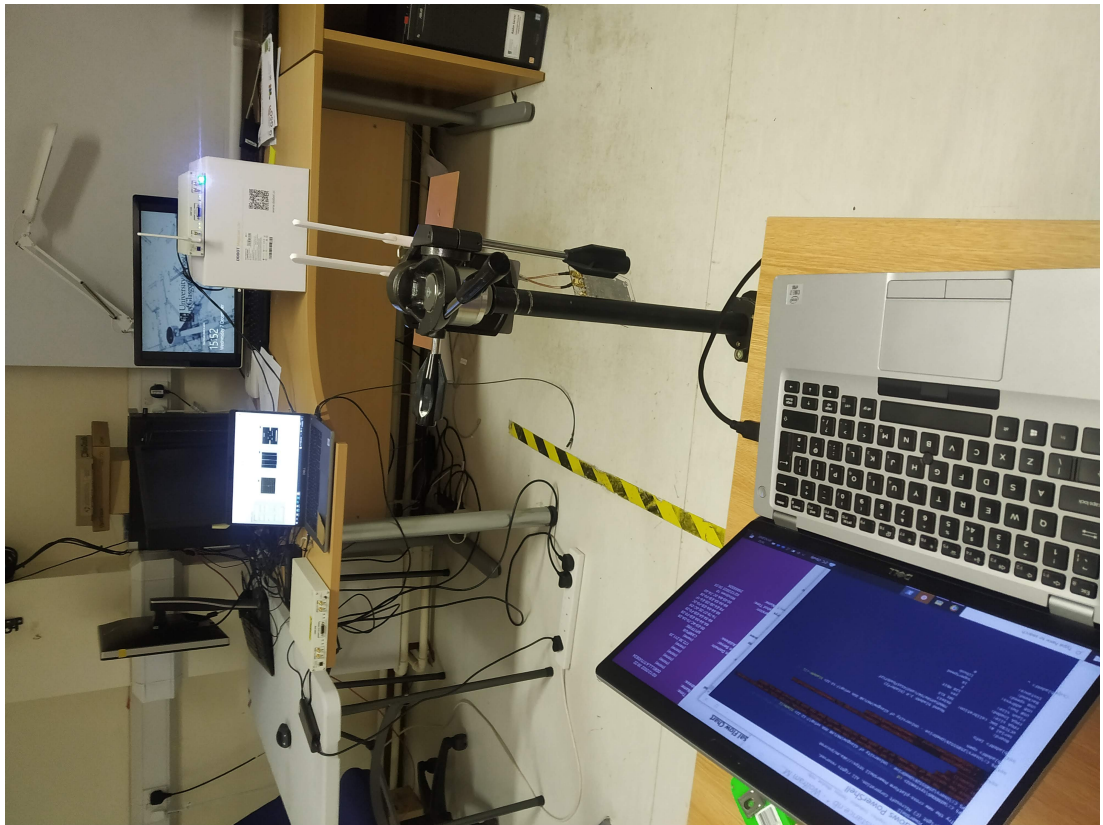
Figure 6.7: Data collection using BladeRF.

6.2.1.6   Results

The collected data was processed and presented in graphical form to demonstrate the functionality of the hardware setup. Notably, the system operated as a beamformer with high accuracy within the frequency range of less than 3 GHz. However, an issue arose when the operating frequency exceeded 3 GHz. This limitation should be taken into account when considering potential use cases and the system's applicability at different frequency bands.

In summary, the BladeRF-based hardware setup, coupled with the dual antenna arrangement, proved effective in wireless communication and UE tracking. The collected data substantiates the system's beamforming capabilities, highlighting its accurate performance up to 3
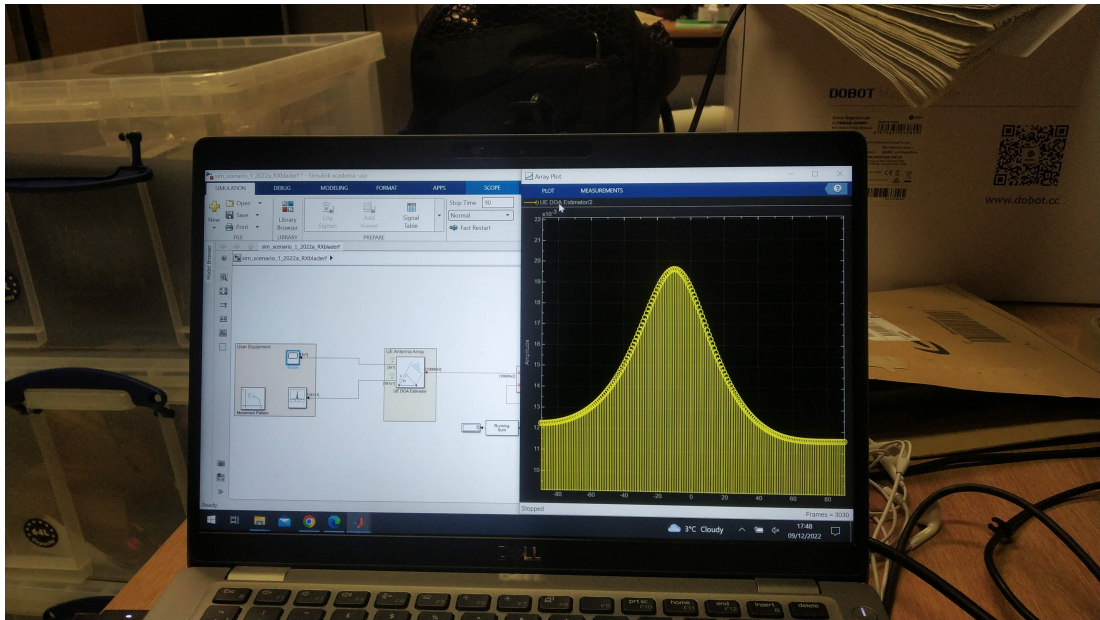
Figure 6.8: DOA estimation using BladeRF.

GHz. Awareness of the frequency-dependent behavior is essential for informed decision-making regarding the setup's deployment and its compatibility with various frequency ranges.

6.2.2 DOA Set-up using LabView and USRPs

This report presents a comprehensive exploration of a DoA setup utilizing LabVIEW and the USRP X300 platform. The primary objective was to develop an efficient and accurate DoA estimation system capable of locating a target user within specified frequency bands. The setup involved a four-element receiving unit paired with a single-antenna transmitter, thereby establishing the basis for accurate DoA estimation and beamforming.

Inspired by the potential offered by the USRP X300 platform and LabVIEW's versatility, this project sought to devise an advanced DoA setup that capitalizes on state-of-the-art technologies. The focal point was the precise Localisation of a target user while employing DoA estimation algorithms and adaptive beamforming techniques.

The setup was designed to operate within two distinct frequency bands: 2.4 GHz and 3.75 GHz. This frequency selection was deliberate, aligning with common wireless communication spectrums and offering a practical demonstration of the setup's adaptability. The project's key components included the four-element receiving unit, a single-antenna transmitter, LabVIEW for control and data acquisition, and the USRP X300 for signal generation and reception.

The experiment's execution involved a multi-step process, from calibrating the system to acquiring and processing signals for DoA estimation. The received signals were analyzed to determine the target user's angle of arrival accurately. By utilizing LabVIEW's intuitive programming environment and the capabilities of the USRP X300, the project successfully demonstrated

the effectiveness of the DoA estimation system.

Results showed that the setup achieved accurate DoA estimation within the specified frequency bands.

6.2.2.1   LabVIEW Scripts for DoA Estimation

In our research on DoA estimation, LabVIEW scripts play a crucial role in orchestrating the communication between the transmitter (TX) and receiver (RX). These scripts serve as the backbone of our DoA estimation system, enabling precise Localisation of signal sources.

The LabVIEW scripts act as intermediaries between the TX and RX, overseeing the signal generation, transmission, reception, and subsequent processing. Their overarching purpose is to facilitate the accurate estimation of the direction from which a signal originates, a critical component of our research.

The TX and RX LabVIEW scripts work in conjunction to achieve DoA estimation. Here's an overview of their functionalities:

6.2.2.2   Transmitter (TX) Script

The TX script in LabVIEW is responsible for generating the signal that will be transmitted to the receiver. It encompasses the following tasks:

- **Signal Generation**: The script generates the signal that carries the required information. This signal can be a test waveform or a modulated signal, depending on the specific DoA estimation technique being employed.

- **Signal Modulation**: If needed, the script modulates the generated signal to fit the modulation scheme and parameters dictated by the experiment's requirements.

- **Data Formatting**: The generated and modulated signal is prepared for transmission by formatting it into packets or frames, incorporating synchronization and error-checking mechanisms.

- **Signal Transmission**: The LabVIEW script interfaces with the hardware to transmit the modulated signal over the air to the receiver.

6.2.2.3   Receiver (RX) Script

The RX script in LabVIEW is designed to capture and process the transmitted signal, enabling accurate estimation of the signal's direction of arrival.

- **Signal Reception**: The script interfaces with the hardware to capture the transmitted signal, which may be affected by noise, interference, and propagation effects.

- **Signal Processing**: Received signals are preprocessed to mitigate noise and interference, enhancing the accuracy of subsequent analysis.

Figure 6.9: LabView script for signal transmission.

- **DoA Estimation Algorithm**: The script applies the DoA estimation algorithm to the received signal. This algorithm might involve techniques such as beamforming, MUSIC, ESPRIT, or others, depending on the specific implementation.

- **Angle Calculation**: Based on the output of the DoA estimation algorithm, the LabVIEW script calculates the angle or angles from which the signal is arriving.

- **Result Presentation**: The calculated DoA angles are then presented graphically or numerically, providing insights into the spatial positioning of the signal source.

Figure 6.10: LabView script for signal reception.

6.2.2.4 Hardware Implementation

The hardware implementation of the system comprises two USRP (Universal Software Radio Peripheral) devices. The first device is a twin RX (receiver) unit designed to accommodate up to four RX antennas. The second device operates as a transmitter (TX) or UE and is equipped with a single antenna. The calibration of the setup was achieved using a 4-port power splitter, enhancing the accuracy of the DoA estimation. Coaxial cables of equal lengths were employed consistently throughout the experiments.

6.2.2.5 Data Collection

Data collection was performed at nine distinct positions to assess the accuracy of the DoA estimation. For reference, angles corresponding to these positions were marked on the floor to facilitate a visual check of the DoA accuracy. Notably, the setup demonstrated optimal performance within a range of 45 degrees and for relatively short distances. However, when subjected to scenarios involving long distances, moving UEs, or outdoor environments, the system exhib-

Figure 6.11: DOA setup using USRPs and LabView.

ited accuracy degradation due to a range of factors, including interference and noise.

6.2.2.6   Results

The obtained results underscore the viability of the setup for demonstration purposes and indoor experimental applications. The system's performance is particularly effective within controlled indoor environments, making it well-suited for showcasing the principles of DoA estimation and enabling experimentation in such settings. However, it is important to acknowledge the limitations of the setup when considering scenarios involving extended distances, dynamic UE movement, or outdoor conditions where external factors can significantly impact its accuracy.

In conclusion, the hardware implementation featuring the twin RX and single-antenna TX/UE USRP configuration provides a practical platform for illustrating DoA estimation concepts and conducting indoor experiments. Careful consideration of the system's limitations and the environmental context is crucial when interpreting its results and potential use cases.
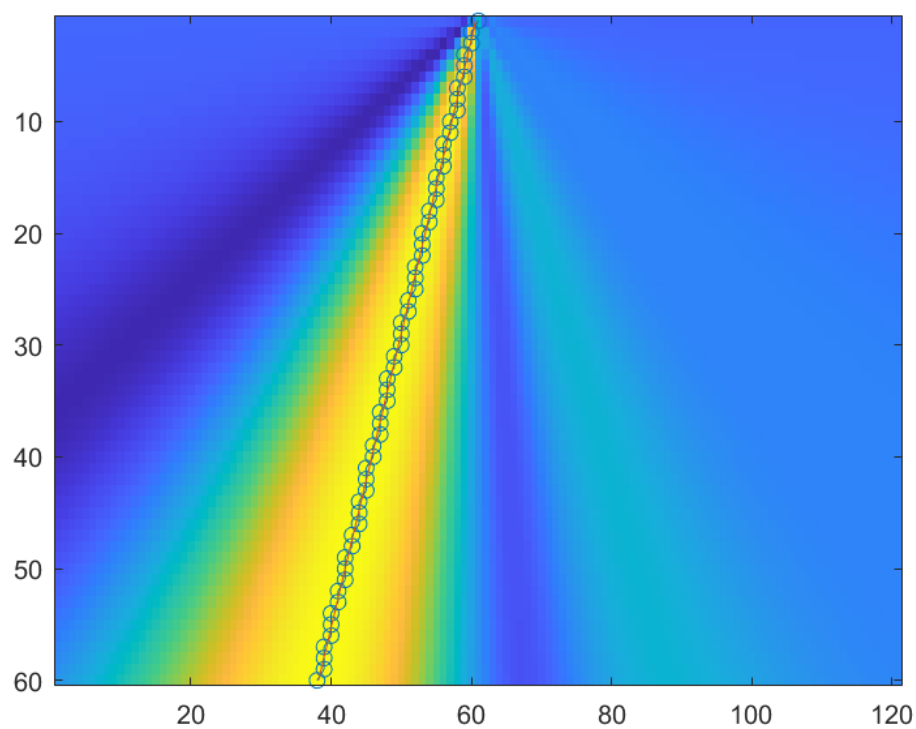
Figure 6.12: DoA estimation at 10 degrees.

Chapter 7

Real-Time Data for Localization via Fingerprinting

This chapter shifts the focus to the application of real-time data sets for localization using fingerprinting methods. The primary objective is to explain the fingerprinting technique and present results from experiments conducted in different scenarios. Through a detailed analysis of the localization process, this chapter contributes valuable insights into the practical application of real-time data in localization.

The chapter on real-time localization delves into the formidable challenge of accurately determining the indoor location of mobile devices, a topic that has sparked significant interest due to the complexities posed by non-line-of-sight propagation and multipath effects. In response to these challenges, this chapter introduces a novel approach to indoor positioning, leveraging channel state information (CSI) and ML techniques to enhance accuracy. The proposed methodology involves the extraction of subcarrier amplitude and phase differences from CSI data, forming fingerprints that are subsequently clustered to identify distinct groups of data. These identified groups are then split into two sub-databases using a defined threshold. ML algorithms and a tailored network architecture are employed to train both sub-databases of fingerprints. The effectiveness of this innovative method is empirically validated through experiments conducted in a standard indoor environment, showcasing its potential to significantly improve the accuracy of indoor localization.

7.1   Localization using LabView and USRPs

This report outlines an in-depth investigation into a localization setup employing LabVIEW and the USRP X300 platform. The core objective of this project was to develop a robust and precise localization system capable of accurately determining the position of a target user within a specific frequency band. The setup encompassed a two-element receiving unit paired with a single-antenna transmitter, enabling accurate localization through DoA estimation and Channel

State Information (CSI) extraction.

Motivated by the capabilities of the USRP X300 and LabVIEW's versatile programming environment, this endeavour aimed to establish a sophisticated localization setup, leveraging cutting-edge technology for accurate positioning. The focus was on precisely determining the location of a target user through advanced DoA estimation techniques and the extraction of CSI data.

The chosen frequency band for this project was 3.75 GHz, a spectrum commonly utilized in wireless communication applications. This frequency selection was strategic, aligning with real-world scenarios and demonstrating the applicability and adaptability of the setup. The primary components included a two-element receiving unit, a single-antenna transmitter, LabVIEW for system control and data processing, and the USRP X300 for generating signals and receiving responses.

The execution of the experiment unfolded through a planned sequence of steps, ranging from system calibration to signal acquisition and processing for localization. The received signals were subjected to rigorous analysis to precisely estimate the target user's location using advanced localization algorithms. Additionally, the setup enabled the extraction of CSI data at nine distinct positions, facilitating a comprehensive understanding of the wireless channel characteristics.

The integration of LabVIEW's intuitive programming interface with the advanced capabilities of the USRP X300 led to the successful demonstration of accurate localization within the specified frequency band. The ability to estimate the user's position and extract CSI data provided valuable insights into the wireless communication environment.

The results indicated that the setup achieved accurate and reliable location estimation within the targeted frequency band. The project's highlight was the successful extraction of CSI data, enhancing the understanding of the wireless channel's behaviour.

7.1.1 Preliminary Requisites

The system architecture created for the device localization procedure is presented in this section, as shown in Fig. 7.6. Additionally, the method for calculating the separation between the two devices is described. The objective function and the experimental setup for device localization are then discussed. Finally, we provide details of the ML model for device localization and sensing applications.

7.1.1.1 RSSI-based Localization

RSSI, or Received Signal Strength Indication, represents the signal strength received by the client, and it is an integral part of the MAC layer. In wireless communication, signals experience phenomena like reflection, diffraction, and scattering, leading to multipath propagation. As a

result, the signal received at a node comes from multiple paths, each with variations in arrival times and phase discrepancies. These variations can either amplify or attenuate the original signal, resulting in multipath attenuation and creating a unique electromagnetic environment indoors. This uniqueness in the channel's multipath structure forms the basis of RSSI-based positioning [157].

The instantaneous value of RSSI can be calculated by integrating the baseband In-phase (I) and Quadrature-phase (Q) power as follows:

$$RSSI_{\text{Instan}} = \sqrt{I^2 + Q^2} \tag{7.1}$$

7.1.1.2 CSI-Based Localization

Channel State Information (CSI) is a valuable metric for localization as it reflects the multipath effects and signal intensity variations during transmission. Small spatial movements can influence CSI values, and due to the complexity of indoor environments, CSI amplitudes vary across different locations. CSI data is part of the physical layer data in wireless communication protocols, such as the 802.11 protocol's physical layer (PHY) [158], which bridges the MAC and wireless media layers.

The channel gain matrix H expresses CSI, with each component having an amplitude $\|H_k\|$ and a phase $\angle H_k$ for the kth subcarrier. It can be written as follows:

$$H_k = \|H_k\| e^{j\angle H_k} \tag{7.2}$$

In this equation, H_k represents the CSI for the kth subcarrier. The terms $\|H_k\|$ and $\angle H_k$ represent the amplitude and phase of the kth subcarriers, respectively. The amplitude and phase of a complex number H can be determined by finding its modulus $\sqrt{(a^2 + b^2)}$ and argument $\theta = \arg\tan\frac{b}{a}$, where a and b are real and imaginary parts of H.

In our research, we have employed RSSI, phase, and CSI-based localization methods and have explored which ML algorithm yields higher accuracy for indoor positioning.

7.2 Experimental configurations

7.2.1 Scenario

In the experiment, we established an indoor environment with a marked floor plan consisting of a square divided into 9 blocks of different sizes (1 meter, 0.75 meters, and 0.5 meters) as shown in Fig. (7.1). Note that this figure is composed in this way for better visuals and may not represent the actual proportion. A transmitting antenna was placed at the center of the floor plan, marked as P1 to P9, and two receiving antennas were positioned at a fixed distance of 0.035 meters at a frequency of 3.75 GHz. We conducted experiments in both line-of-sight (LOS) (7.2,7.3) and
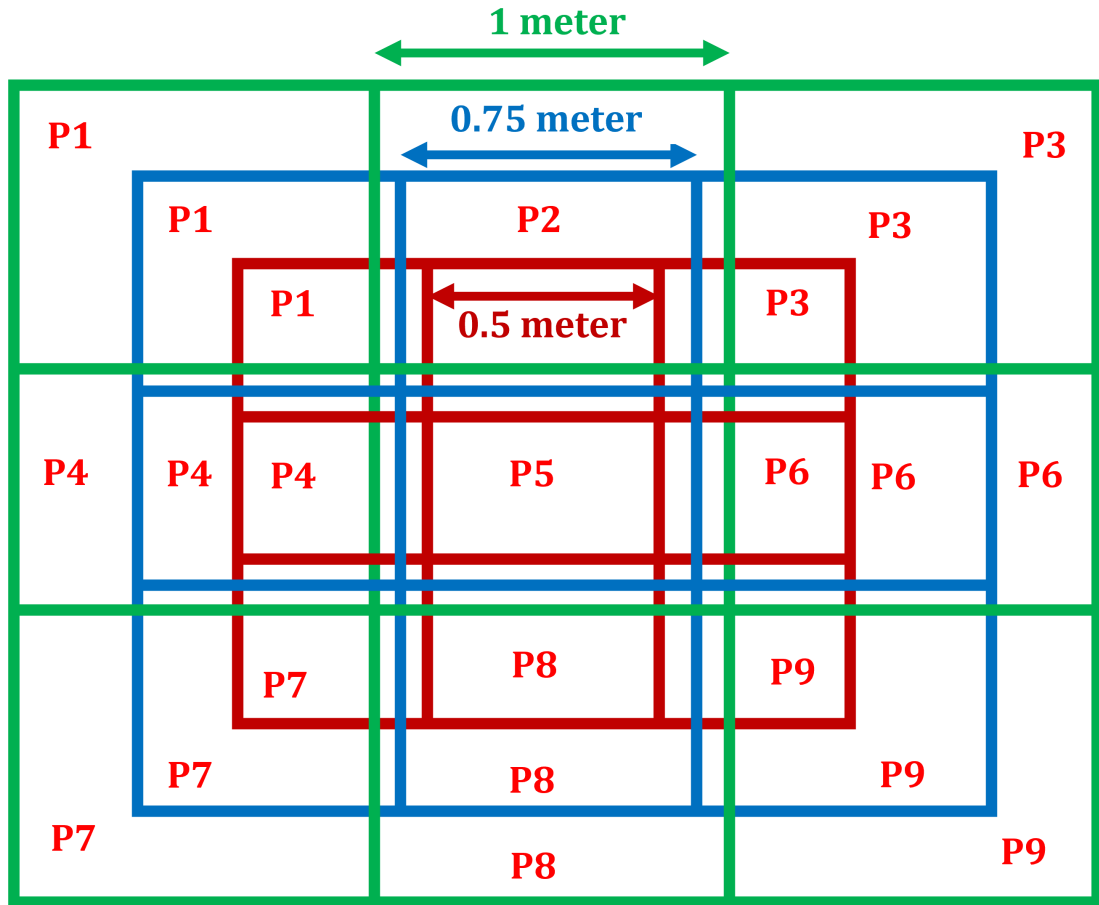
Figure 7.1: Schematic layout of a floor plan.

non-line-of-sight (NLOS) (7.4) scenarios. In the NLOS scenario, we introduced an obstruction by placing a board between the transmitter and receiver, mounted on tripods, which affected the transmitted signal.

The obstruction created by the board in the NLOS scenario had several effects on the transmitted signal. First, it caused multipath propagation, where the signal bounced off the board, creating multiple reflected signals that reached the receiver at different times and angles. This introduced fading, interference, and reduced signal quality, leading to errors and packet loss in communication. Additionally, the obstruction caused diffraction, bending, and spreading the signal around the edges of the board, further complicating the received signal with interference, signal attenuation, and reduced communication range. The significance of obstructions in the transmission of signals cannot be overlooked. They lead to various adverse effects such as diminished signal quality, heightened error rate, and a restricted communication range. These impacts emphasize the utmost importance of considering and addressing such obstructions during the design and implementation of wireless communication systems in real-world situations.
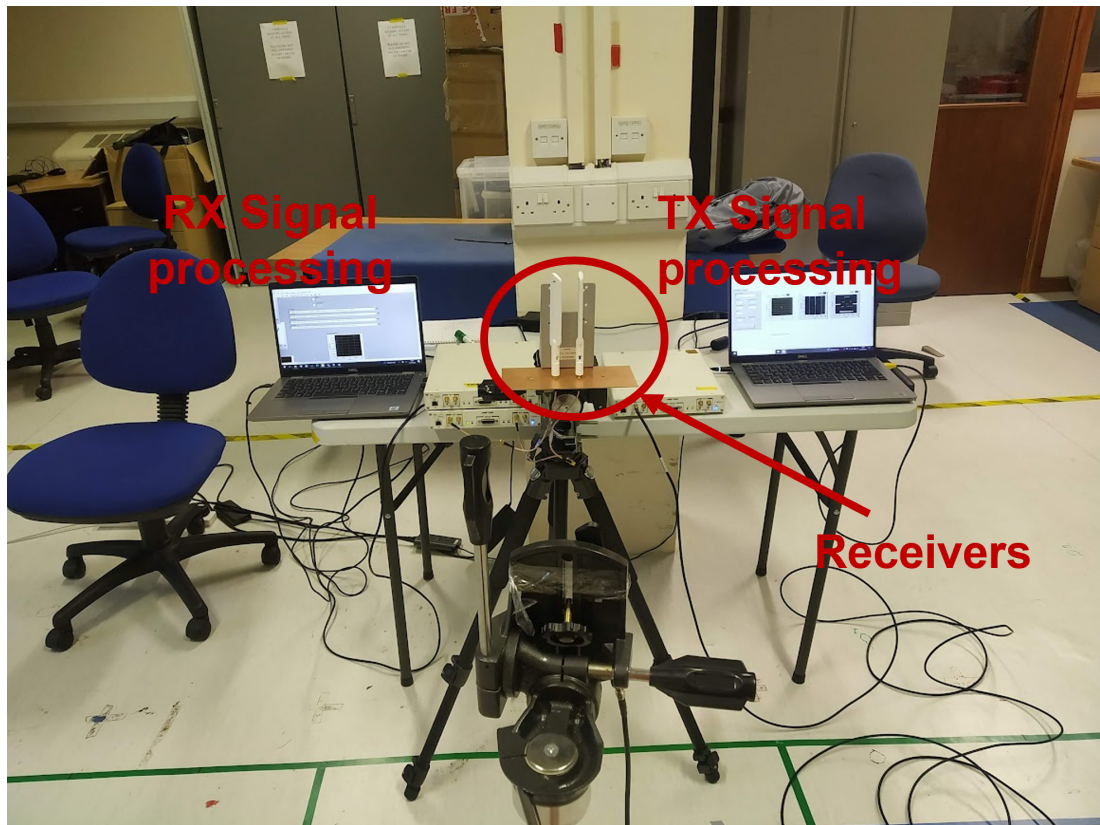
Figure 7.2: Recieving end mounted on a tripod in LOS scene.

7.2.2 Hardware

In this study, we utilized the ETTUS universal software radio peripheral (USRP) X310 device as the transmitter (Tx) and receiver (Rx) terminals. The USRP X310 device provided two channels, which were used separately for Tx and Rx. The experiment was conducted at a carrier frequency (f_c) of 3.75 GHz, and the sampling rate was set to 1 MHz. We utilised a 5G/4G terminal mount monopole antenna manufactured by Taoglas. This indoor passive antenna operates within a frequency range of 600 MHz to 6 GHz and supports various protocols, including 802.11, WLAN, WiFi, WiFi 6E, IoT, and ISM. With its gain ranging from -2.14 dBi to 1.73 dBi, impedance of 50 Ohms, and power rating of 2 W, the antenna is suitable for a wide range of applications, such as gateways, routers, smart metering, vending machines, industrial IoT, smart homes, and connected enterprises.

7.2.3 Software

LabView 2021 was employed as the software-defined radio platform for signal processing. It facilitated the processing of the OFDM signal (7.5), which consisted of 125 data samples at 3.75 GHz at both the transmitting and receiving ends.

The software also incorporated functionalities such as 4-QAM modulation, Least Square-based channel estimation, serial-to-parallel and parallel-to-serial conversion, IFFT and FFT op-
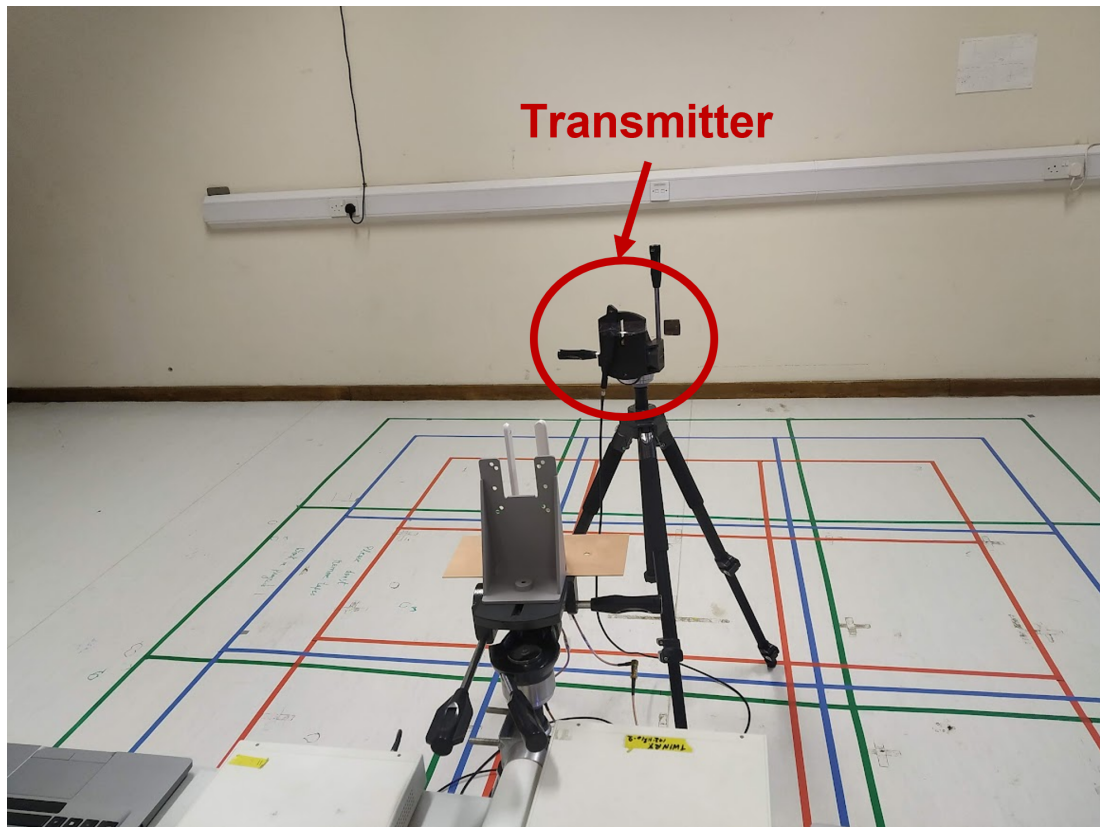
Figure 7.3: Tranmitting end mounted on a tripod in LOS scene.

erations, and cyclic prefix insertion and removal. The system architecture is shown in figure 7.6.

7.3   Data Collection

For channel response analysis, data collection involved recording the characteristics of each receiving antenna and processing the data into a matrix format denoted as [[x1, x2], [y1, y2]] where 'x' represents amplitude and 'y' represents phase.

To train a neural network for position estimation, data was collected for nine positions within the floor plan (see Fig. 7.1). The transmitter was centered at each position, while the uniform linear array receiver remained static.

The transmitter systematically moved from positions P1 to P9, collecting a minimum of 500 samples at each location. Amplitude and phase values, calculated using LabView scripts, were saved in .txt format. To enhance analysis, the .txt files were converted to .csv format, resulting in 36 files representing two receiving channels and 125 subcarriers. Each file had dimensions of $500 \times 1 \times 2$ samples.

Figure 7.7 illustrates the amplitude received on channel-1 for Block 1 at a 0.5-meter distance, showcasing variations in received amplitude across different frequency subcarriers. Similarly,
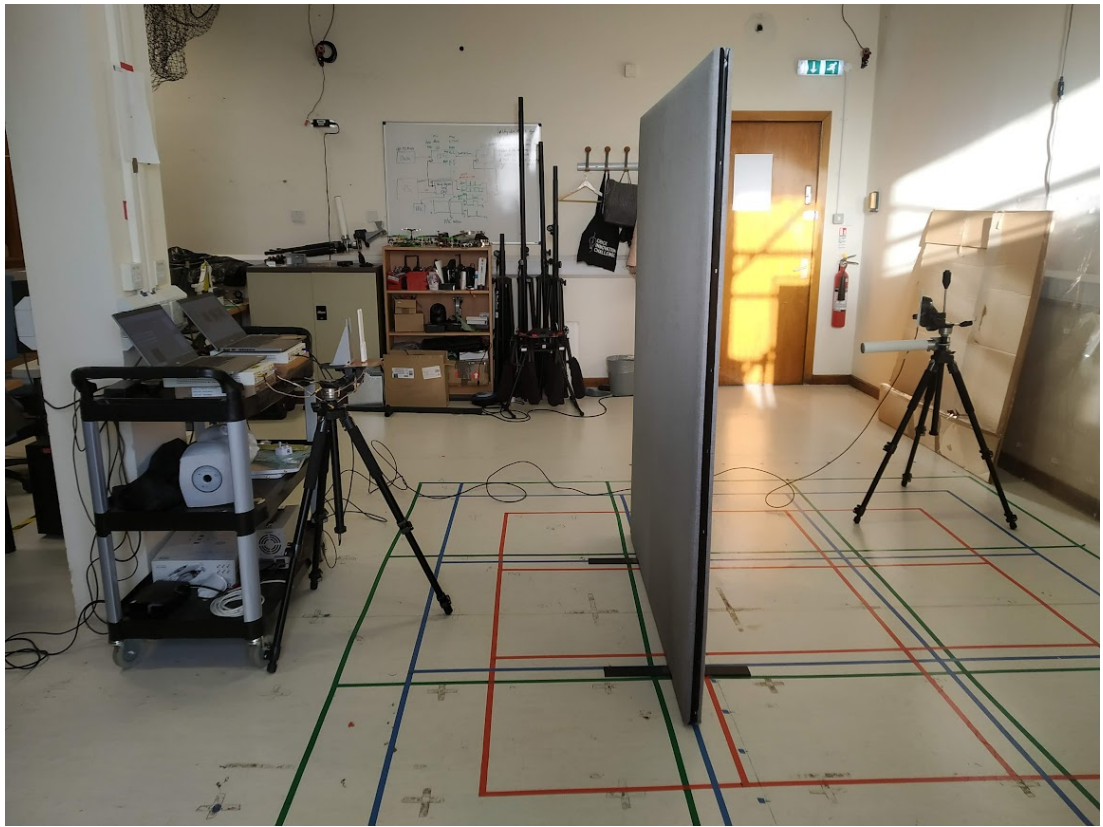
Figure 7.4: Transmitter and Receivers mounted on a tripod in NLOS scene created by placing the board in between.
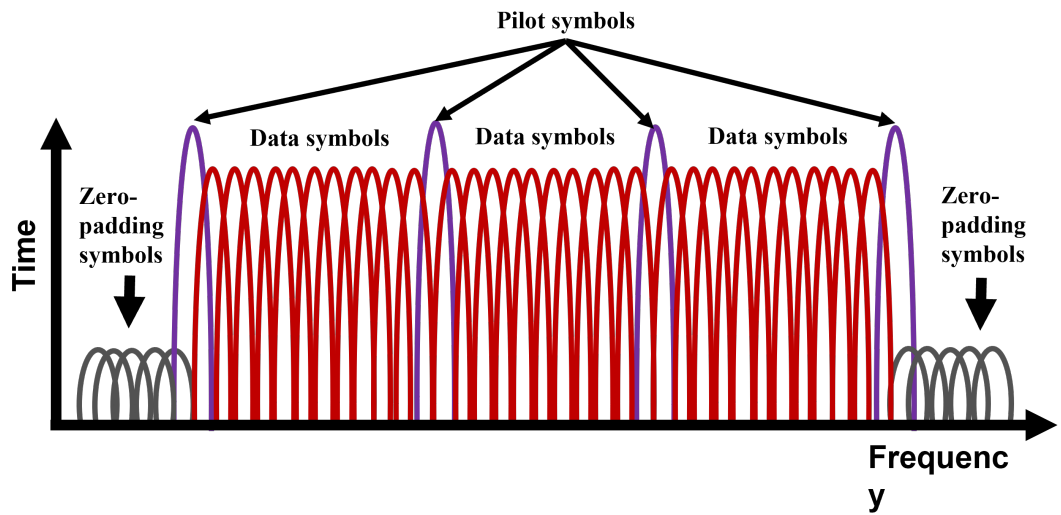
Figure 7.5: Symbols structure for OFDM system of 125 subcarriers.

Fig. 7.8 depicts the phase received on channel-1 for Block 1 at a 0.5-meter distance, providing insight into the phase shift during signal transmission.

These figures offer valuable insights into signal propagation characteristics in both LOS and NLOS scenarios. They effectively visualize sequential operations, including channel response measurement, data processing, and matrix formation.
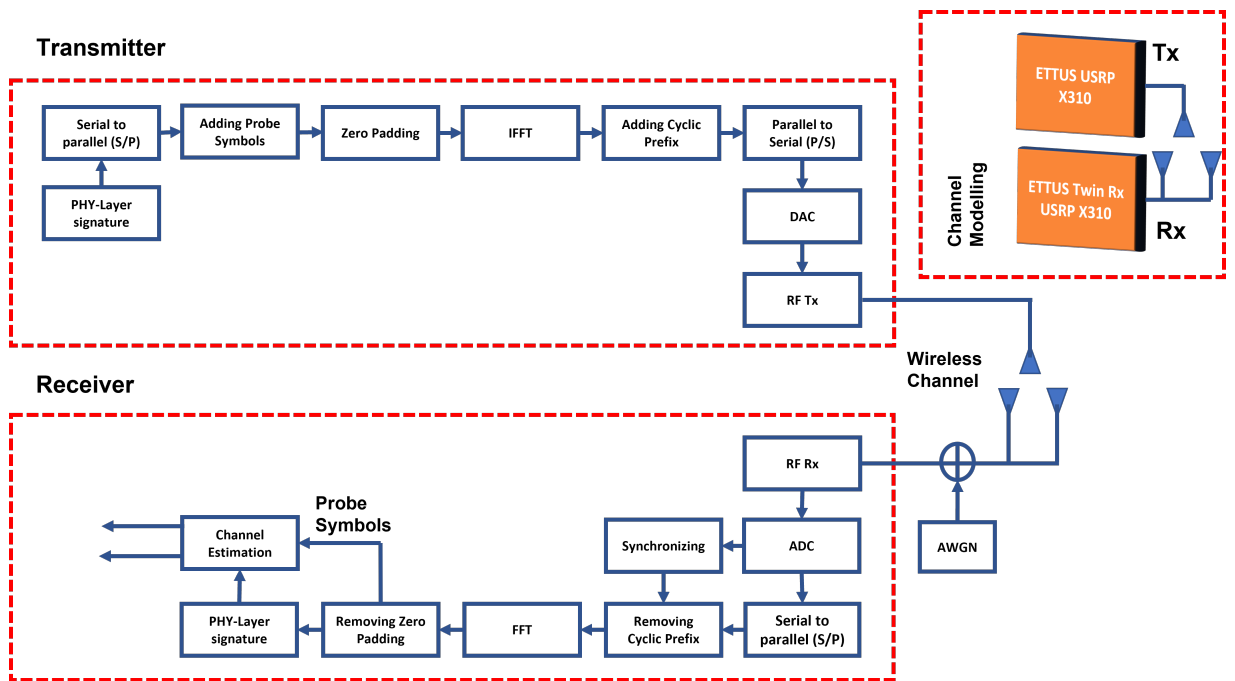
Figure 7.6: System Architecture of OFDM Symbols
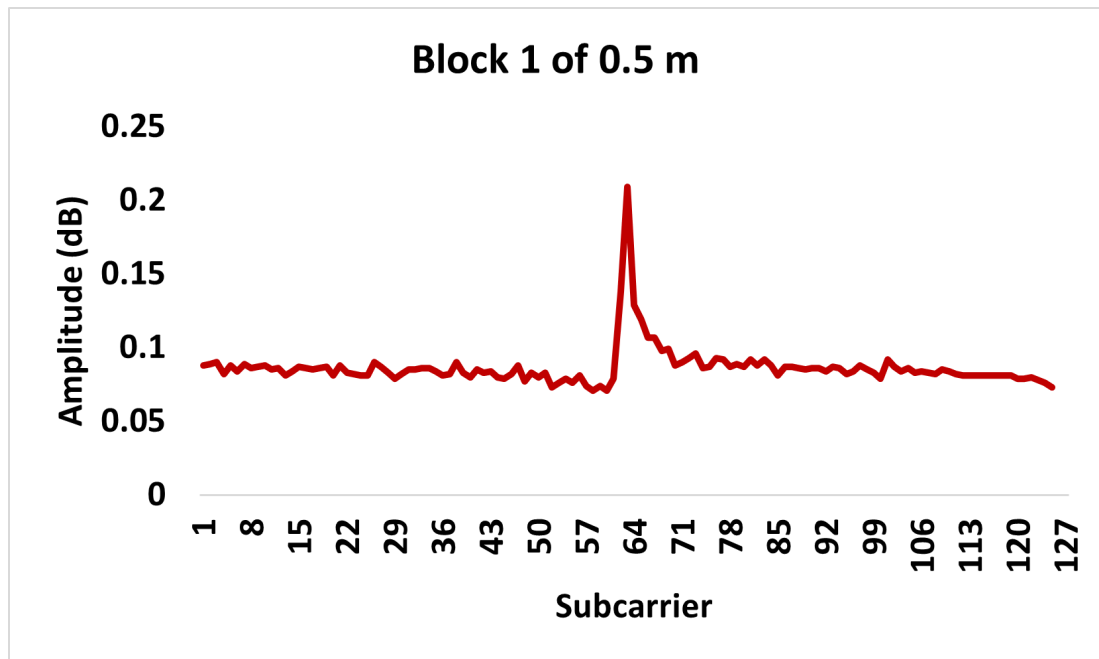
Figure 7.7: Amplitude received on channel 1 on block 1 of 0.5 m for 1 sample with respect to 125 subcarriers.

This methodology ensures a comprehensive dataset with amplitude and phase information for further analysis and exploration of position estimation using neural networks.
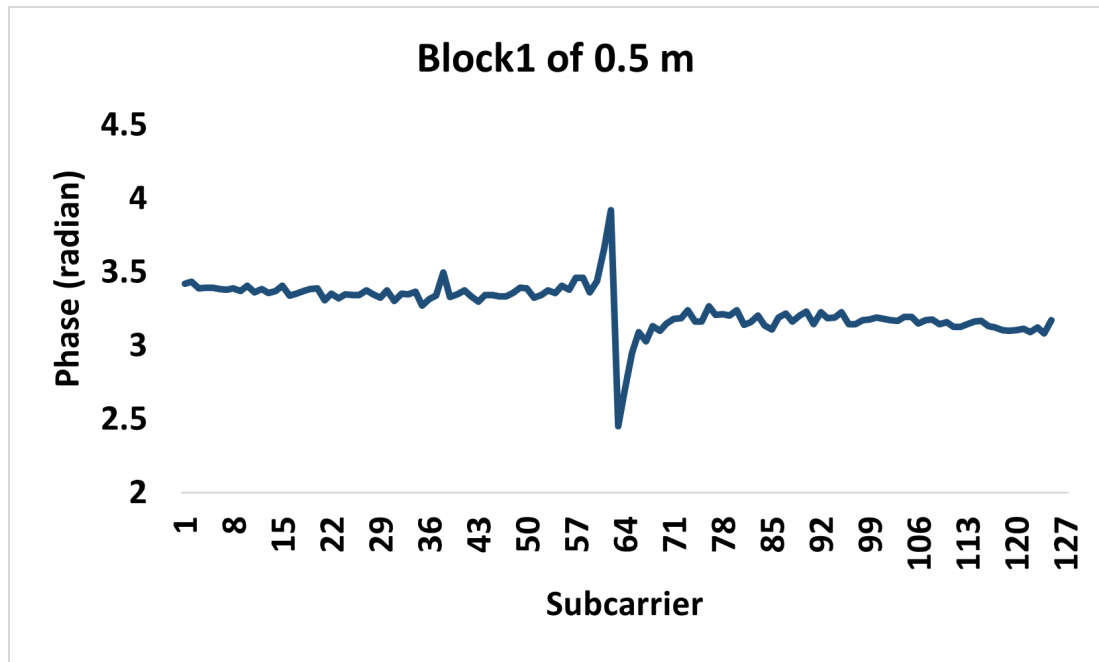
Figure 7.8: Phase received on channel 1 on block 1 of 0.5 m for 1 sample with respect to 125 subcarriers.

7.4 Localization

7.4.1 ML Implementation

In this section, we outline the procedure for position prediction based on machine learning analysis of channel responses. We describe the transformation of channel features and location information into input features and output labels for training a neural network (NN). The flow chart of the procedure is presented in Figure 7.9.
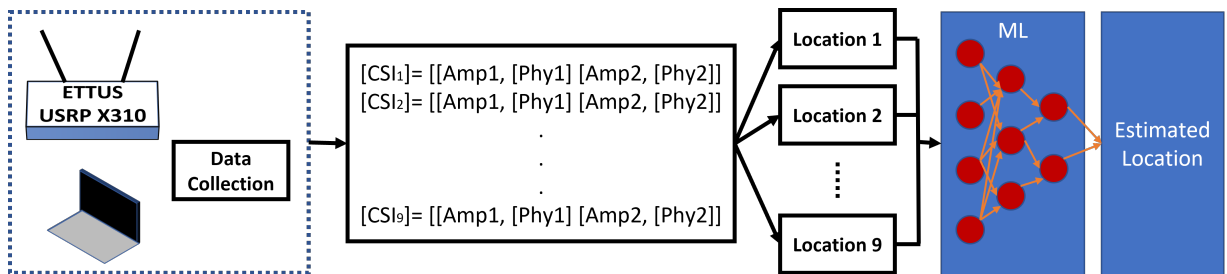
Figure 7.9: System Architecture represents data collection, data processing, ML implementation and results obtained as estimated location.

In this study, we evaluated the performance of two machine learning algorithms, Neural Network and Random Forest (RF), for indoor localization. The hyperparameters and performance metrics for both algorithms are summarized in Table 7.2.

The Neural Network architecture utilized in our experiments consists of two hidden layers, each with 125 neurons, denoted as a 125x2 structure. Similarly, the RF is represented as a 125x2

model. Both algorithms were trained to classify data into nine distinct classes.

7.4.2 Deep Learning Implementation

In the contemporary landscape of location prediction, deep learning techniques are widely employed to automatically extract features from the CSI affected by motion. Leveraging neural networks with multiple layers has the potential to enhance classification Accuracy significantly. However, challenges like overfitting and performance deterioration may emerge, especially when dealing with limited datasets.

Traditional strategies such as adjusting the learning rate, using small batch sizes, and applying weight decay may not suffice to mitigate these challenges. Consequently, achieving optimal performance often necessitates the incorporation of a specific number of dedicated neural layers. In this study, we have chosen to employ DL models specifically configured to handle the complexities of small datasets more efficiently. This approach is driven by the recognition that conventional methods might not adequately address the nuances of our dataset.

While it is acknowledged that certain deep learning models, including CNNs, can become deep and face challenges like overfitting, our selection is deliberate. We contend that, despite potential challenges, CNNs bring valuable capabilities to the task at hand. In the following sections, we delve into the configuration and adaptation of these DL models to address the unique demands of our location prediction framework.

7.4.2.1 Localization using LSTM

We have employed LSTM networks, artificial recurrent neural networks specifically designed to handle time-series data. This choice is motivated by the suitability of LSTM networks for our situation, as mentioned in [159] and [160]. Our primary objective with the LSTM algorithm is to extract CSI values and reduce noise. Each of the 125 subcarriers' raw CSI amplitudes is incorporated into a 125-dimensional feature vector. The hidden layer of the LSTM network has a size of (20, 50) and utilizes the tanh activation function. To minimize the cross-entropy loss, we utilize the Adam optimizer with a batch size of 64, a learning rate of 0.01, and a decay rate of 1e-6. A significant advantage of employing LSTM for classification is the ability to directly learn from raw series data, eliminating the need for manual engineering of input features and providing greater flexibility to domain experts.

7.4.2.2 Localization using CNN

CNN stands out as one of the most widely used deep learning architectures, renowned for its capability to automatically extract intricate, high-dimensional features compared to shallow ones [161, 162]. Based on previous research [163], we assert that CNN and LSTM are compatible deep learning techniques. While LSTM excels in analyzing time-domain data and demonstrates

superior performance for short-duration movement, CNN primarily focuses on capturing frequency domain changes and exhibits a stronger response to long-duration movement. In our implementation, the hidden layers were set to a size of (20, 32), and maximum pooling was applied with a size of (3, 1) using the tanh activation function. Following the general CNN design principle, the final classification prediction can be made in the output layer.

7.4.2.3   Localization using LSTM-CNN

The LSTM (Long Short-Term Memory) is a variant of recurrent neural networks that effectively captures continuous temporal relationships and is well-suited for processing time series data. On the other hand, CNN (Convolutional Neural Network) is adept at reducing frequency domain changes and extracting spatial features [164]. To leverage the advantages of both models, we combine them in the LSTM-CNN model for location prediction. It is worth noting that different variations of LSTM yield diverse results when utilized as input for CSI data. In our study, we compare LSTM with LSTM-CNN to discern localization. The LSTM layer is responsible for analyzing the input data. Signal fluctuations are utilized to gather the input, and time-domain characteristics are extracted from the initial signal. Following the LSTM's output, a 1D-CNN layer is applied. Convolution operations allow for the extraction of high-dimensional implicit features. Subsequently, the resulting convolutions are passed through a maximum pooling layer to obtain the optimal feature sequence, which forms the foundation for the final classification. For our implementation, we have employed an LSTM hidden layer size of (20, 50) and a CNN hidden layer size of (50, 32). The 1D max-pooling size is set to (3, 1), and the activation functions used are tanh and softmax, as mentioned in Table 7.1 of our study.

7.4.3   Training Process

Before concluding this section, it is essential to shed light on the training process of our deep learning models. The training involves presenting the network with labeled examples from the dataset, adjusting the model's internal parameters iteratively, and optimizing them to minimize the classification error. The specifics of this process, including the loss function, optimizer selection, and batch size, are detailed in Table 7.1 for reference.

7.5   Results and Discussion

We emphasize that the evaluation metrics used for performance analysis include Loss, Accuracy, F1 score, and Precision.

These metrics are defined as follows:

- **Loss** ($\mathscr{L}$): Loss is a measure of the model's prediction error. It quantifies the difference

Table 7.1: Hyperparameters of Deep Learning Algorithms

Algorithm	Parameters
LSTM	optimizer='adam', Activation = tanh, 1r=0.01, decay= 1e-6, epochs=50, hidden-layer-units=50, Dropout=0.2 , batch-size=32, connected-layer-activation:'softmax'
CNN	optimizer='adam', Activation = tanh, 1r=(0.1,0.01), loss = 'spares-categorical-crossentropy', hidden-layer-size=(20,32), epochs=(20,50), batch-size=32, Max-pooling-size = (3,1), connected-layer-activation:'softmax'
LSTM + CNN	optimizer='adam', Activation = tanh, 1r=(0.1,0.01), loss = 'spares-categorical-crossentropy', epochs=50, LSTM hidden-layer-units= 50, CNN hidden-layer-size= (50,32), Max-pooling-size = (3,1
NN	optimizer='adam', Activation = relu, 1r=0.01, decay= 1e-6, epochs=50, No.of hidden-layers = 3, batch-size=32, connected-layer-activation:'softmax'

between the predicted and actual values. The goal is to minimize the loss.

$$\mathscr{L} = -\frac{1}{N} \sum_{i=1}^{N} [y_i \log(\hat{y}_i) + (1 - y_i) \log(1 - \hat{y}_i)] \tag{7.3}$$

- **Accuracy (Acc):** Accuracy represents the proportion of correctly classified instances to the total instances.

$$\text{Acc} = \frac{\text{Number of Correct Predictions}}{\text{Total Number of Predictions}} \tag{7.4}$$

- **F1 Score (F1):** F1 score is the harmonic mean of precision and recall, providing a balance between false positives and false negatives.

$$\text{F1} = \frac{2 \cdot \text{Precision} \cdot \text{Recall}}{\text{Precision} + \text{Recall}} \tag{7.5}$$

- **Precision (Precision):** Precision is the ratio of true positives to the sum of true positives and false positives.

$$\text{Precision} = \frac{\text{True Positives}}{\text{True Positives} + \text{False Positives}} \tag{7.6}$$

7.5.1 Location Accuracy Analysis using ML

In this study, we employed two machine learning algorithms for indoor localization: Neural Network and Random Forest (RF). The hyperparameters and performance metrics for both algorithms are summarized in Table 7.2.

The architecture of the Neural Network used in our experiments consists of two hidden layers, each comprising 125 neurons, denoted as a 125x2 structure. The RF model is similarly configured for direct comparison, with settings tailored to optimize classification into nine distinct classes. This clarification is essential to correct the previous inconsistency regarding the RF model's description.

The reported hyperparameter details and performance outcomes stem from our comprehensive experimentation. Detailed results and methodological underpinnings can be referenced in [165]. Table 7.2 succinctly encapsulates this information, offering a comparative glimpse into the effectiveness of both the Neural Network and RF algorithms within the specific context of indoor localization.

Table 7.2: Hyperparameters of Machine Learning Algorithms

Method	Neural Network	RF
Hidden layers	125x2	125x2
Number of Classes	9	9
Loss	0.0953	0.626
Training samples	3600	3600
Accuracy	98.9	89.8

Moreover, Figure 7.10 provides a comparative analysis of location accuracy achieved with single-channel versus two-channel Channel State Information (CSI). Both ML methods exhibit high proximity to the actual positions marked on the floor plan, with minimal loss of probability. In the Line-of-Sight (LOS) scenario, CSI from both channels accurately predicts the location, while in the Non-Line-of-Sight (NLOS) scenario, CSI from two channels shows a slight decrease in location accuracy.

Furthermore, Figure 7.11 offers an in-depth comparative analysis of the CSI data received from single and dual-channel configurations under both Line-of-Sight (LOS) and Non-Line-of-Sight (NLOS) conditions. This analysis is pivotal for understanding the dynamics of indoor localization accuracy in varying environmental conditions.

These findings underscore the importance of considering multiple metrics for a nuanced evaluation of ML algorithms. The choice of features, such as Received Signal Strength Indicator

(RSSI) and CSI, significantly influences the algorithms' ability to accurately estimate location. Additionally, the impact of LOS and NLOS scenarios on performance is evident, emphasizing the need for robust algorithms capable of adapting to real-world wireless communication systems.

The superior performance of Neural Networks and RF, as compared to traditional logistic regression models, reaffirms the significance of utilizing non-linear classification algorithms. These are capable of effectively capturing the complex relationships between the input CSI data and the corresponding block locations. This aligns with our broader goal of developing and implementing localization algorithms that demonstrate high efficacy in real-world scenarios.
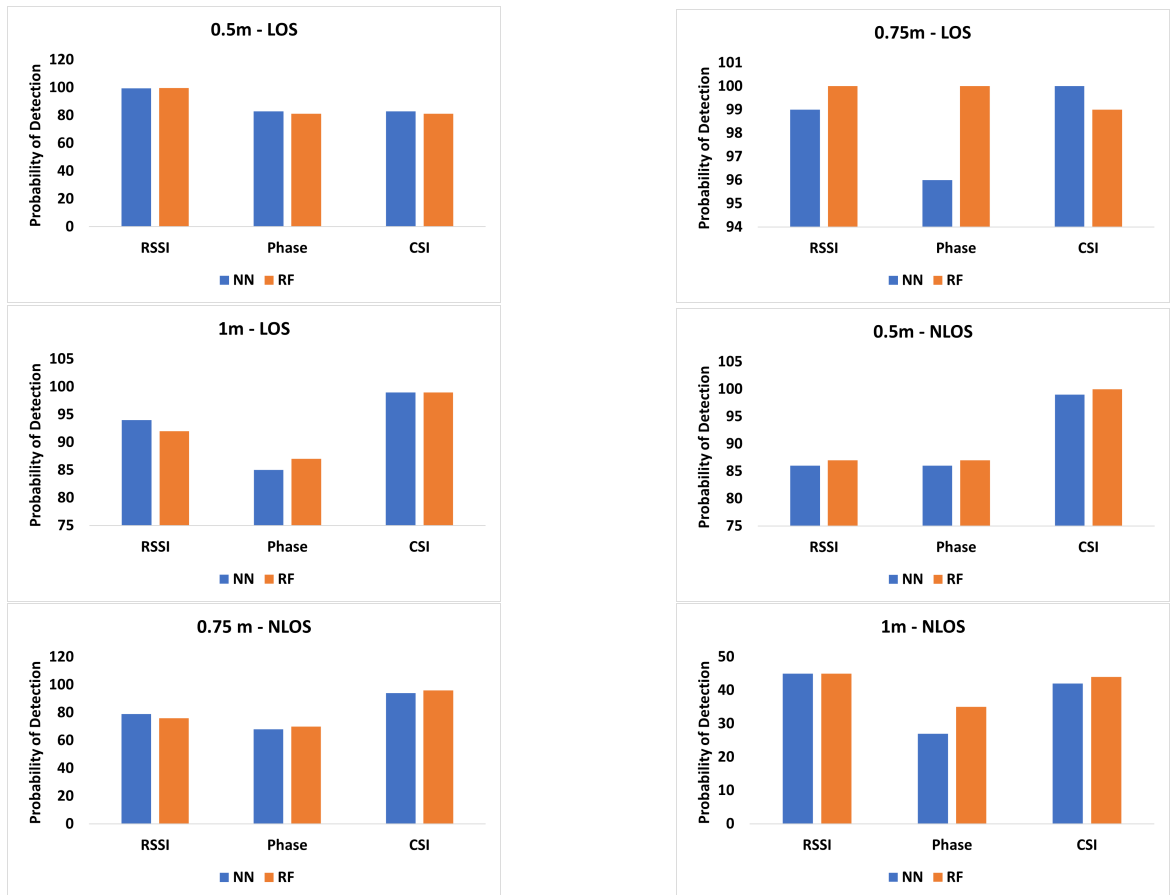
Figure 7.10: Location Accuracy of the floor plan using NN and RF

7.5.2 Position Estimation Performance using DL

In this section, we present the results of our experiments for position estimation using deep learning (DL) algorithms at various distances (0.5 meters, 0.75 meters, and 1 meter), evaluated with four different algorithms: NN, LSTM, CNN, and CNN + LSTM. The performance of each algorithm is assessed based on key metrics, including Loss, Accuracy, F1 score, and Precision (Pre). We provide a detailed analysis of the results for each block case and algorithm.
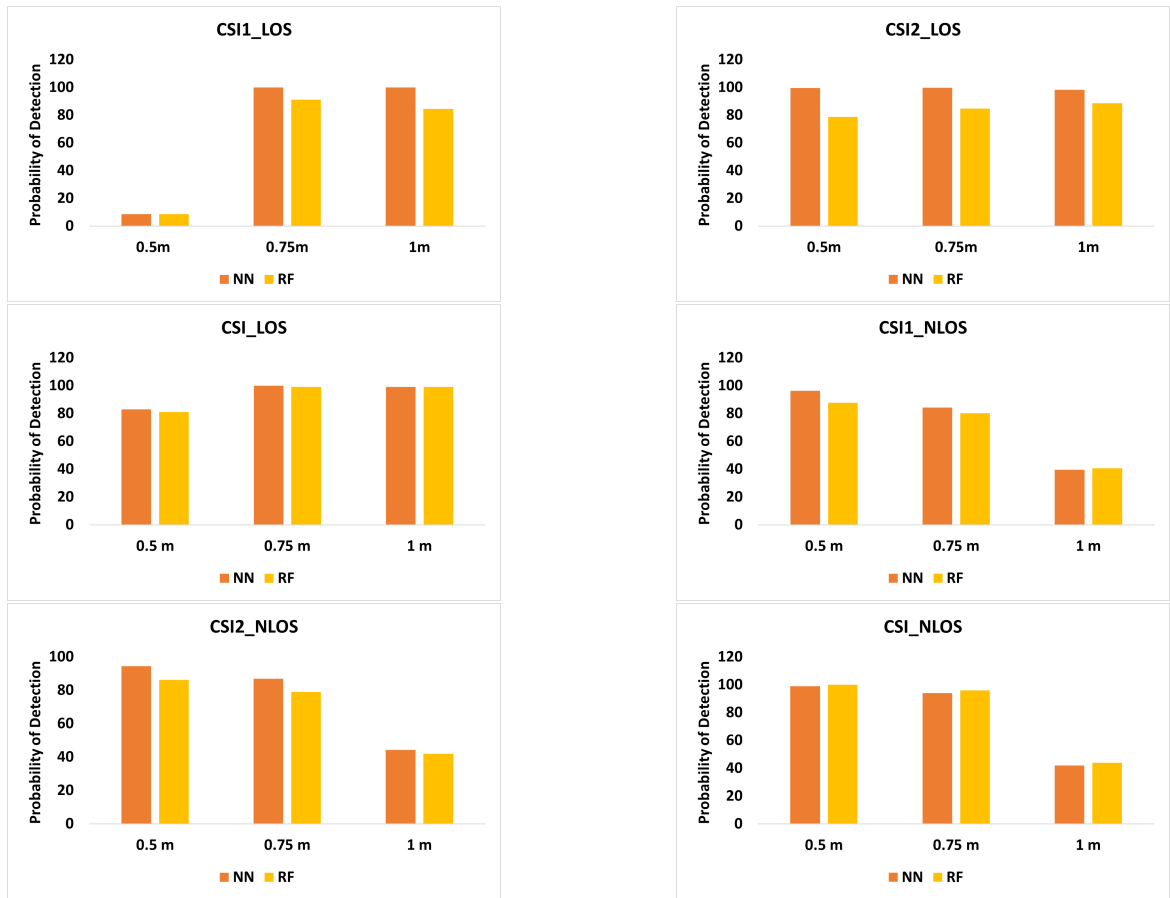
Figure 7.11: Comparison of CSI received on a single channel vs both channels for three cases.

7.5.2.1 0.5 meters Blocks

At blocks of 0.5 meters, the NN algorithm demonstrated competitive performance, achieving a Loss of 0.31, Accuracy of 0.87, F1 score of 1.13, and Precision of 1.08 for Antenna_1. For Antenna_2, it achieved a Loss of 0.30, Accuracy of 0.88, F1 score of 1.14, and Precision of 1.08. Combining both antennas (Antenna_1+2) significantly improved the algorithm's performance, resulting in a lower Loss of 0.06, high Accuracy of 0.97, F1 score of 0.98, and Precision of 0.92.

The LSTM algorithm exhibited robust performance at these blocks, with notable results for Antenna_1, Antenna_2, and the combined scenario. The CNN algorithm showed mixed results, while the CNN + LSTM algorithm performed reasonably well (refer Table 7.3).

Table 7.3: Results for 0.5 meter block

	0.5 meters											
Algorithms	**Antenna_1**				**Antenna_2**				**Antenna_1+2**			
	Loss	**Accuracy**	**F1**	**Pre**	**Loss**	**Accuracy**	**F1**	**Pre**	**Loss**	**Accuracy**	**F1**	**Pre**
NN	0.31	0.87	1.13	1.08	0.30	0.88	1.14	1.08	0.06	0.97	0.98	0.92
LSTM	0.20	0.92	1.05	0.99	0.25	0.90	1.16	1.10	0.02	0.99	0.95	0.90
CNN	0.41	0.83	1.39	1.29	0.46	0.80	1.41	1.32	0.14	0.91	0.95	0.90
CNN + LSTM	0.27	0.90	1.12	1.08	0.29	0.85	1.15	1.10	0.09	0.94	0.96	0.91

7.5.2.2 0.75 meters Blocks

At a distance of 0.75 meters, the NN algorithm maintained competitive performance with a Loss of 0.33, Accuracy of 0.85, F1 score of 1.18, and Precision of 1.14 for Antenna_1. Similar results were observed for Antenna_2, with an improved Accuracy of 0.90. Combining antennas (Antenna_1+2) further enhanced the NN algorithm's Accuracy.

The LSTM algorithm demonstrated strong and consistent performance at this distance, outperforming other algorithms in terms of Loss, Accuracy, F1 score, and Precision. The CNN algorithm showed consistent performance, with perfect Accuracy when both antennas were combined. The CNN + LSTM algorithm exhibited promising results, although a slight decrease in Accuracy was noted (refer Table 7.4).

Table 7.4: Results for 0.75 meter block

| Algorithms | 0.75 meters | | | | | | | | | | | |
| | Antenna_1 | | | | Antenna_2 | | | | Antenna_1+2 | | | |
	Loss	Accuracy	F1	Pre	Loss	Accuracy	F1	Pre	Loss	Accuracy	F1	Pre
NN	0.33	0.85	1.18	1.14	0.31	0.90	1.13	1.08	0.06	0.97	0.98	0.92
LSTM	0.34	0.88	1.16	1.12	0.14	0.93	1.0	9.4	0.018	0.99	0.93	0.88
CNN	0.31	0.89	1.13	1.08	0.14	0.94	0.98	0.92	0.00	1.00	0.94	0.88
CNN + LSTM	0.29	0.88	1.15	1.10	0.17	0.92	1.04	0.98	0.020	0.98	0.94	0.88

7.5.2.3 1 meter Blocks

At a distance of 1 meter, the NN algorithm maintained stability, achieving competitive results. The LSTM algorithm exhibited consistent performance, while the CNN algorithm showed a slight decrease in Accuracy. The CNN + LSTM algorithm experienced a minor decline in performance.

Overall, the LSTM algorithm consistently performed well across all distances, demonstrating strong Accuracy and precision. The CNN algorithm had mixed results, performing well at shorter distances but showing a decrease in performance at longer distances. The CNN + LSTM algorithm showed promising performance but also experienced a slight decline as the distance increased. The NN algorithm showed relatively stable performance but generally achieved lower Accuracy compared to the other algorithms (refer table 7.5).

Table 7.5: Results for 1 meter block

| Algorithms | 1 meters | | | | | | | | | | | |
| | Antenna_1 | | | | Antenna_2 | | | | Antenna_1+2 | | | |
	Loss	Accuracy	F1	Pre	Loss	Accuracy	F1	Pre	Loss	Accuracy	F1	Pre
NN	0.35	0.87	1.16	1.12	0.27	0.90	1.12	1.08	0.03	0.98	0.95	0.90
LSTM	0.22	0.92	1.05	0.99	0.24	0.91	1.18	1.13	0.019	0.99	0.93	0.88
CNN	0.37	0.79	1.34	1.27	0.24	0.90	1.16	1.10	0.017	0.99	0.94	0.89
CNN + LSTM	0.35	0.77	1.37	1.29	0.27	0.88	1.20	1.14	0.018	0.99	0.93	0.88

7.5.2.4 Bar Graph

Figure 7.12 presents a bar graph illustrating the comparison of Accuracy among the algorithms (LSTM, CNN, CNN + LSTM, and NN) with respect to the three different antennas: Antenna_1, Antenna_2, and Antenna_1+2. The variations in Accuracy for each algorithm across different antennas are displayed.

It's important to note that the training process and methodology, including the handling of Antenna_1, Antenna_2, and the combined scenario, were conducted systematically. The distinctions among these antennas were introduced during the training phase, contributing to the nuanced evaluation presented in this section.

In conclusion, we have developed a method for estimating the position of a wireless device using advanced signal processing techniques and machine learning algorithms. We have tested our method in LOS, and have compared its performance to other machine learning methods. Our results show that the use of machine learning algorithms, particularly neural networks and support vector machines, can improve the accuracy of position estimation in both LOS environments. Additionally, our results show that the NN used in this study outperforms other machine learning methods in LOS environments. Overall, these results demonstrate the potential of our method for improving the accuracy of position estimation in wireless networks.
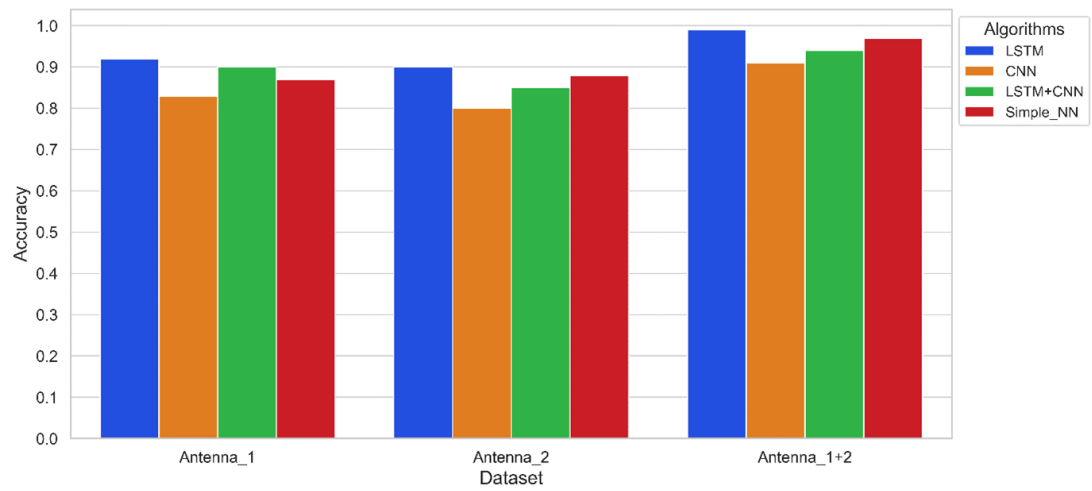
(a) 0.5 meter
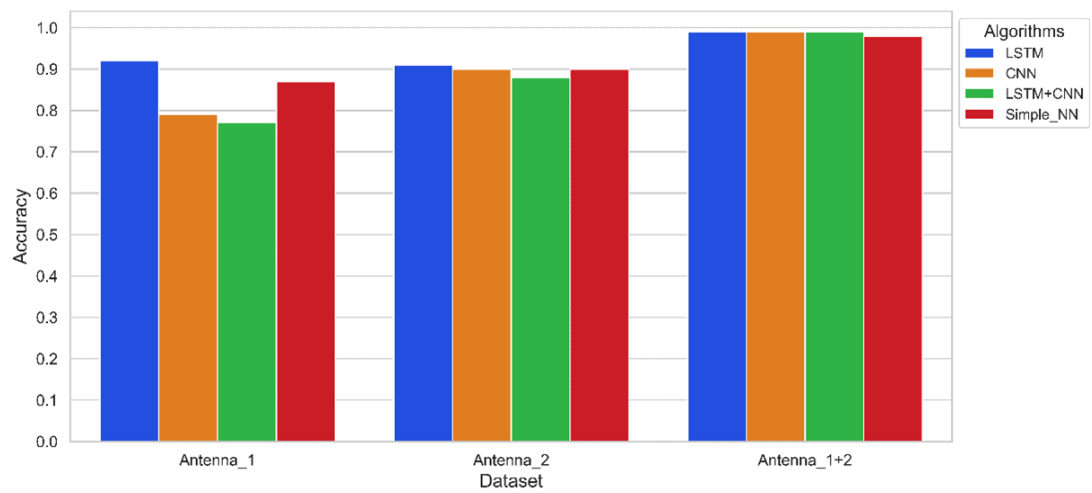
(b) 0.75 meter
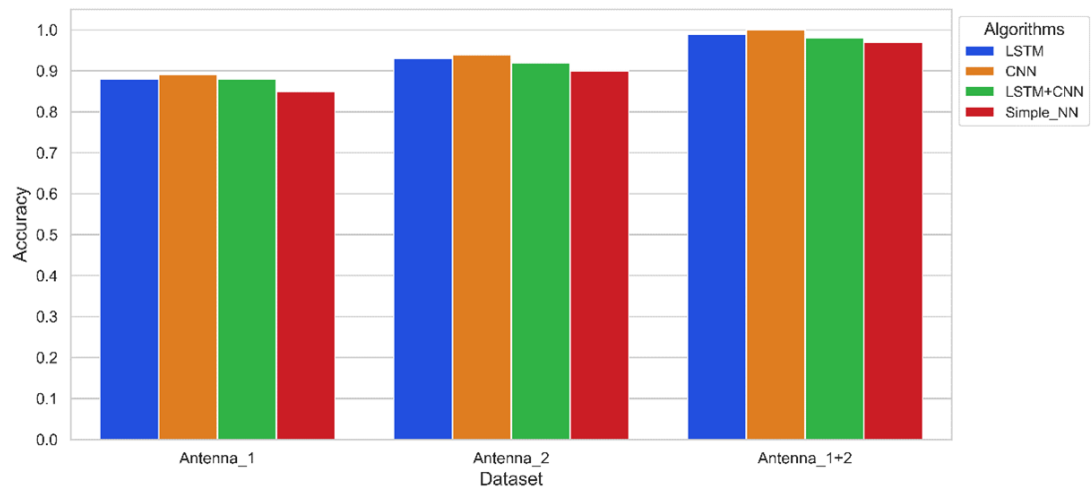
(c) 1 meter

Figure 7.12: Location Accuracy of floor plan using NN, LSTM, CNN

Chapter 8

Extended Research Work

The main objective of this chapter [1] is to elucidate additional work conducted beyond the primary scope of the thesis. It outlines the specific objectives and contributions of this extra work, providing readers with a comprehensive understanding of the extended efforts undertaken during the research.

8.1 In-network Angle Approximation for Supporting Adaptive Beamforming

This approach presents a novel network paradigm with the potential to reduce both complexity and latency. The integration of beamforming has become essential in modern wireless communication systems, requiring accurate beam alignment achieved through precise estimation of signal arrival direction. However, this estimation process is computationally complex, particularly in dynamic environments where users are constantly in motion.

We propose a user-assisted in-network method to optimally approximate the angle of arrival. This is achieved by segmenting the cell area into an exponentially binned grid, leveraging the capabilities of programmable data planes and their match-action table (MAT) logic. The method relies on periodic location messages reported by the UE, which are processed within the network to dynamically reconfigure base station antennas. This results in the implementation of user-assisted in-network beam control.

The proposed method is implemented in P4 [2] and executed on a Tofino ASIC. Our evaluation establishes a theoretical bound on the absolute error of the MAT-based angle approximation, demonstrating its alignment with empirical error distributions. Importantly, we observe no significant increase in errors related to latency, considering various control cycle times (less than 100 ms) and user movement at moderate speeds (less than 90 km/h). Additionally, resource

---

[1]This work is from one of our published work [166]
[2]Description of P4 is in appedix

usage is found to be influenced solely by the size of the Ternary content-addressable memory (TCAM) table storing angle approximation values, with no notable per-stage resource impact on the pipeline.

8.1.1 Introduction

The evolution of wireless networks towards accommodating escalating data service demands has necessitated the exploration of the electromagnetic spectrum's higher frequencies. This exploration is driven by the urgent need for bandwidth to support the burgeoning data traffic, leading to the consideration of millimeter-wave (mmWave) frequencies for the deployment of 5G wireless communication networks. The mmWave spectrum, defined as the range from 30 to 300 GHz, is particularly attractive for its potential to offer substantial bandwidths, thereby enabling higher data transfer rates [17].

Nevertheless, the deployment of mmWave communications is challenged by significant hurdles, including pronounced propagation loss, limited signal travel distances, and a high vulnerability to obstruction by physical barriers such as buildings and vegetation, and even human bodies. To mitigate these limitations, particularly the issue of limited propagation distances in mmWave communications, beamforming emerges as a viable technological solution. Beamforming is advantageous for its capacity to extend coverage, enhance signal quality, enable precise tracking of UE and facilitate coordination among base stations (BS) [80].

This research focuses on refining beamforming techniques to improve the accuracy of aligning mmWave signals. Given the directional propagation of mmWave signals, achieving accurate beam alignment represents a formidable challenge. Traditional strategies often rely on exhaustive search methods, which are resource-intensive. Our proposed methodology introduces an innovative use of P4-enabled switches, which are capable of performing elementary mathematical operations and storing previous information in tables, to determine the Angle of Arrival (AoA) between the transmitter and receiver. This method leverages straightforward trigonometric calculations to offer a more efficient solution.

8.1.1.1 Research Motivation

Our investigation is driven by several pivotal considerations:

Efficiency at the Network Switch Level: By conducting complex operations at the network switch level (data link layer), our approach aims to enhance processing efficiency and optimize the use of resources.

Vision for Distributed Architecture: This study contributes to the development of a distributed architecture, pushing network functionalities beyond the conventional boundaries of the network layer.

Exploitation of P4-Enabled Switches: Utilizing the capabilities of P4 technology, our ap-

proach seeks to alleviate network layer congestion by delegating specific operations to the data link layer. This strategy promises greater network customization and adaptability, which are critical for the success of 5G networks.

Adaptation through Software-Defined Radio (SDR): The flexibility afforded by software-defined radio technology aligns perfectly with the dynamic requirements of 5G networks, offering a versatile framework for network customization.

8.1.1.2 Potential Applications

The proposed methodology holds promise for a variety of applications, including but not limited to:

Security Enhancement: Applying P4-enabled switches to bolster the security measures within 5G networks.

Backhaul Network Optimization: Evaluating performance improvements in the backhaul network, extending the focus beyond the end-user experience.

Edge Computing Integration: Investigating the potential for integrating edge computing capabilities within the proposed network architecture.

8.1.1.3 Challenges in Beamforming Training

While advanced beamforming techniques aim to boost network performance at the user level, it's crucial to assess their overall impact, particularly on the backhaul network. The conventional approach of pre-configuring beamforming at the Media Access Control (MAC) sub-layer, which oversees the operation of physical devices like antennas, necessitates a reevaluation of its effectiveness in enhancing backhaul network performance.

8.1.1.4 Proposed Approach

We propose a user-assisted in-network approach to accurately steer the beam towards the UE. The method involves periodic location reporting by the UE to an in-network computing node (P4 switch in the transport network or Radio Access Network), which processes this information to compute the angle used for beam reconfiguration. The complex task of angle computation is approximated using match-action tables (MATs) in the data plane, with bounded approximation errors.

8.1.1.5 Evaluation

The accuracy of the proposed system is evaluated in dynamic scenarios involving a moving UE and varying control latency. Additionally, the resource usage of the Tofino-based implementation is analyzed. The study demonstrates the potential of P4 and P4-enabled devices in devel-

oping unique edge-cloud or fog network architectures, facilitating the provision of personalized network services.

This work contributes to the ongoing discourse on enhancing wireless communication networks, particularly in the context of 5G, and underscores the potential of P4 technology in optimizing network performance and customization.

8.1.2 System Design

Figure 8.1 illustrates the segmented network scenario considered. Mobile users are connected to the 5G network and indirectly linked to switches in the access aggregation network through core network protocols. In this network, it is assumed that some switches are P4-programmable. The proposed system involves mobile users periodically sending their GPS locations to a P4 switch. The P4 switch calculates the angle of the UE around the corresponding base station and sends a configuration message to the base station to adjust the beam direction towards the UE. This user-assisted in-network method is anticipated to reduce control latency and enhance beam steering compared to traditional approaches.
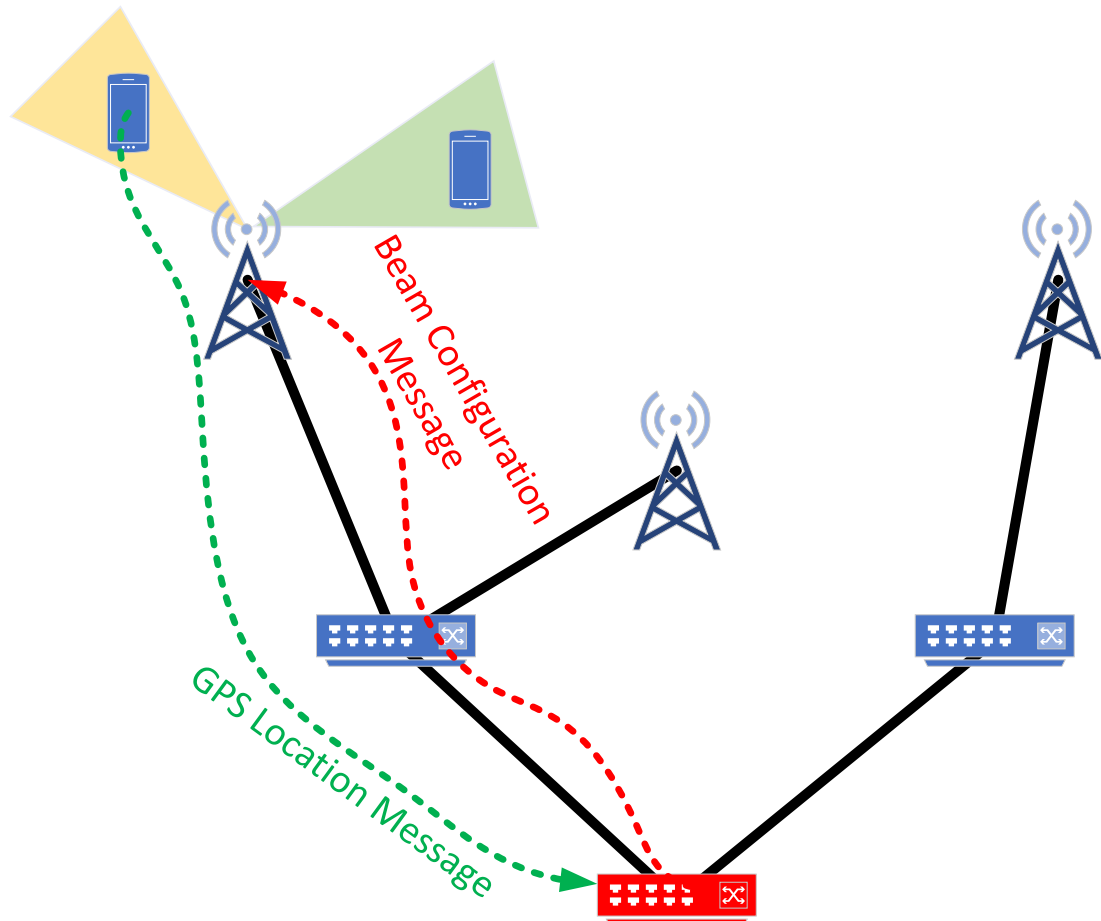
Figure 8.1: Main concept of the proposed user-assisted in-network beam-control.

8.1.3   Angle Approximation in the Data Plane

The angle approximation process in the data plane involves several key steps, as illustrated in Figure 8.2. Figure 8.2a depicts the positions of two UEs within the range of a base station and the desired Angles of Arrival (α_1, α_2) that need to be determined for steering the beams.

| (a) Direct Angle of Arrival | (b) Base-angle Approximation on a Grid | (c) Final Angle Transformation |
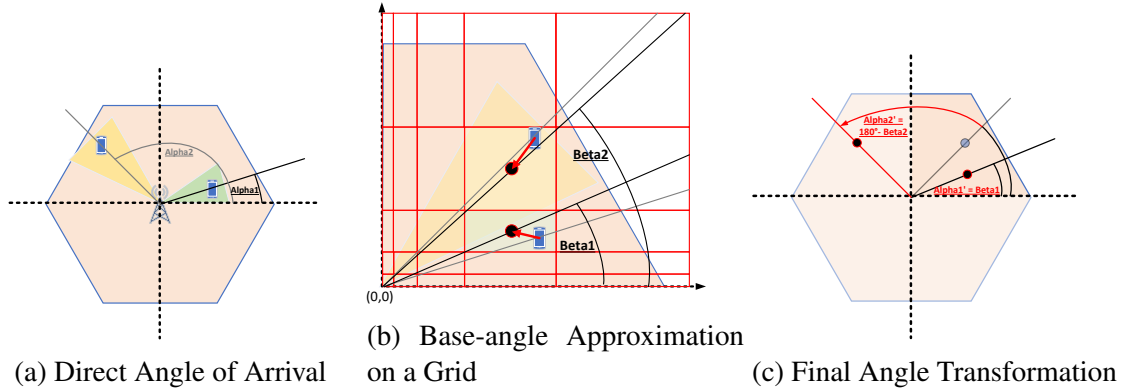
Figure 8.2: Key steps of beam angle approximation with an exponentially binned grid.

The absolute coordinates of UEs are initially transformed into a relative coordinate system, with the base station's location as the origin. The base angle of a UE with relative location (a,b) can be computed as $\beta = \arctan|b|/|a|$. However, due to the complexity of the arctangent function, an alternative approach is needed.
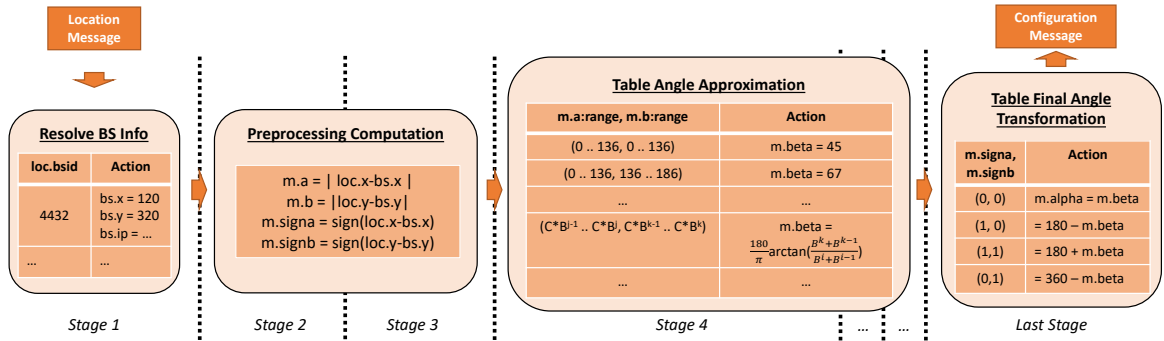
Figure 8.3: Data Plane Design of the Angle Approximation

The approximation method, as shown in Figure 8.2b, involves using an exponential binning grid to approximate the UE's location with the centroid of the containing grid cell. The centroid points are then used to determine the approximated base angles (β_1 and β_2). The final angle transformation corrects the quadrant, resulting in the approximated angle (α_1' and α_2') of the beam for the given UE.

The implementation design of the Angle Approximation method in the data plane is depicted in Figure 8.3. When a location message is received, it is parsed, and the UE's location with information about the base station is stored in a new header instance (*loc*). The base station coordinates are resolved using an exact match-action table (MAT). The angle approximation relies on two match-action tables: Angle Approximation and Final Angle Transformation.

The Angle Approximation table performs range matching on keys *m.a* and *m.b*, representing the exponential binning grid. The Final Angle Transformation table matches on keys *m.signa* and *m.signb* to obtain the final angle approximation α'. The data plane design allows for efficient and accurate angle computation, paving the way for improved beam steering in mmWave communication networks.

8.1.4 Validation of Concept

We have successfully implemented the proposed methodology using P4 within the TNA (Tofino Native Architecture) model and conducted comprehensive evaluations on a Tofino ASIC. Our assessment revolves around three primary aspects: 1) The accuracy of the MAT-based angle estimation under various granularity factors (number of bins, N=20, 40, 60, and 80), 2) the impact of mobile UE movement and non-zero control cycle delays on the method's precision, and 3) the correlation between Tofino resource utilization (stages, SRAM, TCAM memories) and the applied granularity factor N.

8.1.5 Accuracy of Angle Approximation

Figure 8.5 illustrates the absolute error distribution of angle approximation for different grid granularities (N=20, 40, 60, and 80) across varying cell diameters (200m to 1km). The evaluation, performed with 100,000 UE locations randomly distributed within a specific diameter around a base station, emphasizes that grid granularity has a more substantial impact on approximation error than cell diameter. The maximum errors for N=20, 40, 60, and 80 are approximately 8, 5, 4, and 2.5 degrees, respectively.

Practically, larger errors necessitate wider beams. In static scenarios, the beam width needs to be twice the maximum approximation error. For example, with a 5-degree wide beam and a maximum error of 2.5 degrees, the system ensures that the UE remains within the beam. In addition to empirical analysis, we present a theoretical bound on the error of the applied grid-based angle approximation.

Lemma 1 *The absolute error of the proposed MAT-based angle approximation is bounded by* $2 \times \arctan(\sqrt{B}) - \frac{\pi}{2}$ *(in radians), where B is the base number in* $B^N = D$*, for a predefined maximum distance D and granularity factor N.*

(Proof sketch.) If the user's relative coordinates (a, b) lie in a cell grid $|a| \in [B^i, B^{(i+1)})$ and $|b| \in [B^k, B^{(k+1)})$ for any positive integers i and k, the angle is approximated according to the central point of the cell. The deviation from the real angle is largest at one of the corner points of the cell. By defining error functions for the corner points and taking derivatives in i and k to find the location of maximum errors, we establish the error bound.

This theoretical bound aligns with empirical error distributions. For instance, in a cell with a diameter of 800 meters, the theoretical error bounds for granularity factors N=20, 40, 60, and 80 are 9.5, 4.8, 3.2, and 2.4 degrees, respectively.

8.1.6   Impact of Mobile UEs and Control Latency

To showcase our concept in a dynamic scenario, we simulate a small cell in a semi-urban environment at the UofG, UK (Figure 8.4). A user moves along a predefined route at speeds ranging from 5 to 200 kmph. We emulate UE movement, assessing the impact of displacement on the UE's location concerning the feedback loop of angle approximation and beam reconfiguration, which takes more than zero time. The round trip delay between UE location information departure and control message arrival at the base station varies between 5, 20, and 100 ms.

Figure 8.4: University campus showing the transmitter and the mobile user.

Figures 8.6-8.7 present angle approximation errors at the time of arrival of the configuration message to the base station, accounting for UE movement. The results demonstrate that a larger granularity factor (N) yields better angle approximation, even with longer control cycle times and moderate UE speeds. Comparing $N = 20$ to $N = 80$, the increase in error due to latency and movement is less significant for $N = 20$ when the base error is high (around 9 degrees). These error distributions resemble static scenarios shown in Figure 8.5.

Significant deviation occurs only at a control cycle time of 100 ms and high UE speed (>90 kmph), as shown in Figure 8.7c. This indicates that wider beams are required at high speeds; otherwise, the UE may exit the coverage area as the beam cannot track the UE effectively.

Note that real-world environments are more complex, where radio propagation is influenced by various environmental factors, impacting the UE's quality of experience.
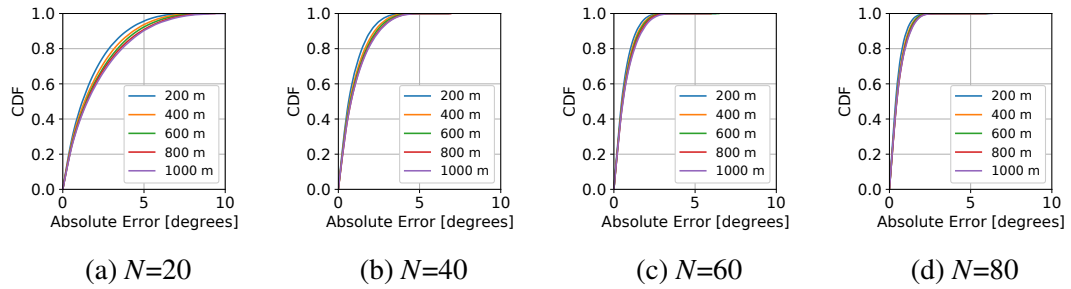
Figure 8.5: Error Distribution of MAT-based Angle Approximation.
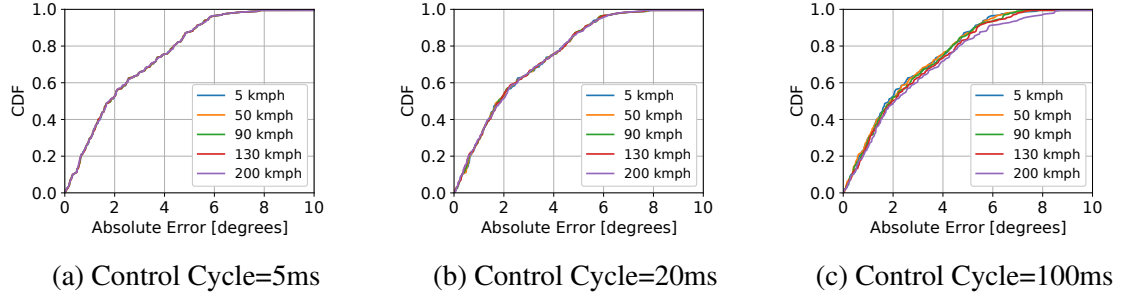
Figure 8.6: Angle approximation error when the user moves at a constant speed and the control cycle is not zero. N is set to 20.

8.1.7 Resource Utilization

Figure 8.8 illustrates the trade-off between granularity factor (N) and resource usage (stages, SRAM, and TCAM) on a Tofino ASIC. The grid resolution defined by N significantly impacts angle approximation accuracy. While larger N values result in better accuracy, they require a larger TCAM space for grid-searching logic in MAT.

Observations from the figure include constant SRAM usage, independent of the granularity factor. The grid-based angle approximation leverages a TCAM table, and therefore, the granularity factor correlates strongly with the required TCAM space. For N=20 and 40, the TCAM table occupies a single stage; for N=50 and 60, the TCAM table is distributed across two stages. For N=80, three stages are required. Although the proposed method occupies TCAM space on one or more stages, per-stage resource usage is not significant. Other network functions/pipelines related to mobile transport or RAN can be co-located with the proposed pipeline. The TCAM space of stages implementing the MAT-based angle approximation table is essentially fully occupied, but other resources like SRAM and ALUs can potentially be used in these stages by other pipelines.

8.1.8 Customization

Environmental variations around a base station can lead to non-linear radio propagation due to reflections from buildings and other objects. To address these effects, customization of the proposed method may be necessary. Two potential approaches are: 1) introducing customized

(a) Control Cycle=5ms   (b) Control Cycle=20ms   (c) Control Cycle=100ms
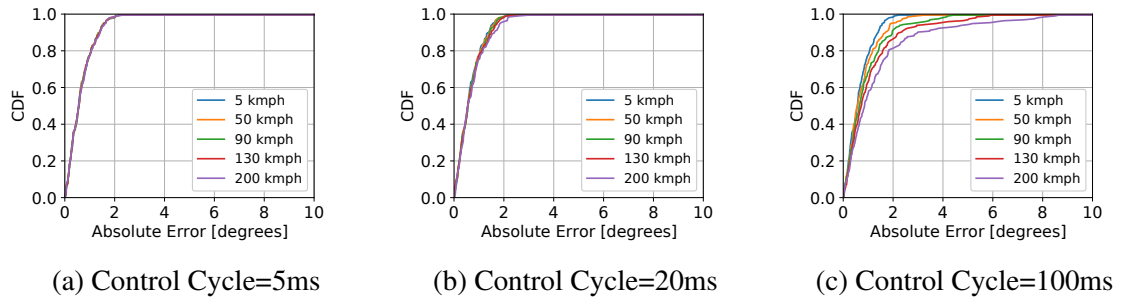
Figure 8.7: Angle approximation error when the user moves at a constant speed (5kmph to 200kmph) and the control cycle is 5ms, 20ms, or 100ms. N is fixed to 80.
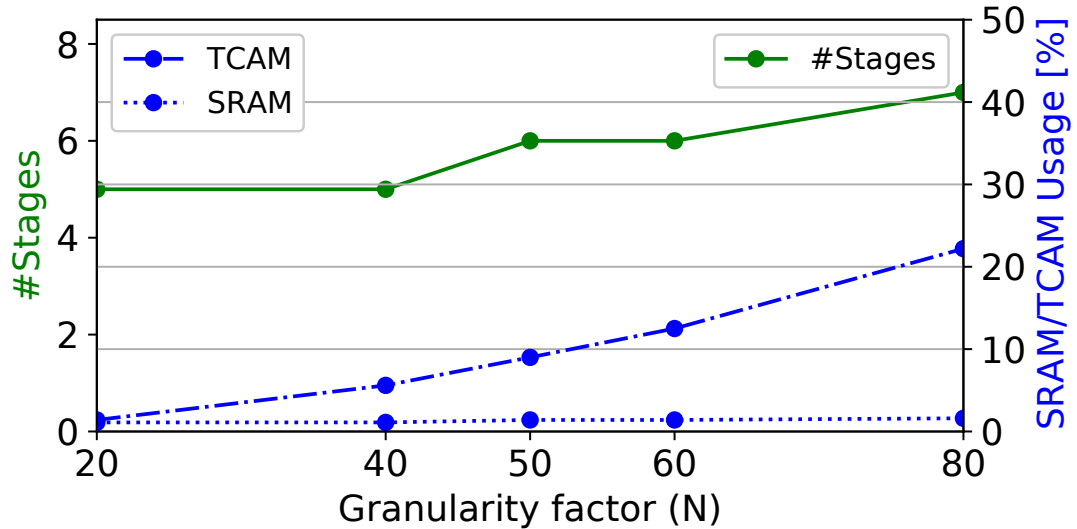
Figure 8.8: The trade-off between granularity factor (N) and resource usage (stages, SRAM and TCAM) on a Tofino ASIC.

tables for each base station, and 2) extending the angle approximation grid to cover all possible quadrants around the base station, accommodating asymmetric signal propagation in the cell. In the latter case, the approximation table requires four times more TCAM entries to cover all four quadrants of the cell. However, in the first case, separate tables for each base station would be needed, increasing the required TCAM space. Future work includes a more detailed analysis of customization scenarios and their efficient implementation.

These comprehensive evaluations validate the effectiveness and feasibility of our proposed angle approximation method using the MAT-based approach within the P4 framework and Tofino ASIC.

8.1.9   Conclusion

Accurate estimation of the direction of arrival is pivotal for effective adaptive beamforming in wireless communications. Traditional beamforming algorithms, operating at the link layer, introduce latency concerns, particularly in the context of backhaul networks. To enhance net-

work responsiveness, we propose a novel user-assisted beamforming strategy leveraging programmable data planes and in-network computation facilitated by P4.

In our approach, UE periodically reports its location to the network, and beam parameter computation (specifically, the angle of arrival) is performed by a programmable switch within the network. Our preliminary results indicate that the additional computation, which involves dividing the cell area into binned grids, yields angle approximations with manageable error bounds and requires moderate per-stage resources. The proposed scheme has been demonstrated on a Tofino ASIC.

Chapter 9

Conclusion and Future Work

This project represents a significant advancement in the field of wireless communication systems, with a particular focus on the areas of DoA estimation, beamforming, and localization techniques. At the heart of this endeavor was the use of innovative methods and state-of-the-art technology, including tools such as MATLAB, BladeRF, LabVIEW, and USRP X300. These tools were instrumental in achieving the project's ambitious goals, providing valuable insights and laying the groundwork for future advancements in the field.

One of the notable achievements of this project was the effective implementation of DoA estimation, beamforming, and localization. These implementations were not only theoretical but also practical, as they utilized various tools to demonstrate their efficacy in real-world scenarios. In particular, the use of Software Defined Radio (SDR) units proved to be a game-changer in achieving precise signal arrival angle estimation. This precision is pivotal in enhancing the accuracy and reliability of wireless communication systems.

The project also delved deep into the detailed analysis of DoA techniques. This analysis was crucial in highlighting the practical applications of these techniques in modern communication systems. By understanding their nuances, the project was able to showcase the versatility and utility of DoA estimation in various contexts.

Furthermore, the exploration of digital and hybrid beamforming techniques was a key aspect of this research. This exploration emphasized the critical role these techniques play in managing signal direction and mitigating interference, which are core challenges in wireless communications.

Another major achievement was the successful demonstration of localization capabilities, particularly using LabVIEW and USRP X300. This demonstration not only validated the theoretical concepts developed in the project but also showcased their practical applicability in real-world scenarios.

Collaboration was also a cornerstone of this project's success. By partnering with esteemed institutions such as the University of Iran, ELTE, and the UofG, the project was able to enrich its research scope. This collaborative effort brought together diverse perspectives and expertise,

contributing significantly to the depth and breadth of the research.

Limitations: The main limitation identified in this project pertains to sub-optimal configuration schemes, which indicates a need for further optimization to enhance system performance. Specifically, a notable challenge encountered was with the BladeRF Software Defined Radio (SDR) units, particularly their performance in high-frequency over-the-air communications. The BladeRF, while robust in many scenarios, demonstrated limitations when operating at higher frequencies, which is a critical aspect for advanced wireless communication systems.

Moreover, there's a potential need for phase and clock synchronization when using two BladeRF boards in tandem, especially in the context of a 4x4 antenna setup. This synchronization is crucial for ensuring coherent signal processing and effective beamforming, which are fundamental for the accuracy and efficiency of DoA estimation and other advanced communication techniques.

Additionally, the beam steering setup in the project encountered limitations due to the number of antenna elements. The current configuration, while functional, could greatly benefit from an increased number of antenna elements. This expansion would enable a narrower beam width, which is essential for more precise beam steering. A narrower beam width contributes significantly to improved signal directionality and interference mitigation, enhancing overall system performance.

9.1 Future Work

Future work should focus on:

1. Optimizing configuration schemes.

2. Advancing beamforming techniques and algorithms.

3. Investigating novel localization methods.

4. Collaborating with industry for practical implementation.

The project demonstrates the effectiveness of modern technologies in wireless communications, laying a foundation for future research and innovation in the field. The following work is a part of the future work.

9.1.1 6-Bit Digital Phase Shifter for Electronic Beam Steering Applications

Phased array antennas (PAAs) are of great interest for next-generation wireless systems due to their fast and accurate electronic beam steering capabilities, surpassing traditional mechanical scanning methods [167, 168]. However, the widespread adoption of PAAs is hindered by high

costs and complex designs associated with conventional analog phase shifter arrays. This work presents an innovative solution—a low-cost, compact PAA system with integrated digital phase shifters for precise beam control. The system employs a modular antenna array architecture with decentralized phase shifting to reduce complexity and enhance scalability.

Key contributions include optimizing a 5-element microstrip subarray meeting size and frequency requirements, and introducing a series-fed distribution network for seamless integration of custom digital phase shifters, allowing incremental phase adjustments. Practical beam steering at 3.75 GHz demonstrates the system's effectiveness. The streamlined architecture and low-cost digital phase shifters offer a groundbreaking approach, potentially overcoming traditional barriers in PAA implementations and expanding applications like fast-tracking objects.

The work is structured as follows: Section 9.2 details the methodology for developing the proposed PAA system. Section 9.3 discusses obtained results, highlighting system performance. Finally, Section 9.4 summarizes key findings and conclusions from this exploration of low-cost, compact PAA systems with integrated digital phase shifters.

9.2 Model Design

The model design encompasses a systematic approach, beginning with the creation of a 5-element uniform linear microstrip antenna array optimized for the operational frequency of 3.75 GHz. The design, simulated in CST Microwave Studio (Figure 9.1), utilizes FR-4 substrate boards (30x30 cm) with a permittivity of 4.5 and a thickness of 1.6 mm. The optimization process involved a trade-off between gain, directivity, and size. Each antenna element was fine-tuned to achieve maximum performance, ensuring that the array operates efficiently within the desired frequency band.

The series-fed network plays a crucial role in distributing power from the input port to each antenna element, allowing seamless integration with custom 6-bit digital phase shifters. The feeding network design considerations include minimizing power losses, maintaining compactness, and accommodating the integration of digital phase shifters. To achieve these objectives, a series feed configuration was chosen for its inherent advantages in terms of low insertion losses, simplicity of design, and compatibility with the integration of phase shifters.

These custom 4-channel 6-bit Analog devices (HMC649ALP6E) digital phase shifters were implemented to allow precise beam steering control. Each phase shifter provides 64 possible phase states with a phase step of 5.625 degrees. The 4-channel phase shifters enable independent phase control for each antenna element, facilitating dynamic and adaptive beam steering. The fabrication process involved a combination of printed circuit board (PCB) manufacturing techniques and surface-mount device (SMD) technology, resulting in compact and cost-effective phase shifters.

This phase shifter is controlled directly through the FPGA. The advantage of parallel control
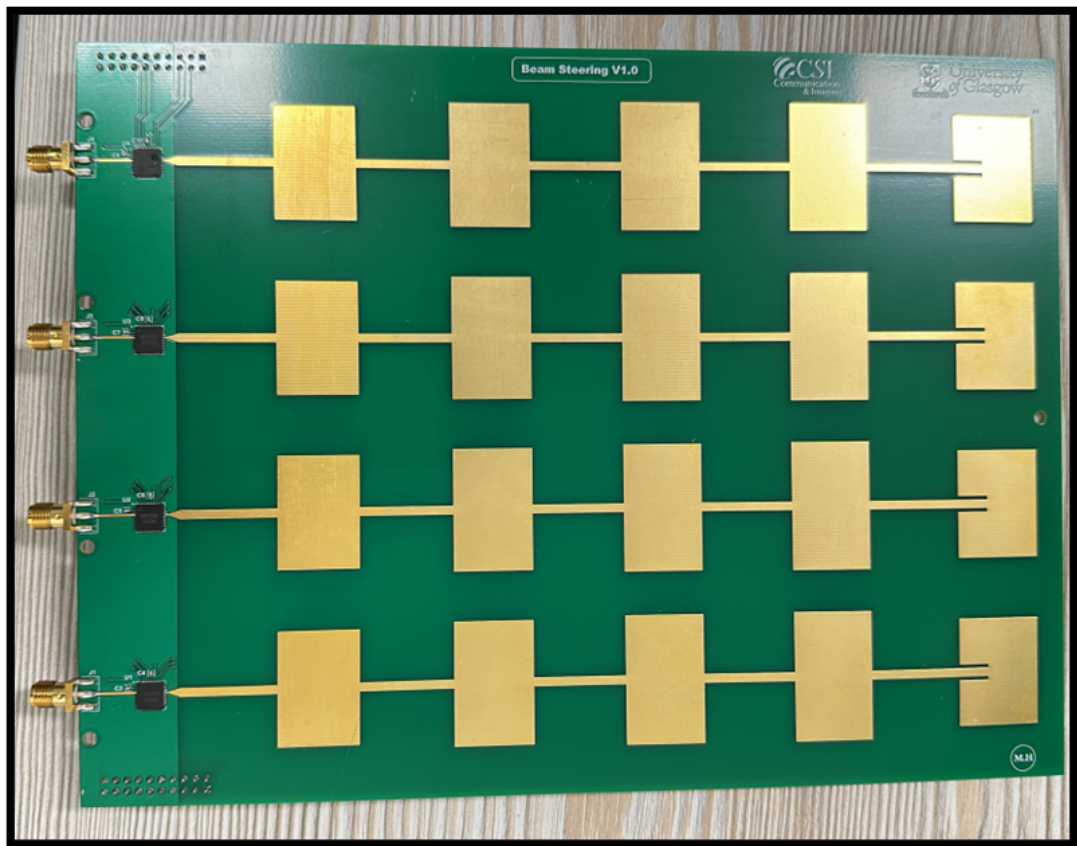
Figure 9.1: 4 channel antenna array containing 4X5 elements. Each channel feeds a series of 5 patch antennas.

for the phase shifters enhanced the steering speed. The Xilinx Spartan-7 FPGA is used in the proposed design. The internal clock frequency in the FPGA is 100 MHz, which enables a steering speed of 10 ns. Moreover, the FPGA is connected to the proposed Graphical User Interface (GUI) using the UART protocol to configure a fixed steering angle or electronic scanning mode with a reconfigurable scan time and scan angle.

The interconnected components, namely the microstrip antenna array, series-fed network, and digital phase shifters, form a compact and efficient phased array system. The design choices made in each subsystem aim to strike a balance between performance, cost-effectiveness, and ease of integration, laying the foundation for advanced beamforming capabilities.

9.3   Results and Discussion

The results highlight the successful implementation and testing of the compact phased array antenna system. Preliminary testing conducted in an anechoic chamber produced promising outcomes, validating the system's beamforming capabilities. The measured radiation pattern is closely aligned with simulated results (Figure 9.2), indicating the effectiveness of the antenna array in achieving the desired directional characteristics. The system demonstrated precise beam
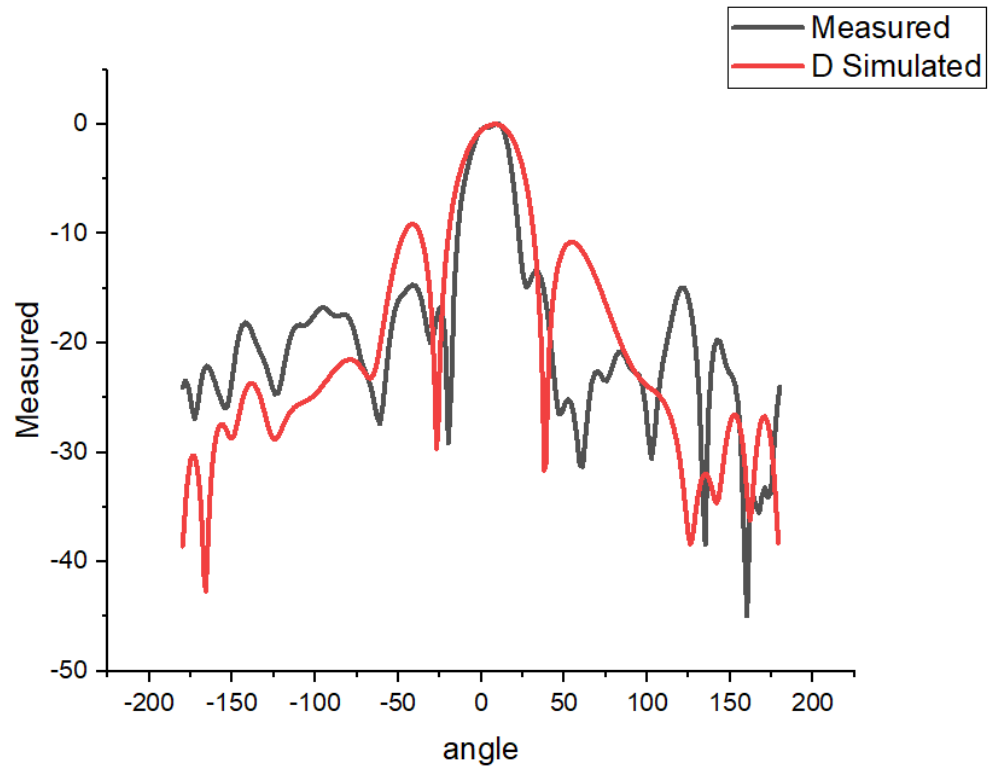
Figure 9.2: Measured vs. simulated antenna pattern.

steering at angles of 0°, and 90°, showcasing a gain variation of less than 1 dB, sidelobe levels below -10 dB, and minimal impact on the radiation pattern.
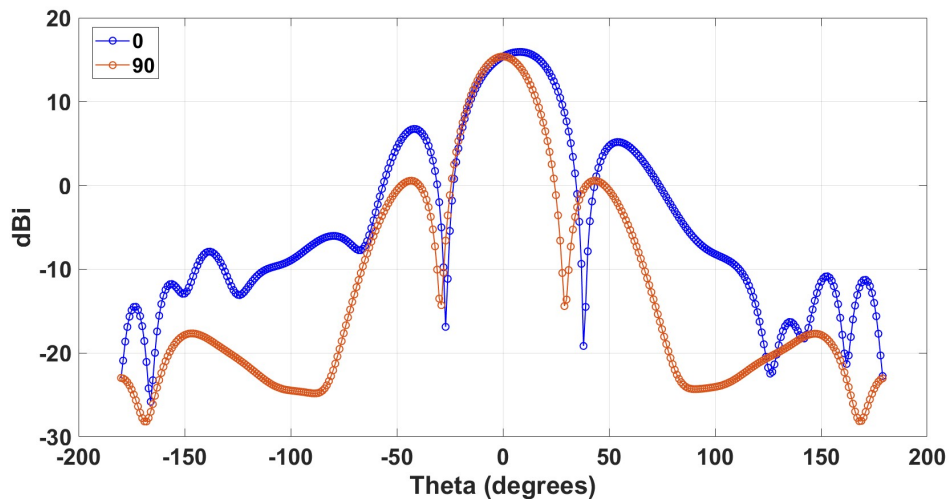
Figure 9.3: Simulated results of beam steering at 0 and 90 degrees.

Figure 9.3 illustrates the simulated beam steering capabilities, providing insights into the system's dynamic control. The phased array system achieved reliable and consistent beam steering across the specified angles, demonstrating its adaptability to changing operational requirements.

Further testing involved varying environmental conditions, such as temperature and humidity, to assess the robustness of the system.

Ongoing developments include the creation of a graphical user interface (GUI) (Figure 9.4) for enhanced user interaction and FPGA coding to augment dynamic control over the phase shifter and antenna array. The GUI provides a user-friendly platform for adjusting beam steering parameters, making the system accessible to operators with varying levels of expertise. Simultaneously, the FPGA coding efforts focus on enhancing the real-time adaptability of the phased array, ensuring rapid response to changing operational scenarios. The integration of beamform-

Figure 9.4: GUI interface for Phase Shifter.

ing with location estimation techniques adds a layer of sophistication, positioning the phased array system as a versatile solution for electronic beam steering applications. By leveraging received signals for both beamforming and localization, the system can be employed in scenarios requiring accurate target tracking, localization of communication sources, and improved situational awareness.

9.4   Conclusion

This work demonstrates an innovative phased array architecture using low-cost digital phase shifters that reduce complexity and cost compared to conventional implementations relying solely on high-end analog phase shifters. The system's reliable beam steering capabilities and ongoing efforts to incorporate automatic beam control and localization techniques will represent a significant advancement over existing benchtop phased array systems.

Bibliography

[1] P. Wang, J. Zhang, X. Zhang, Z. Yan, B. G. Evans, and W. Wang, "Convergence of satellite and terrestrial networks: A comprehensive survey," *IEEE access*, vol. 8, pp. 5550–5588, 2019.

[2] W. Ejaz, M. Naeem, A. Shahid, A. Anpalagan, and M. Jo, "Efficient energy management for the internet of things in smart cities," *IEEE Communications magazine*, vol. 55, no. 1, pp. 84–91, 2017.

[3] S. A. Bagloee, M. Tavana, M. Asadi, and T. Oliver, "Autonomous vehicles: challenges, opportunities, and future implications for transportation policies," *Journal of modern transportation*, vol. 24, pp. 284–303, 2016.

[4] F. Boccardi, R. W. Heath, A. Lozano, T. L. Marzetta, and P. Popovski, "Five disruptive technology directions for 5g," *IEEE communications magazine*, vol. 52, no. 2, pp. 74–80, 2014.

[5] R. Di Taranto, S. Muppirisetty, R. Raulefs, D. Slock, T. Svensson, and H. Wymeersch, "Location-aware communications for 5g networks: How location information can improve scalability, latency, and robustness of 5g," *IEEE Signal Processing Magazine*, vol. 31, no. 6, pp. 102–112, 2014.

[6] X. Zhang, S. Pan, and Q. Miao, "Adaptive beamforming-based gigabit message dissemination for highway vanets," *IEEE Transactions on Intelligent Transportation Systems*, vol. 23, no. 7, pp. 7666–7679, 2021.

[7] N. Shoaib, S. Shoaib, R. Y. Khattak, I. Shoaib, X. Chen, and A. Perwaiz, "Mimo antennas for smart 5g devices," *IEEE access*, vol. 6, pp. 77014–77021, 2018.

[8] J. Kaur, S. Bhatti, K. Tan, O. R. Popoola, M. A. Imran, R. Ghannam, Q. H. Abbasi, and H. T. Abbas, "Contextual beamforming: Exploiting location and ai for enhanced wireless telecommunication performance," *APL Machine Learning*, vol. 2, no. 1, 2024.

[9] R. Chataut and R. Akl, "Massive MIMO systems for 5G and beyond networks—overview, recent trends, challenges, and future research direction," *Sensors*, vol. 20, no. 10, p. 2753, 2020.

[10] P. Kumar *et al.*, "Review paper on development of mobile wireless technology," in *Journal of Physics: Conference Series*, vol. 1979, p. 012024, IOP Publishing, 2021.

[11] A. Gohar and G. Nencioni, "The role of 5G technologies in a smart city: The case for intelligent transportation system," *Sustainability*, vol. 13, no. 9, p. 5188, 2021.

[12] Y. Huo, X. Dong, and W. Xu, "5G cellular user equipment: From theory to practical hardware design," *IEEE Access*, vol. 5, pp. 13992–14010, 2017.

[13] Z. Zhang, X. Wang, K. Long, A. V. Vasilakos, and L. Hanzo, "Large-scale mimo-based wireless backhaul in 5G networks," *IEEE Wireless Communications*, vol. 22, no. 5, pp. 58–66, 2015.

[14] B. Alhayani, A. S. Kwekha-Rashid, H. B. Mahajan, H. Ilhan, N. Uke, A. Alkhayyat, and H. J. Mohammed, "5G standards for the Industry 4.0 enabled communication systems using artificial intelligence: Perspective of smart healthcare system," *Applied nanoscience*, pp. 1–11, 2022.

[15] R. M. Sandoval, A.-J. Garcia-Sanchez, F. Garcia-Sanchez, and J. Garcia-Haro, "Evaluating the more suitable ISM frequency band for IoT-based smart grids: A quantitative study of 915 MHz vs. 2400 MHz," *Sensors*, vol. 17, no. 1, p. 76, 2016.

[16] P. Sethi and S. R. Sarangi, "Internet of things: architectures, protocols, and applications," *Journal of Electrical and Computer Engineering*, vol. 2017, 2017.

[17] T. S. Rappaport, S. Sun, R. Mayzus, H. Zhao, Y. Azar, K. Wang, G. N. Wong, J. K. Schulz, M. Samimi, and F. Gutierrez, "Millimeter wave mobile communications for 5G cellular: It will work!," *IEEE access*, vol. 1, pp. 335–349, 2013.

[18] M. Attaran, "The impact of 5G on the evolution of intelligent automation and industry digitization," *Journal of Ambient Intelligence and Humanized Computing*, pp. 1–17, 2021.

[19] K. Pahlavan and P. Krishnamurthy, *Principles of wireless networks*, vol. 1. Prentice Hall PTR, 2001.

[20] I. F. Akyildiz, C. Han, and S. Nie, "Combating the distance problem in the millimeter wave and terahertz frequency bands," *IEEE Communications Magazine*, vol. 56, no. 6, pp. 102–108, 2018.

[21] S. Tripathi, N. V. Sabu, A. K. Gupta, and H. S. Dhillon, "Millimeter-wave and terahertz spectrum for 6G wireless," in *6G Mobile Wireless Networks*, pp. 83–121, Springer, 2021.

[22] T. L. Marzetta, "Noncooperative cellular wireless with unlimited numbers of base station antennas," *IEEE transactions on wireless communications*, vol. 9, no. 11, pp. 3590–3600, 2010.

[23] L. Zhang, M. Z. Chen, W. Tang, J. Y. Dai, L. Miao, X. Y. Zhou, S. Jin, Q. Cheng, and T. J. Cui, "A wireless communication scheme based on space-and frequency-division multiplexing using digital metasurfaces," *Nature electronics*, vol. 4, no. 3, pp. 218–227, 2021.

[24] A. Zakrzewska, S. Ruepp, and M. S. Berger, "Towards converged 5G mobile networks-challenges and current trends," in *Proceedings of the 2014 ITU kaleidoscope academic conference: Living in a converged world-Impossible without standards?*, pp. 39–45, IEEE, 2014.

[25] H. Sharma, N. Kumar, and R. Tekchandani, "Physical layer security using beamforming techniques for 5G and beyond networks: A systematic review," *Physical Communication*, vol. 54, p. 101791, 2022.

[26] D. d. S. Brilhante, J. C. Manjarres, R. Moreira, L. de Oliveira Veiga, J. F. de Rezende, F. Müller, A. Klautau, L. Leonel Mendes, and F. A. P. de Figueiredo, "A literature survey on AI-aided beamforming and beam management for 5G and 6G systems," *Sensors*, vol. 23, no. 9, p. 4359, 2023.

[27] E. Björnson, L. Sanguinetti, H. Wymeersch, J. Hoydis, and T. L. Marzetta, "Massive MIMO is a reality—what is next?: Five promising research directions for antenna arrays," *Digital Signal Processing*, vol. 94, pp. 3–20, 2019.

[28] B. Zhou, A. Liu, and V. Lau, "Successive localization and beamforming in 5g mmwave mimo communication systems," *IEEE Transactions on Signal Processing*, vol. 67, no. 6, pp. 1620–1635, 2019.

[29] Y. Lu, M. Koivisto, J. Talvitie, M. Valkama, and E. S. Lohan, "Positioning-aided 3d beamforming for enhanced communications in mmwave mobile networks," *IEEE Access*, vol. 8, pp. 55513–55525, 2020.

[30] N. Sharma, P. Ahlawat, and R. K. Aggarwal, "Artificial intelligence enabled 5g-nr optimisation," *International Journal of Sensor Networks*, vol. 42, no. 1, pp. 41–51, 2023.

[31] M. S. Islam, T. Jessy, M. S. Hassan, K. Mondal, and T. Rahman, "Suitable beamforming technique for 5g wireless communications," in *2016 International Conference on Computing, Communication and Automation (ICCCA)*, pp. 1554–1559, IEEE, 2016.

[32] W. Chen, X. Lin, J. Lee, A. Toskala, S. Sun, C. F. Chiasserini, and L. Liu, "5g-advanced toward 6g: Past, present, and future," *IEEE Journal on Selected Areas in Communications*, vol. 41, no. 6, pp. 1592–1619, 2023.

[33] B. M. ElHalawany, S. Hashima, K. Hatano, K. Wu, and E. M. Mohamed, "Leveraging machine learning for millimeter wave beamforming in beyond 5g networks," *IEEE Systems Journal*, vol. 16, no. 2, pp. 1739–1750, 2021.

[34] S. Sand, R. Tanbourgi, C. Mensing, and R. Raulefs, "Position aware adaptive communication systems," in *2009 Conference Record of the Forty-Third Asilomar Conference on Signals, Systems and Computers*, pp. 73–77, IEEE, 2009.

[35] M. Cheng and X. Fang, "Location information-assisted opportunistic beamforming in LTE system for high-speed railway," *EURASIP Journal on Wireless Communications and Networking*, vol. 2012, no. 1, pp. 1–7, 2012.

[36] H. Ruan and R. C. de Lamare, "Low-complexity robust adaptive beamforming algorithms exploiting shrinkage for mismatch estimation," *IET Signal Processing*, vol. 10, no. 5, pp. 429–438, 2016.

[37] T. E. Bogale, "Adaptive beamforming and modulation design for 5G V2I networks," in *2020 10th Annual Computing and Communication Workshop and Conference (CCWC)*, pp. 0090–0096, IEEE, 2020.

[38] F. Maschietti, D. Gesbert, and P. de Kerret, "Location-aided coordinated analog precoding for uplink multi-user millimeter wave systems," *arXiv preprint arXiv:1711.03031*, 2017.

[39] O. Igbafe, J. Kang, H. Wymeersch, and S. Kim, "Location-aware beam alignment for mmWave communications," *arXiv preprint arXiv:1907.02197*, 2019.

[40] N. J. Myers, Y. Wang, N. González-Prelcic, and R. W. Heath, "Deep learning-based beam alignment in mmWave vehicular networks," in *ICASSP 2020-2020 IEEE International Conference on Acoustics, Speech and Signal Processing (ICASSP)*, pp. 8569–8573, IEEE, 2020.

[41] X. Li, A. Alkhateeb, and C. Tepedelenlioğlu, "Generative adversarial estimation of channel covariance in vehicular millimeter wave systems," in *2018 52nd Asilomar Conference on Signals, Systems, and Computers*, pp. 1572–1576, IEEE, 2018.

[42] A. Alkhateeb, S. Alex, P. Varkey, Y. Li, Q. Qu, and D. Tujkovic, "Deep learning coordinated beamforming for highly-mobile millimeter wave systems," *IEEE Access*, vol. 6, pp. 37328–37348, 2018.

[43] J. S. Blogh, J. Blogh, and L. L. Hanzo, *Third-generation systems and intelligent wireless networking: smart antennas and adaptive modulation*. John Wiley & Sons, 2002.

[44] R. A. Monzingo and T. W. Miller, *Introduction to adaptive arrays*. Scitech publishing, 2004.

[45] Q. Li, G. Li, W. Lee, M.-i. Lee, D. Mazzarese, B. Clerckx, and Z. Li, "MIMO techniques in WiMAX and LTE: a feature overview," *IEEE Communications magazine*, vol. 48, no. 5, pp. 86–92, 2010.

[46] A. O. Steinhardt and B. D. Van Veen, "Adaptive beamforming," *International Journal of Adaptive Control and Signal Processing*, vol. 3, no. 3, pp. 253–281, 1989.

[47] S. Applebaum, "Adaptive arrays," *IEEE Transactions on Antennas and Propagation*, vol. 24, no. 5, pp. 585–598, 1976.

[48] B. Widrow, P. Mantey, L. Griffiths, and B. Goode, "Adaptive antenna systems," *Proceedings of the IEEE*, vol. 55, no. 12, pp. 2143–2159, 1967.

[49] J. Capon, "High-resolution frequency-wavenumber spectrum analysis," *Proceedings of the IEEE*, vol. 57, no. 8, pp. 1408–1418, 1969.

[50] I. S. Reed, J. D. Mallett, and L. E. Brennan, "Rapid convergence rate in adaptive arrays," *IEEE Transactions on Aerospace and Electronic Systems*, no. 6, pp. 853–863, 1974.

[51] D. Ricks, P. Cifuentes, and J. Goldstein, "Adaptive beamforming using the multistage Wiener filter with a soft stop," in *Conference Record of Thirty-Fifth Asilomar Conference on Signals, Systems and Computers (Cat.No.01CH37256)*, vol. 2, pp. 1401–1406 vol.2, 2001.

[52] S. A. Vorobyov, "Adaptive and robust beamforming," in *Academic Press Library in Signal Processing*, vol. 3, pp. 503–552, Elsevier, 2014.

[53] S. Lukose and M. Mathurakani, "A study on various types of beamforming algorithms," 2010.

[54] S. Werner *et al.*, *Reduced complexity adaptive filtering algorithms with applications to communications systems*. Helsinki University of Technology, 2002.

[55] S. Dai, *Adaptive beamforming and switching in smart antenna systems*. PhD thesis, University of Glasgow, 2021.

[56] R. Parihar, "Branch prediction techniques and optimizations," *University of Rochester, NY, USA*, 2015.

[57] M. Kim, H. Momose, and T. Nakayama, "Development of link context-aware millimeter-wave beam switching system using depth-sensor," in *2018 International Symposium on Antennas and Propagation (ISAP)*, pp. 1–2, IEEE, 2018.

[58] A. Sellami, L. Nasraoui, and L. Najjar, "Outdoor neighbor-assisted localization algorithm for massive MIMO systems," in *2021 IEEE 94th Vehicular Technology Conference (VTC2021-Fall)*, pp. 1–5, IEEE, 2021.

[59] H. Wang, Z. Zhang, H. Shi, J. Dang, L. Wu, W. Zheng, and L. Zhao, "Location aware multi-cell MIMO communications assisted by optical positioning," in *2021 13th International Conference on Wireless Communications and Signal Processing (WCSP)*, pp. 1–5, IEEE, 2021.

[60] H. Döbler and B. Scheuermann, "Lama: Location-assisted medium access for position-beaconing applications," in *Proceedings of the 22nd International ACM Conference on Modeling, Analysis and Simulation of Wireless and Mobile Systems*, pp. 253–260, 2019.

[61] V. Lazarev, G. Fokin, and I. Stepanets, "Positioning for location-aware beamforming in 5G ultra-dense networks," in *2019 IEEE International Conference on Electrical Engineering and Photonics (EExPolytech)*, pp. 136–139, IEEE, 2019.

[62] Z. Xing, R. Wang, X. Yuan, and J. Wu, "Location-aware beamforming design for reconfigurable intelligent surface aided communication system," in *2021 IEEE/CIC International Conference on Communications in China (ICCC)*, pp. 201–206, IEEE, 2021.

[63] B. Zhu, Z. Zhang, and J. Cheng, "Outage analysis and beamwidth optimization for positioning-assisted beamforming," *IEEE Communications Letters*, 2022.

[64] C. Liu, W. Yuan, Z. Wei, X. Liu, and D. W. K. Ng, "Location-aware predictive beamforming for UAV communications: A deep learning approach," *IEEE Wireless Communications Letters*, vol. 10, no. 3, pp. 668–672, 2020.

[65] I. Orikumhi, J. Kang, C. Park, J. Yang, and S. Kim, "Location-aware coordinated beam alignment in mmWave communication," in *2018 56th Annual Allerton Conference on Communication, Control, and Computing (Allerton)*, pp. 386–390, IEEE, 2018.

[66] S. Khosravi, H. S. Ghadikolaeiy, J. Zander, and M. Petrova, "Location-aided beamforming in mobile millimeter-wave networks," *arXiv preprint arXiv:2205.09887*, 2022.

[67] A. El-Komy, O. R. Shahin, R. M. Abd El-Aziz, and A. I. Taloba, "Integration of computer vision and natural language processing in multimedia robotics application," *Inf. Sci*, vol. 7, no. 6, 2022.

[68] W. Xia, G. Zheng, Y. Zhu, J. Zhang, J. Wang, and A. P. Petropulu, "A deep learning framework for optimization of MISO downlink beamforming," *IEEE Transactions on Communications*, vol. 68, no. 3, pp. 1866–1880, 2019.

[69] C. Liu and H. J. Helgert, "An improved adaptive beamforming-based machine learning method for positioning in massive MIMO systems," *International Journal On Advances in Internet Technology*, vol. 6, no. 1-2, pp. 1–12, 2020.

[70] U. Bhattacherjee, C. K. Anjinappa, L. Smith, E. Ozturk, and I. Guvenc, "Localization with deep neural networks using mmWave ray tracing simulations," in *2020 Southeast-Con*, pp. 1–8, IEEE, 2020.

[71] U. Bhattacherjee, *Experimental Study of Localizing an Aerial User and Application of Deep Neural Network in Localization.* North Carolina State University, 2021.

[72] U. Bhattacherjee, E. Ozturk, O. Ozdemir, I. Guvenc, M. L. Sichitiu, and H. Dai, "Experimental study of outdoor UAV localization and tracking using passive rf sensing," in *Proceedings of the 15th ACM Workshop on Wireless Network Testbeds, Experimental evaluation & CHaracterization*, pp. 31–38, 2022.

[73] W. Wang, B. Li, Z. Huang, and L. Zhu, "Deep learning-based localization with urban electromagnetic and geographic information," *Wireless Communications and Mobile Computing*, vol. 2022, 2022.

[74] J. Kaur, O. R. Popoola, M. A. Imran, Q. H. Abbasi, and H. T. Abbas, "Deep neural network for localization of mobile users using raytracing," in *2022 IEEE USNC-URSI Radio Science Meeting (Joint with AP-S Symposium)*, 2022.

[75] A. Klautau and Pedro Batista, "5G MIMO Data for Machine Learning : Application to Beam-Selection using Deep Learning."

[76] H. Huang, Y. Cheng, and R. Weibel, "Transport mode detection based on mobile phone network data: A systematic review," *Transportation Research Part C: Emerging Technologies*, vol. 101, pp. 297–312, 4 2019.

[77] K. Aljohani, I. Elshafiey, and A. Al-Sanie, "Implementation of deep learning in beamforming for 5G MIMO systems," in *2022 39th National Radio Science Conference (NRSC)*, vol. 1, pp. 188–195, IEEE, 2022.

[78] D. H. Silva, D. A. Ribeiro, M. A. Ramírez, R. L. Rosa, S. Chaudhary, and D. Z. Rodríguez, "Selection of beamforming in 5G MIMO scenarios using machine learning approach," in *2022 19th International Conference on Electrical Engineering/Electronics, Computer, Telecommunications and Information Technology (ECTI-CON)*, pp. 1–4, IEEE, 2022.

[79] H. Huang, Y. Peng, J. Yang, W. Xia, and G. Gui, "Fast beamforming design via deep learning," *IEEE Transactions on Vehicular Technology*, vol. 69, no. 1, pp. 1065–1069, 2019.

[80] P. Jeyakumar, N. Tharanitaran, E. Malar, and P. Muthuchidambaranathan, "Beamforming design with fully connected analog beamformer using deep learning," *INTERNATIONAL JOURNAL OF COMMUNICATION SYSTEMS*, vol. 35, no. 7, 2022.

[81] J. M. Huttunen, D. Korpi, *et al.*, "DeepTx: Deep learning beamforming with channel prediction," *arXiv preprint arXiv:2202.07998*, 2022.

[82] I. Hameed, P. V. Tuan, and I. Koo, "Deep learning–based energy beamforming with transmit power control in wireless powered communication networks," *IEEE Access*, vol. 9, pp. 142795–142803, 2021.

[83] R. Yadav and A. Tripathi, "3D MIMO beamforming using spatial distance SVM algorithm and interference mitigation for 5G wireless communication network," *Journal of Cases on Information Technology (JCIT)*, vol. 24, no. 4, pp. 1–26, 2022.

[84] H. J. Kwon, J. H. Lee, and W. Choi, "Machine learning-based beamforming in two-user MISO interference channels," in *2019 International Conference on Artificial Intelligence in Information and Communication (ICAIIC)*, pp. 496–499, IEEE, 2019.

[85] M. M. Ramón, N. Xu, and C. G. Christodoulou, "Beamforming using support vector machines," *IEEE Antennas and Wireless Propagation Letters*, vol. 4, pp. 439–442, 2005.

[86] S. Lavdas, P. K. Gkonis, Z. Zinonos, P. Trakadas, L. Sarakis, and K. Papadopoulos, "A machine learning adaptive beamforming framework for 5G millimeter wave massive MIMO multicellular networks," *IEEE Access*, vol. 10, pp. 91597–91609, 2022.

[87] C. Liu and H. J. Helgert, "Beammap: Beamforming-based machine learning for positioning in massive MIMO systems," in *Proceedings of the Eleventh International Conference on Evolving Internet, Rome, Italy*, vol. 30, 2019.

[88] A. J. Singh and M. Jayakumar, "Machine learning based digital beamforming for line-of-sight optimization in satcom on the move technology," in *2020 4th International Conference on Electronics, Communication and Aerospace Technology (ICECA)*, pp. 422–427, IEEE, 2020.

[89] L. Le Magoarou, T. Yassine, S. Paquelet, and M. Crussière, "Deep learning for location based beamforming with NLOS channels," in *ICASSP 2022-2022 IEEE International Conference on Acoustics, Speech and Signal Processing (ICASSP)*, pp. 8812–8816, IEEE, 2022.

[90] C.-H. Lin, Y.-T. Lee, W.-H. Chung, S.-C. Lin, and T.-S. Lee, "Unsupervised resnet-inspired beamforming design using deep unfolding technique," in *GLOBECOM 2020-2020 IEEE Global Communications Conference*, pp. 1–7, IEEE, 2020.

[91] H. Hojatian, J. Nadal, J.-F. Frigon, and F. Leduc-Primeau, "Flexible unsupervised learning for massive MIMO subarray hybrid beamforming," in *GLOBECOM 2022-2022 IEEE Global Communications Conference*, pp. 3833–3838, IEEE, 2022.

[92] S. T. Spantideas, A. E. Giannopoulos, N. C. Kapsalis, A. Kalafatelis, C. N. Capsalis, and P. Trakadas, "Joint energy-efficient and throughput-sufficient transmissions in 5g cells with deep q-learning," in *2021 IEEE International Mediterranean Conference on Communications and Networking (MeditCom)*, pp. 265–270, IEEE, 2021.

[93] T. Maksymyuk, J. Gazda, O. Yaremko, and D. Nevinskiy, "Deep learning based massive mimo beamforming for 5G mobile network," in *2018 IEEE 4th International Symposium on Wireless Systems within the International Conferences on Intelligent Data Acquisition and Advanced Computing Systems (IDAACS-SWS)*, pp. 241–244, IEEE, 2018.

[94] C. Sun, Z. Shi, and F. Jiang, "A machine learning approach for beamforming in ultra dense network considering selfish and altruistic strategy," *IEEE Access*, vol. 8, pp. 6304–6315, 2020.

[95] A. M. Ahmed, A. A. Ahmad, S. Fortunati, A. Sezgin, M. S. Greco, and F. Gini, "Reinforcement learning based beamforming for massive mimo radar multi-target detection," *arXiv preprint arXiv:2005.04708*, 2020.

[96] V. Raj, N. Nayak, and S. Kalyani, "Deep reinforcement learning based blind mmWave mimo beam alignment," *IEEE Transactions on Wireless Communications*, vol. 21, no. 10, pp. 8772–8785, 2022.

[97] L. Bai and Z. Pang, "Multiagent reinforcement learning based energy beamforming control," *arXiv preprint arXiv:2006.08829*, 2020.

[98] L. Wang, S. Fortunati, M. S. Greco, and F. Gini, "Reinforcement learning-based waveform optimization for MIMO multi-target detection," in *2018 52nd Asilomar Conference on Signals, Systems, and Computers*, pp. 1329–1333, IEEE, 2018.

[99] I. Nasim, A. S. Ibrahim, and S. Kim, "Learning-based beamforming for multi-user vehicular communications: a combinatorial multi-armed bandit approach," *IEEE Access*, vol. 8, pp. 219891–219902, 2020.

[100] W. Yuan, C. Liu, F. Liu, S. Li, and D. W. K. Ng, "Learning-based predictive beamforming for UAV communications with jittering," *IEEE Wireless Communications Letters*, vol. 9, no. 11, pp. 1970–1974, 2020.

[101] Y. Arjoune and S. Faruque, "Double deep Q-learning and SAC based hybrid beamforming for 5G and beyond millimeter-wave systems," in *2021 IEEE International Conference on Electro Information Technology (EIT)*, pp. 422–428, IEEE, 2021.

[102] M. S. Aljumaily and H. Li, "Machine learning aided hybrid beamforming in massive-MIMO millimeter wave systems," in *2019 IEEE International Symposium on Dynamic Spectrum Access Networks (DySPAN)*, pp. 1–6, IEEE, 2019.

[103] M. S. Aljumaily and H. Li, "Hybrid beamforming for multiuser MIMO mmWave systems using artificial neural networks," in *2021 International Conference on Advanced Computer Applications (ACA)*, pp. 150–155, IEEE, 2021.

[104] H. Hojatian, J. Nadal, J.-F. Frigon, and F. Leduc-Primeau, "Unsupervised deep learning for massive MIMO hybrid beamforming," *IEEE Transactions on Wireless Communications*, vol. 20, no. 11, pp. 7086–7099, 2021.

[105] T. Peken, S. Adiga, R. Tandon, and T. Bose, "Deep learning for SVD and hybrid beamforming," *IEEE Transactions on Wireless Communications*, vol. 19, no. 10, pp. 6621–6642, 2020.

[106] Y. Su, J. Slottow, and A. Mozes, "Distributing proprietary geographic data on the world wide web—ucla gis database and map server," *Computers & Geosciences*, vol. 26, no. 7, pp. 741–749, 2000.

[107] H. Khelifi, S. Luo, B. Nour, H. Moungla, Y. Faheem, R. Hussain, and A. Ksentini, "Named data networking in vehicular ad hoc networks: State-of-the-art and challenges," *IEEE Communications Surveys & Tutorials*, vol. 22, no. 1, pp. 320–351, 2019.

[108] S. Uppoor, O. Trullols-Cruces, M. Fiore, and J. M. Barcelo-Ordinas, "Generation and analysis of a large-scale urban vehicular mobility dataset," *IEEE Transactions on Mobile Computing*, vol. 13, no. 5, pp. 1061–1075, 2013.

[109] I. Mesogiti, E. Theodoropoulou, F. Setaki, G. Lyberopoulos, A. Tzanakaki, M. Anastassopoulos, C. Politi, P. Papaioannou, C. Tranoris, S. Denazis, *et al.*, "5G-VICTORI: Future railway communications requirements driving 5G deployments in railways," in *Artificial Intelligence Applications and Innovations. AIAI 2021 IFIP WG 12.5 International Workshops: 5G-PINE 2021, AI-BIO 2021, DAAI 2021, DARE 2021, EEAI 2021, and MHDW 2021, Hersonissos, Crete, Greece, June 25–27, 2021, Proceedings*, pp. 21–30, Springer, 2021.

[110] L. Bassbouss, M. B. Fadhel, S. Pham, A. Chen, S. Steglich, E. Troudt, M. Emmelmann, J. Gutiérrez, N. Maletic, E. Grass, *et al.*, "5G-VICTORI: Optimizing media streaming in mobile environments using mmWave, NBMP and 5G edge computing," in *Artificial*

Intelligence Applications and Innovations. AIAI 2021 IFIP WG 12.5 International Workshops: 5G-PINE 2021, AI-BIO 2021, DAAI 2021, DARE 2021, EEAI 2021, and MHDW 2021, Hersonissos, Crete, Greece, June 25–27, 2021, Proceedings, pp. 31–38, Springer, 2021.

[111] E. Coronado, S. N. Khan, and R. Riggio, "5G-EmPOWER: A software-defined networking platform for 5g radio access networks," *IEEE Transactions on Network and Service Management*, vol. 16, no. 2, pp. 715–728, 2019.

[112] G. F. Riley and T. R. Henderson, "The ns-3 network simulator," *Modeling and tools for network simulation*, pp. 15–34, 2010.

[113] L. F. Perrone, T. R. Henderson, M. J. Watrous, and V. D. Felizardo, "The design of an output data collection framework for ns-3," in *2013 Winter Simulations Conference (WSC)*, pp. 2984–2995, IEEE, 2013.

[114] J. Sperling, S. E. Young, V. Garikapati, A. L. Duvall, and J. Beck, "Mobility data and models informing smart cities," tech. rep., National Renewable Energy Lab.(NREL), Golden, CO (United States), 2019.

[115] D. Tosi, "Cell phone big data to compute mobility scenarios for future smart cities," *International Journal of Data Science and Analytics*, vol. 4, pp. 265–284, 2017.

[116] A. Alkhateeb, G. Charan, T. Osman, A. Hredzak, J. Morais, U. Demirhan, and N. Srinivas, "DeepSense 6G: A large-scale real-world multi-modal sensing and communication dataset," *arXiv preprint arXiv:2211.09769*, 2022.

[117] D. Uvaydov, S. D'Oro, F. Restuccia, and T. Melodia, "Deepsense: Fast wideband spectrum sensing through real-time in-the-loop deep learning," in *IEEE INFOCOM 2021-IEEE Conference on Computer Communications*, pp. 1–10, IEEE, 2021.

[118] A. Oliveira and T. Vazão, "Generating synthetic datasets for mobile wireless networks with SUMO," in *Proceedings of the 19th ACM international symposium on mobility management and wireless access*, pp. 33–42, 2021.

[119] C.-D. Phung, N.-E.-H. Yellas, S. B. Ruba, and S. Secci, "An Open Dataset for Beyond-5G Data-driven Network Automation Experiments," in *2022 1st International Conference on 6G Networking (6GNet)*, IEEE, jul 6 2022.

[120] D. Raca, D. Leahy, C. J. Sreenan, and J. J. Quinlan, "Beyond throughput, the next generation," in *Proceedings of the 11th ACM Multimedia Systems Conference*, ACM, may 27 2020.

[121] I. Karim, K. S. Mubasshir, M. M. Rahman, and E. Bertino, "SPEC5G: A Dataset for 5G Cellular Network Protocol Analysis," 2023.

[122] S. Bouchelaghem, H. Boudjelaba, M. Omar, and M. Amad, "User Mobility Dataset for 5G Networks Based on GPS Geolocation," in *2022 IEEE 27th International Workshop on Computer Aided Modeling and Design of Communication Links and Networks (CAMAD)*, IEEE, nov 2 2022.

[123] G. Lee, J. Lee, Y. Kim, and J.-G. Park, "Network Flow Data Re-collecting Approach Using 5G Testbed for Labeled Dataset," in *2022 24th International Conference on Advanced Communication Technology (ICACT)*, IEEE, feb 13 2022.

[124] F. Mehmeti and T. F. L. Porta, "Analyzing a 5G Dataset and Modeling Metrics of Interest," in *2021 17th International Conference on Mobility, Sensing and Networking (MSN)*, IEEE, 12 2021.

[125] A. Narayanan, E. Ramadan, J. Quant, P. Ji, F. Qian, and Z.-L. Zhang, "5G tracker," in *Proceedings of the SIGCOMM '20 Poster and Demo Sessions*, ACM, aug 10 2020.

[126] Y. Lei, L. Qiang, Z. Yonghao, L. Hao, Y. Peng, F. Lei, L. Wenjing, and Q. Xuesong, "Data Mining and Statistical Analysis on Smart City Services Based on 5G Network," in *2019 15th International Wireless Communications amp; Mobile Computing Conference (IWCMC)*, IEEE, 6 2019.

[127] Q. Yang, C. zhang, C. Hu, H. Zhou, and H. Lou, "Big data collection and application based on 5G Industrial Internet Three-level edge layer," *Journal of Physics: Conference Series*, vol. 1684, p. 012025, nov 1 2020.

[128] S. Song, C. Su, B. Rountree, and K. W. Cameron, "A simplified and accurate model of power-performance efficiency on emergent GPU architectures," in *2013 IEEE 27th International Symposium on Parallel and Distributed Processing*, pp. 673–686, IEEE, 2013.

[129] M. Romer, *Beamforming adaptive arrays with graphics processing units*. PhD thesis, University of Texas at Austin, 2008.

[130] Z. Tang, D. Wang, and Z. Zhang, "Recurrent neural network training with dark knowledge transfer," in *2016 IEEE international conference on acoustics, speech and signal processing (ICASSP)*, pp. 5900–5904, IEEE, 2016.

[131] M. Zhang, J. Gao, and C. Zhong, "A deep learning-based framework for low complexity multiuser MIMO precoding design," *IEEE Transactions on Wireless Communications*, vol. 21, no. 12, pp. 11193–11206, 2022.

[132] S. Wassermann, T. Cuvelier, P. Mulinka, and P. Casas, "Adaptive and reinforcement learning approaches for online network monitoring and analysis," *IEEE Transactions on Network and Service Management*, vol. 18, no. 2, pp. 1832–1849, 2020.

[133] J. Verbraeken, M. Wolting, J. Katzy, J. Kloppenburg, T. Verbelen, and J. S. Rellermeyer, "A survey on distributed machine learning," *Acm computing surveys (csur)*, vol. 53, no. 2, pp. 1–33, 2020.

[134] L. Prechelt, "Automatic early stopping using cross validation: quantifying the criteria," *Neural networks*, vol. 11, no. 4, pp. 761–767, 1998.

[135] W. Webb, *Wireless communications: The future*. John Wiley & Sons, 2007.

[136] H. Tataria, M. Shafi, A. F. Molisch, M. Dohler, H. Sjöland, and F. Tufvesson, "6g wireless systems: Vision, requirements, challenges, insights, and opportunities," *Proceedings of the IEEE*, vol. 109, no. 7, pp. 1166–1199, 2021.

[137] T. K. Lo, "Maximum ratio transmission," in *1999 IEEE international conference on communications (Cat. No. 99CH36311)*, vol. 2, pp. 1310–1314, IEEE, 1999.

[138] T. Yoo and A. Goldsmith, "Optimality of zero-forcing beamforming with multiuser diversity," in *IEEE International Conference on Communications, 2005. ICC 2005. 2005*, vol. 1, pp. 542–546, IEEE, 2005.

[139] H. Al Kassir, Z. D. Zaharis, P. I. Lazaridis, N. V. Kantartzis, T. V. Yioultsis, and T. D. Xenos, "A review of the state of the art and future challenges of deep learning-based beamforming," *IEEE Access*, 2022.

[140] A. E. Ferreira, F. M. Ortiz, L. H. M. Costa, B. Foubert, I. Amadou, and N. Mitton, "A study of the lora signal propagation in forest, urban, and suburban environments," *Annals of Telecommunications*, vol. 75, pp. 333–351, 2020.

[141] M. Tuchler, A. C. Singer, and R. Koetter, "Minimum mean squared error equalization using a priori information," *IEEE Transactions on Signal processing*, vol. 50, no. 3, pp. 673–683, 2002.

[142] L. D. Nguyen, H. D. Tuan, T. Q. Duong, and H. V. Poor, "Multi-user regularized zero-forcing beamforming," *IEEE Transactions on Signal Processing*, vol. 67, no. 11, pp. 2839–2853, 2019.

[143] R. Onrubia, D. Pascual, J. Querol, H. Park, and A. Camps, "The global navigation satellite systems reflectometry (gnss-r) microwave interferometric reflectometer: Hardware, calibration, and validation experiments," *Sensors*, vol. 19, no. 5, p. 1019, 2019.

[144] P. Kela, M. Costa, J. Turkka, M. Koivisto, J. Werner, A. Hakkarainen, M. Valkama, R. Jantti, and K. Leppanen, "Location based beamforming in 5g ultra-dense networks," in *2016 IEEE 84th Vehicular Technology Conference (VTC-Fall)*, pp. 1–7, IEEE, 2016.

[145] F. Tao, B. Xiao, Q. Qi, J. Cheng, and P. Ji, "Digital twin modeling," *Journal of Manufacturing Systems*, vol. 64, pp. 372–389, 2022.

[146] E. VanDerHorn and S. Mahadevan, "Digital twin: Generalization, characterization and implementation," *Decision support systems*, vol. 145, p. 113524, 2021.

[147] D. López-Pérez, A. De Domenico, N. Piovesan, G. Xinli, H. Bao, S. Qitao, and M. Debbah, "A survey on 5g radio access network energy efficiency: Massive mimo, lean carrier design, sleep modes, and machine learning," *IEEE Communications Surveys & Tutorials*, vol. 24, no. 1, pp. 653–697, 2022.

[148] C. K. Anjinappa and I. Guvenc, "Angular and temporal correlation of v2x channels across sub-6 ghz and mmwave bands," in *2018 IEEE International Conference on Communications Workshops (ICC Workshops)*, pp. 1–6, IEEE, 2018.

[149] R. W. E. e. Stewart, K. W. Barlee, D. S. W. Atkinson, and L. H. Crockett, *Software defined radio using MATLAB® & Simulink® and the RTL-SDR*. Glassgow: Strathclyde Academic Media, 1st (revised) ed., 2 2017.

[150] Analog Devices, "AD7AD7476A/AD7477A/AD7478A Datasheet and Product Info," tech. rep., Analog Devices, Norwood, 11 2011.

[151] Lime Microsystems, "LimeSDR | Crowd Supply," 2016.

[152] RTL-SDR.com, "RTL-SDR Blog V3 Datasheet," tech. rep., 2020.

[153] Nuand, "bladeRF 2.0 micro," 11 2018.

[154] D. Gaydos, P. Nayeri, and R. Haupt, "Experimental Demonstration of a Software-Defined-Radio Adaptive Beamformer," in *2018 48th European Microwave Conference (EuMC)*, pp. 1581–1584, 2018.

[155] P. Nayeri and R. L. Haupt, "A testbed for adaptive beamforming with software defined radio arrays," in *2016 IEEE/ACES International Conference on Wireless Information Technology and Systems (ICWITS) and Applied Computational Electromagnetics (ACES)*, pp. 1–2, 2016.

[156] P. Delos, "Receiver Design Considerations in Digital Beamforming Phased Arrays," 2017.

[157] W. K. Zegeye, S. B. Amsalu, Y. Astatke, and F. Moazzami, "Wifi rss fingerprinting indoor localization for mobile devices," in *2016 IEEE 7th Annual Ubiquitous Computing, Electronics & Mobile Communication Conference (UEMCON)*, pp. 1–6, IEEE, 2016.

[158] Y. Chapre, A. Ignjatovic, A. Seneviratne, and S. Jha, "Csi-mimo: An efficient wi-fi fingerprinting using channel state information with mimo," *Pervasive and Mobile Computing*, vol. 23, pp. 89–103, 2015.

[159] I. Santos, L. Castro, N. Rodriguez-Fernandez, A. Torrente-Patino, and A. Carballal, "Artificial neural networks and deep learning in the visual arts: A review," *Neural Computing and Applications*, vol. 33, pp. 121–157, 2021.

[160] M. Al-Sarem, A. Alsaeedi, F. Saeed, W. Boulila, and O. AmeerBakhsh, "A novel hybrid deep learning model for detecting covid-19-related rumors on social media based on lstm and concatenated parallel cnns," *Applied Sciences*, vol. 11, no. 17, p. 7940, 2021.

[161] S. Ben Atitallah, M. Driss, W. Boulila, A. Koubaa, and H. Ben Ghezala, "Fusion of convolutional neural networks based on dempster–shafer theory for automatic pneumonia detection from chest x-ray images," *International Journal of Imaging Systems and Technology*, vol. 32, no. 2, pp. 658–672, 2022.

[162] S. Ben Atitallah, M. Driss, W. Boulila, and H. Ben Ghezala, "Randomly initialized convolutional neural network for the recognition of covid-19 using x-ray images," *International journal of imaging systems and technology*, vol. 32, no. 1, pp. 55–73, 2022.

[163] K. Greff, R. K. Srivastava, J. Koutník, B. R. Steunebrink, and J. Schmidhuber, "Lstm: A search space odyssey," *IEEE transactions on neural networks and learning systems*, vol. 28, no. 10, pp. 2222–2232, 2016.

[164] N. Y. Hammerla, S. Halloran, and T. Plötz, "Deep, convolutional, and recurrent models for human activity recognition using wearables," *arXiv preprint arXiv:1604.08880*, 2016.

[165] A. H. Salamah, M. Tamazin, M. A. Sharkas, and M. Khedr, "An enhanced wifi indoor localization system based on machine learning," in *2016 International conference on indoor positioning and indoor navigation (IPIN)*, pp. 1–8, IEEE, 2016.

[166] H. Mallouhi, J. Kaur, H. T. Abbas, and S. Laki, "In-network angle approximation for supporting adaptive beamforming," in *Proceedings of the 5th International Workshop on P4 in Europe*, pp. 61–66, 2022.

[167] A. Abbaspour-Tamijani and K. Sarabandi, "An affordable millimeter-wave beam-steerable antenna using interleaved planar subarrays," *IEEE Transactions on Antennas and Propagation*, vol. 51, no. 9, pp. 2193–2202, 2003.

[168] K. M. Younus, A. A. Jasim, and R. W. Clarke, "A beam steering system design based on phased array antennas," in *IOP Conference Series: Materials Science and Engineering*, vol. 1152, p. 012002, IOP Publishing, 2021.

Appendix A

Simulated Data from Ray Tracing Tool

The key objective of this chapter is to detail the process of generating simulated data using Wireless InSite with a focus on ray tracing principles. It aims to define the simulation setup, parameters, and scenarios considered, laying the groundwork for subsequent simulations and experiments. Through a thorough exploration of the simulated data generation process, this chapter seeks to provide readers with a clear understanding of the foundational elements of the research.

A.1   Introduction

Ray tracing, as a simulation technique, assumes a crucial role in the exploration of location-based adaptive beamforming within transport systems. Its capability to model intricate signal propagation scenarios aligns seamlessly with the objective of exploiting location information. By employing ray tracing, this research seeks to unravel the dynamics of adaptive beamforming in the context of transport systems, focusing on the specific parameters critical for localization.

A.2   Ray Tracing Principles

Ray tracing, a fundamental computational technique, plays a pivotal role in simulating the complex behavior of electromagnetic waves. By tracing individual rays and simulating their interactions with surfaces and objects, it accurately models phenomena such as reflection, refraction, and diffraction. This approach provides a realistic representation of signal propagation, capturing the nuances of real-world scenarios.

Memory Requirements and Computational Considerations

Ray tracing simulations are computationally intensive, demanding substantial memory resources to handle the complexity of large-scale environments. The accuracy and resolution of simulations directly impact memory requirements. High-fidelity simulations with detailed spatial information necessitate more memory for storing intermediate results and complex geome-

try representations. Computational considerations involve optimizing algorithms and employing parallel processing to manage the computational load efficiently.

Large-Area Compilations

The research incorporates large-area compilations within ray tracing simulations to replicate real-world scenarios accurately. Large-area compilations involve modeling extensive geographical regions, such as urban environments or transport systems, to capture the complexities of signal propagation across significant distances. This ensures that the adaptive beamforming strategies derived from these simulations are applicable to diverse and expansive transport scenarios.

A.3   Objectives of Ray Tracing Simulation

Precise Localization Parameters

The foremost objective of employing ray tracing simulations in the context of adaptive beamforming for transport systems is to extract precise localization parameters. This includes crucial elements such as DoD, DoA, power levels, SNR, path gain, and other relevant metrics. The aim is to obtain a detailed spatial understanding that forms the foundation for adaptive beamforming.

Realistic Propagation Scenarios

Ray tracing facilitates the creation of realistic propagation scenarios, mimicking the intricacies of signal behavior in transport environments. The simulations are designed to capture the complexities of urban landscapes, vehicular movement, and varying terrains. By doing so, the research aims to ensure that the adaptive beamforming strategies derived from these simulations are robust and applicable to real-world scenarios.

Impact of Location on Signal Characteristics

Through ray tracing, the research seeks to explore how the location of entities within transport systems influences key signal characteristics. This includes investigating how signals propagate in Line of Sight (LOS) and Non-Line of Sight (NLOS) scenarios, the impact of obstacles on signal strength, and the variation in propagation time delay based on location. Understanding these nuances is integral to tailoring adaptive beamforming strategies.

Optimization of Adaptive Beamforming Strategies

The ultimate objective is to optimize adaptive beamforming strategies based on the location insights obtained through ray tracing. By comprehensively analyzing the simulated data, the research aims to propose and refine adaptive beamforming techniques that leverage the extracted localization parameters. This optimization is geared towards enhancing the efficiency and performance of beamforming in diverse transport scenarios.

A.4   Features Obtained from Ray Tracing

AoA: Ray tracing simulations yielded precise information about the AoA of signals within the transport environment. AoA is a fundamental parameter as it defines the direction from which a signal arrives at the receiving antenna. This data is crucial for understanding the spatial distribution of signals and forms the basis for adaptive beamforming.

DoA: DoA information was extracted through ray tracing, providing insights into the angle indicating the direction from which a signal is transmitted. DoA is essential for determining the orientation of signal sources within the transport system, aiding in the development of adaptive beamforming strategies.

ToA: The simulation results included ToA data, indicating the time taken for a signal to travel from the transmitter to the receiver. This temporal information is valuable in understanding signal propagation delays based on location, contributing to the temporal aspects of adaptive beamforming.

Power Levels: Ray tracing simulations provided measurements of signal strength at various points in the transport scenario. Power levels are critical for assessing the intensity of signals, guiding the optimization of beamforming strategies to enhance communication reliability and efficiency.

Path Loss: Evaluation of Path Loss was conducted through ray tracing, offering insights into signal attenuation as it propagates through the open space of the transport system. Understanding path loss is vital for adjusting beamforming parameters to compensate for signal weakening over distance.

Path Gain: Quantification of Path Gain was derived from the simulations, detailing the gain experienced by the signal along its propagation path. Path gain information is instrumental in designing adaptive beamforming techniques to maximize signal strength and coverage.

SNR: Assessment of the SNR was a key outcome of the ray tracing tool. SNR evaluation is crucial for determining the quality of signals in the presence of background noise, influencing decisions in adaptive beamforming to ensure optimal communication performance.

The features obtained through ray tracing provide a comprehensive dataset for understanding the intricacies of signal propagation within transport systems, setting the stage for informed and effective adaptive beamforming strategies.

A.5   Utilization of Ray Tracing Features in Subsequent Analyses

The features obtained from ray tracing simulations served as foundational elements in subsequent analyses, employing a combination of statistical methods, ML algorithms, and data processing techniques. The utilization of these features can be outlined as follows:

Statistical Analysis: Statistical methods were applied to analyze key features such as AoA, DoA, ToA, Power Levels, Path Loss, Path Gain, and SNR. Descriptive statistics provided insights into the central tendencies, variabilities, and distributions of these parameters, forming the basis for establishing baseline characteristics of the wireless environment.

Feature Engineering: Feature engineering techniques were employed to derive new parameters or enhance existing ones. This involved transformations, aggregations, or combinations of ray tracing features to create more informative variables for subsequent analyses. Feature engineering aimed to capture nuanced aspects of signal propagation and enhance the discriminative power of the dataset.

ML Algorithms: ML algorithms, including but not limited to Support Vector Machine (SVM), Convolutional Neural Network (CNN), and Gated Recurrent Unit (GRU), were incorporated into the analysis pipeline. The features extracted from ray tracing simulations served as input variables for training and testing these models. The ML algorithms were designed to learn patterns, correlations, and associations within the dataset, contributing to the development of predictive models.

Localization Algorithms: The angle-related features, such as AoA and DoA, played a crucial role in developing localization algorithms. By leveraging these features, algorithms were designed to estimate the spatial coordinates of signal sources within the transport system. This localization information is integral for adaptive beamforming, as it enables the system to dynamically adjust based on the locations of users or communication nodes.

Dynamic Beamforming Strategies: The temporal characteristics provided by ToA were utilized to design dynamic beamforming strategies. Adaptive beamforming algorithms were developed to adjust the directionality and focus of antenna arrays based on the temporal dynamics of signal propagation. This dynamic adaptation ensures optimal communication performance in time-varying transport scenarios.

Quality-Aware Communication: Signal quality assessments derived from SNR values were integrated into the analyses to create quality-aware communication strategies. ML models were trained to predict signal quality based on ray tracing features, enabling adaptive beamforming systems to prioritize high-quality communication links.

A.6   Integration with Other Datasets

The integration of ray tracing data with other datasets was a crucial step in enhancing the comprehensiveness of the analyses. This integration aimed to provide a holistic view of the wireless communication environment within transport systems. The process and outcomes of integrating ray tracing data with other datasets are detailed below:

Wireless InSite and SUMO Integration: The ray tracing data obtained from Wireless InSite simulations was integrated with datasets generated through the Simulation of Urban Mobil-

ity (SUMO) tool. This integration facilitated a unified analysis of wireless communication and vehicular mobility scenarios. By correlating the spatial information from ray tracing with the movement patterns of vehicles simulated in SUMO, a more realistic representation of dynamic communication environments was achieved. This combined dataset enabled the exploration of how varying vehicular trajectories impact signal propagation and communication quality.

5G Test Bed Integration: Real-time data from 5G test beds available at the university was integrated with ray tracing results. This integration allowed for a comparison between simulated scenarios and actual experimental conditions, validating the accuracy and reliability of the ray-tracing simulations. The 5G test bed data provided empirical insights into the performance of wireless communication technologies in practical, on-the-ground settings. Discrepancies or similarities between ray tracing predictions and real-world measurements were scrutinized to refine the predictive capabilities of the simulation tool.

Literature Result Reproduction: The ray tracing results were cross-referenced and integrated with findings from relevant literature, particularly in the context of beamforming techniques and wireless communication in transport systems. Reproducing literature results within the ray tracing framework provided a benchmark for validating the simulation accuracy. Discrepancies or agreements with established results contributed to refining the ray-tracing model parameters and ensuring their alignment with real-world phenomena.

Wireless InSite Datasets: Datasets generated within Wireless InSite, beyond ray tracing-specific outputs, were integrated for a comprehensive analysis. This included information on antenna configurations, signal characteristics, and environmental conditions. Integrating these additional datasets allowed for a more nuanced exploration of the factors influencing wireless communication beyond the direct impact of ray-tracing features.

ML Training Data: The ray-tracing features served as a foundational element for training ML models. Integrating this training data with diverse datasets enriched the ML algorithms' exposure to various scenarios and conditions. This integration contributed to the development of robust and adaptive models capable of generalizing insights beyond the specific conditions simulated through ray tracing.

The integration of ray tracing data with other datasets brought a synergistic perspective to the analyses, combining simulated scenarios with real-world measurements, vehicular mobility patterns, established literature results, and additional information from Wireless InSite. This comprehensive approach ensured a more thorough understanding of the dynamics of wireless communication in transport systems.

A.7 Case Studies or Examples

In this section, we present illustrative case studies and simulations that showcase the pivotal role of ray tracing in obtaining relevant data and drawing meaningful conclusions for your research

on Exploiting Location Information for Adaptive Beamforming in Transport Systems.

A.7.1 Cont-BF in Cellular Communications

In the realm of cellular communications, the occurrence of handoffs or handovers during user transitions between BS presents challenges. Addressing this, highly directional antennas, especially in millimeter-wave systems, offer solutions by reducing interference and enhancing network efficiency. Cont-BF, a technique integrating ML and deep learning (DL) to predict a mobile user's location and reconfigure antenna arrays, stands out. This thesis explores the application of Cont-BF, emphasizing its role in reducing computational overhead and improving communication.

A.7.2 Challenges in Predicting Object Positions

Predicting an object's future position, especially in networking, has proven challenging. To overcome this, Cont-BF, a spatial filtering technique, minimizes interference by steering transmitted signals based on predicted location information. This technique aims to focus beam emissions toward the receiver direction, with the work emphasizing its role in reducing computational overhead.

A.7.3 Simulation Setup Using Wireless InSite in Rosslyn City

To illustrate the Cont-BF process, we established a simulation using Remcom Wireless InSite 3.3.0 (WI). Utilizing an existing profile of Rosslyn City, Virginia, USA, the simulation incorporated various transmitters and receiver routes, symbolizing moving vehicles. The scenario involved a mobile vehicle communicating with three cellular BS. The specific configurations of the BS antennas, the route of the moving vehicle, and the variations in power levels are detailed in Figures A.1, A.2, and A.3.

A.7.4 Integration with ML Models

Results from the ray-tracing simulation, including received power, path loss, propagation path, angle of arrival, time of arrival, direction of arrival, and more, were exported. These results serve as inputs for training the antenna network for location information. The integration of various ML models, such as support vector machine (SVM), convolutional neural network (CNN), gated recurrent unit (GRU), among others, with the outcomes from Wireless InSite facilitates the generation of a self-learned network.
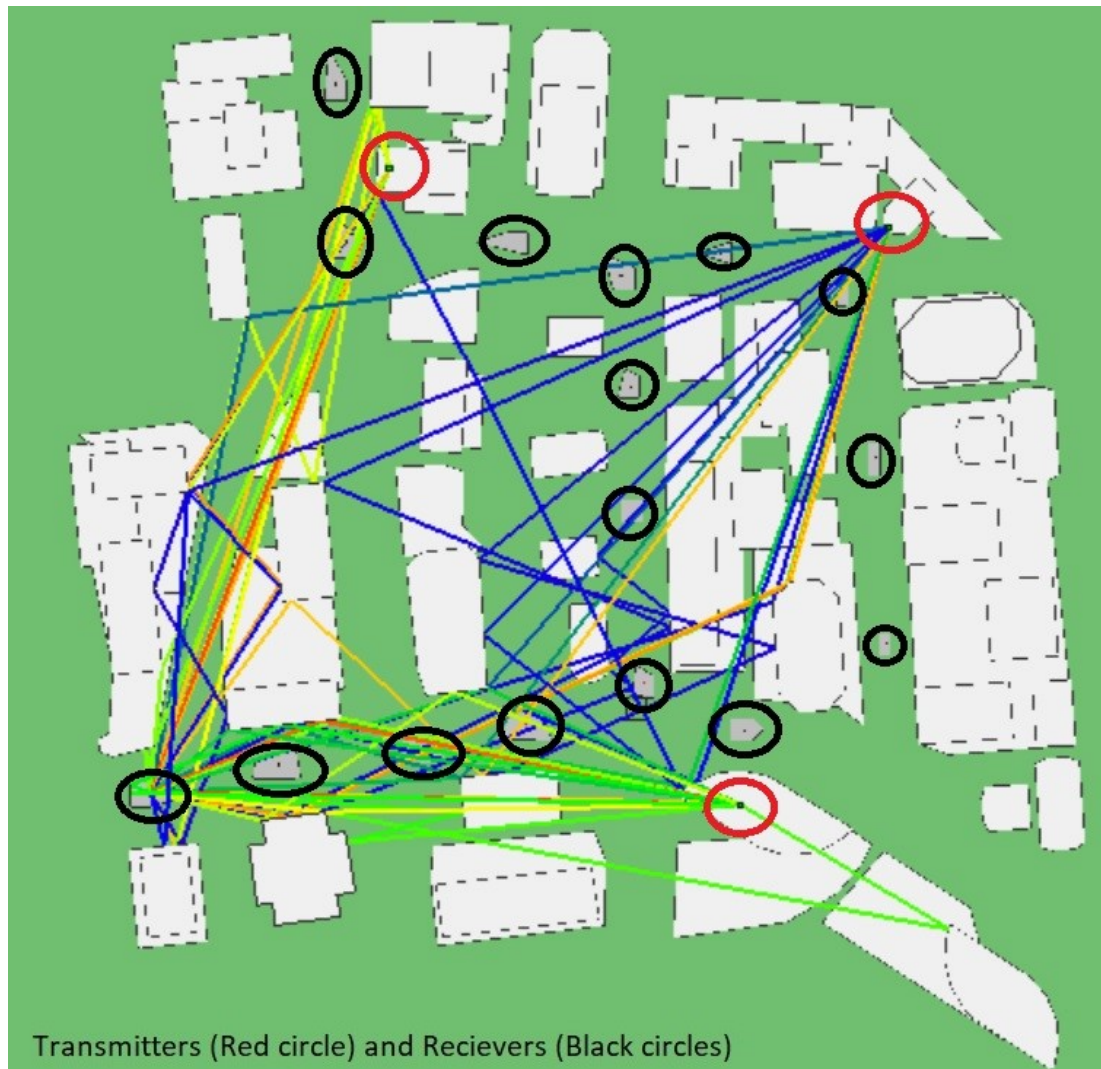
Figure A.1: Propagation paths of 3 Transmitters to 1st receiver in vehicular ray tracing scenario in Rosslyn, Virginia.

A.7.5 Creation of Open Space Scenario

As an integral part of the research methodology, an open space scenario was crafted to simulate radio wave propagation in unobstructed environments. This scenario was designed with a transmitter strategically positioned at one corner, emitting signals across the open space. A grid configuration consisting of more than 1000 receivers was employed to capture a broad spectrum of data points, enriching the dataset with diverse signal characteristics.

In both iterations of the open space scenario, we utilized a variety of antennas to comprehensively explore the wireless channel characteristics. Half-wave dipole antennas, directional antennas, and MIMO antennas were strategically employed to observe the impact of different antenna types on signal propagation. This approach aimed to understand how varying antenna configurations influenced key parameters such as AoA, DoA, RSSI, and Path Gain (PG).

To ensure a nuanced understanding of the wireless channel, each simulation involved the
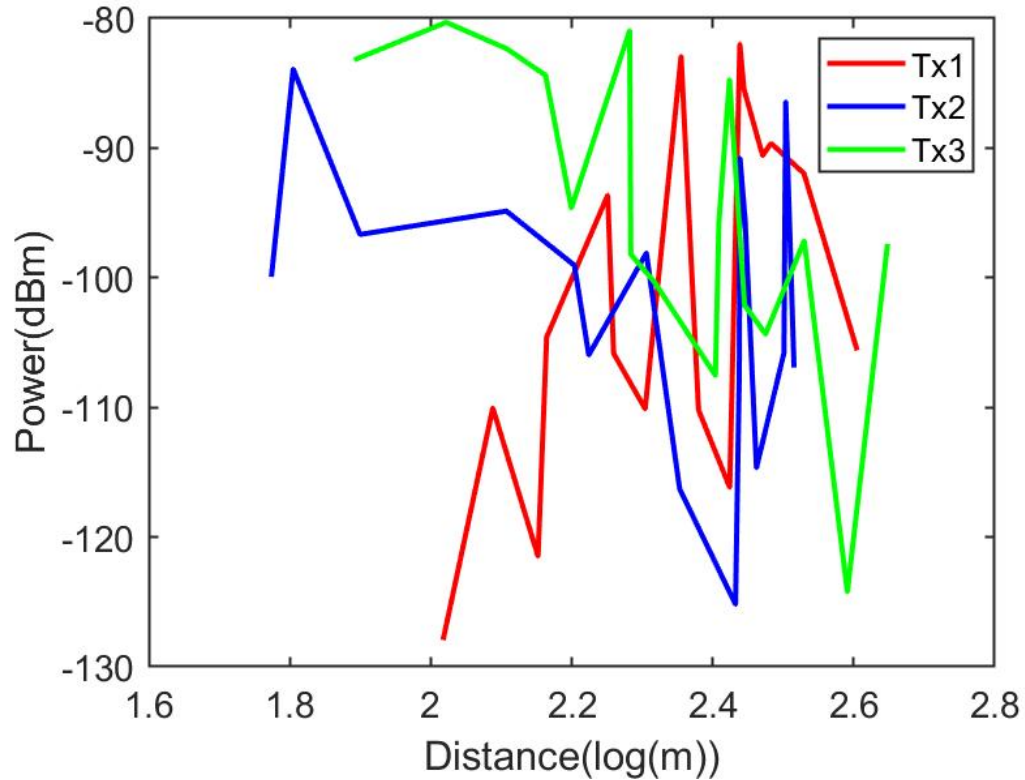
Figure A.2: Received power vs Distance.

consideration of 250 paths. This meticulous approach was taken to capture a detailed representation of the wireless channel and enhance the realism of the simulated scenarios. The outcomes from these simulations contribute significantly to the overarching goal of exploiting location information for adaptive beamforming in transport systems.

A.7.6   UofG Campus Scenario

This section provides a detailed overview of the simulation setup designed for location estimation within the UofG campus, emphasizing the application of ML techniques to predict UE locations based on channel features and location information.

To illustrate the concept of localization, a small cell scenario was constructed within the urban environment of the UofG's Gilmorehill campus, situated in Glasgow, Scotland, UK. Figure A.4 offers a visual representation of this scenario.

The defined cell operated at a carrier frequency of 3.75 GHz with a 100 MHz bandwidth. A strategically positioned set of receivers, located 2 meters above the ground and spaced 5 meters apart, simulated the movement of vehicles along a designated route at speeds of 5, 10, and 15 meters per second. The route covered key locations, including Byres Road, JMS, the library, and UofG Union (GUU). This arrangement ensured the capture of both line-of-sight (LOS) and non-line-of-sight (NLOS) paths.
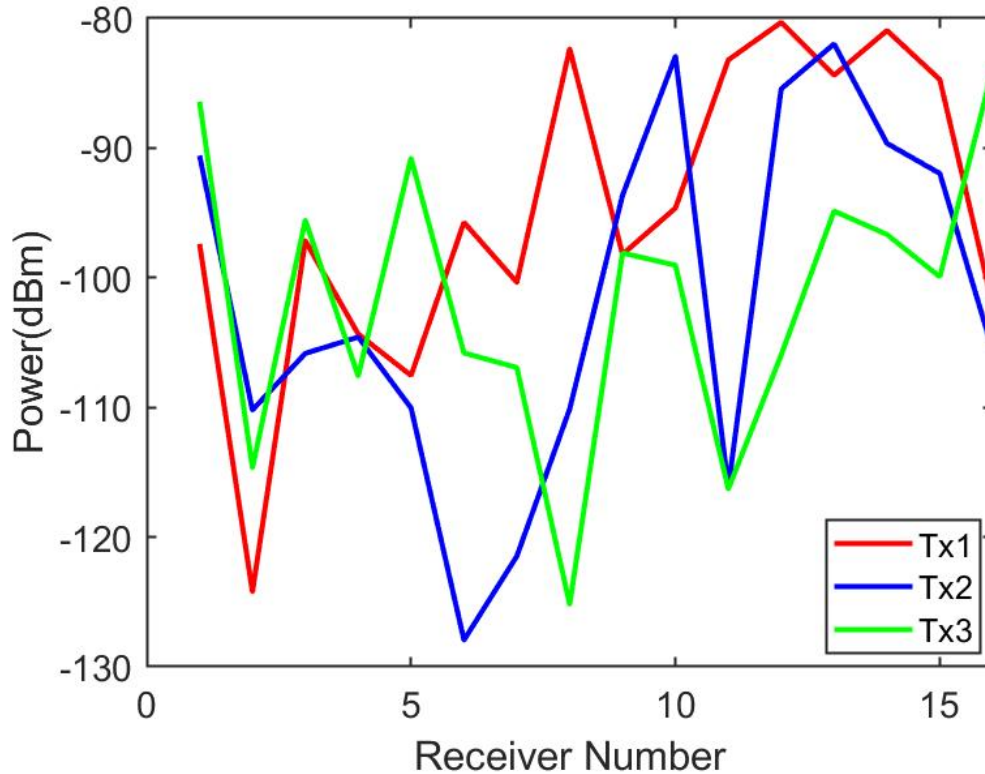
Figure A.3: Received power vs Receivers.

The ground truth for Deep Neural Network (DNN) output was established using UE locations corresponding to the receiver points. The simulation parameters encompassed MIMO directional array antennas at both transmitters, 49 dBm transmitter power, a 15-degree downtilt, and -100 dBm receiver sensitivity. The simulations were executed on an Intel(R) Core(TM) i7-9700 CPU @ 3.00GHz, 32GB RAM PC, utilizing Wireless InSite® MIMO version 3.3.

This designed scenario serves as a critical component in the exploration of location-based adaptive beamforming within an urban context, contributing valuable insights to the broader research endeavor.

A.7.7   Data Extraction and Analysis

Following the simulations, a crucial step involved the extraction of data pertaining to the parameters discussed earlier, including but not limited to AoA, DoA, ToA, RSSI, Path Gain (PG), and others. The Wireless InSite tool facilitated the retrieval of detailed results, enabling a comprehensive analysis of signal behavior in both open-space and campus scenarios.

This extracted data played a pivotal role in establishing a profound understanding of wireless propagation intricacies. Moreover, it laid a robust foundation for subsequent phases of the research, specifically focusing on the development and training of ML and DL algorithms. These algorithms were instrumental in predictive modeling and system optimization, particularly in

Figure A.4: UofG Campus Scenario

the context of location-based adaptive beamforming.

Details regarding the acquisition of each parameter and their specific roles in the localization process will be thoroughly elucidated in the subsequent chapter, providing an in-depth exploration of the methodology employed and the insights gained.

Appendix B

P4 Programming Language

P4, which stands for "Programming Protocol-independent Packet Processors," is a domain-specific language that has revolutionized the way network packets are processed in modern networking environments. Unlike traditional networking devices that come with fixed functionality, P4 enables network engineers and researchers to define and modify the behavior of network devices programmatically. This is achieved through a high-level abstraction that allows for the specification of how network packets are processed, independent of the underlying hardware.

The coding approach in P4 is unique and powerful. P4 code typically defines a packet-processing pipeline, which includes specifying how packets are parsed, the match-action tables that decide how packets are processed, and how packets are to be modified or forwarded. P4 programs define these processes in a clear, declarative manner, allowing for custom packet-forwarding logic that can be tailored to specific network needs. The language's syntax is similar to C, making it accessible to those familiar with conventional programming languages.

P4's programmability opens up opportunities for implementing a wide range of networking functions, from basic forwarding to more complex operations like network telemetry, load balancing, and security monitoring. In the context of 5G and mmWave technologies, P4's ability to rapidly process and adapt to packet-level information in real-time is crucial for tasks like dynamic beamforming, where efficient handling of data such as UE location is essential for optimizing network performance. As such, P4 has become an indispensable tool in the modern networking landscape, driving innovations in network functionality, performance, and flexibility.